NONLINEAR PERFORMANCE ASSESSMENT OF RC BUILDINGS BASED ON DISPLACEMENT DESIGN BY IMPLEMENTING TSC2018 WITH COMPARISON TO THE EUROCODE

AROVA KONAK

March 2022

DİYARBAKIR

GRADUATE SCHOOL
OF NATURAL AND APPLIED SCIENCES
OF DICLE UNIVERSITY

NONLINEAR PERFORMANCE ASSESSMENT OF RC BUILDINGS BASED ON DISPLACEMENT DESIGN BY IMPLEMENTING TSC2018 WITH COMPARISON TO THE EUROCODE

BY
AROVA KONAK

IN PARTIAL FULFILLMENT OF THE REQUIREMENTS
FOR
THE DEGREE OF MASTER OF SCIENCE
IN
CIVIL ENGINEERING

March 2022
DİYARBAKIR

NONLINEAR PERFORMANCE ASSESSMENT OF RC BUILDINGS BASED ON DISPLACEMENT DESIGN BY IMPLEMENTING TSC2018 WITH COMPARISON TO THE EUROCODE

This study, prepared by **Arova KONAK** as part of the Dicle University Graduate Education and Examination Regulation, was evaluated by the jury members with the following information and accepted as a **Master's Thesis in the Department of Civil Engineering**.

Prof. Dr. Neslihan DALKILIÇ ____________________
Dean, Graduate School of **Natural and Applied Science**

Assoc. Prof. Dr. İdris BEDİRHANOĞLU ____________________
Supervisor, **Civil Engineering Dept., Dicle University**

Examining Committee Members:

Assoc. Prof. Dr. Barış ERDİL (*) ____________________
Civil Engineering Dept.,Yüzüncü Yıl University

Assoc. Prof. Dr. İdris BEDİRHANOĞLU (**) ____________________
Civil Engineering Dept., Dicle University

Assoc. Prof. Dr. Mehmet Emin ÖNCÜ ____________________
Civil Engineering Dept., Dicle University

APPROVAL

Date: *01.03.2022*

(*) Write the title, name and affiliation of the head of the examining committee in the first row.
(**) Write the title, name and affiliation of the superviso in the second row.

I hereby declare that all information in this document has been obtained and presented following the Thesis Manual (prepared by the Dicle University Graduate School of Natural and Applied Sciences), academic rules and ethical conduct. I also declare that, as required by these rules and conduct, I have fully cited and referenced all material and results that are not original to this work. I shall be solely responsible if any evidence is found against my declaration.

Name, Surname: AROVA KONAK

Signature: ……………………………

ACKNOWLEDGMENTS

I would like to acknowledge the following people whose enormous contributions led to the successful completion of this thesis:

I would like to thank my advisor Associate Prof. Dr. IDRIS BEDIRHANOĞLU and Dr. FEVZI SARITAŞ. for their continuous guidance.

I would like to express my gratitude to my father SUBHI KALLO, my mother, husband, daughter, and dear sisters.

I would like to thank to Dicle University, department of Civil Engineering for their facilities that they provided to me.

I would like to extend my thanks to the DUBAP for grant they provided me to do this research (Project number: FBE.21.023).

CONTENT

LIST OF FIGURES

LIST OF TABLE

ANNOTATION AND SYMBOL

Symbol	Explanation
A_s	Area of a section of tensile reinforcement
S_a	Spectral acceleration.
S_d	Spectral displacement (Sa and the associated Sd make up points on the capacity spectrum)
V	Base shear
Δ_{roof}	Roof displacement (V and the associated Δroof make up points on the capacity curve)
W	Building dead weight plus likely live loads.
wi/g	mass assigned to level
α_1	The modal mass coefficient for the first natural mode.
$\Theta i,1$	The amplitude of mode 1 at level i
N	Level N, the level which is the uppermost in the main portion of the structure
εc	Concrete strain value
εs	Steel strain value
Θp	Plastic curvature
$Ø_U$	Ultimate curvature
ωwe	Mechanical reinforcement ratio of effective confinement reinforcement
LP	Plastic hinge length
LS	Shear span
d_b	Longitudinal reinforcement diameter
d_{bL}	The diameter of the tension reinforcement.
εsh	Steel strain at hardening point
Θy	Yiled rotation
εsu	The confined concrete ultimate strain
B_0	Hysteretic damping represented as equivalent viscous damping.
E_D	Energy dissipated by damping.
E_{SO}	Maximum strain energy
M_y	Yield moment

θ_y	The chord rotation at yield
Øy	The yield curvature of the end section.
h	The depth of cross-section
a	The confinement effectiveness factor
ω, ω'	The mechanical reinforcement ratio of the tension and compression, respectively, longitudinal reinforcement.
ρ_{sx}	The ratio of transverse steel parallel to the direction x of loading.
L_P	The length of plastic hinge.
L_V	The length of shear.
P_d	The steel ratio of diagonal reinforcement, in each diagonal direction.
f_c, f_{yw}	The concrete compressive strength (Mpa) and the stirrup yield (Mpa)
a_v	Shear cracking is expected to precede flexural yielding at the end section.
d and d'	The depths of the tension and compression reinforcement respectively.

Annotation	**Explanation**
TSC2018	Turkish Seismic Code Published In 2018
EC8	European Seismic Code
ABYYHY1998	Regulation on Buildings to be Built in Disaster Areas
FEMA356	The American Pre-Standard And Commentary For The Seismic Rehabilitation of Buildings**.**
ASCE 41-06	A valuable tool for structural engineers and the public for improving seismic performance of existing buildings.

ABSTRACT

NONLINEAR PERFORMANCE ASSESSMENT OF RC BUILDINGS BASED ON DISPLACEMENT DESIGN BY IMPLEMENTING TSC2018 WITH COMPARISON TO THE EUROCODE

Arova KONAK
Master of Science in Department of Civil engineering
Supervisor: Associate Prof. Dr. İdris BEDİRHANOĞU
March 2022,130 pages

Turkey is located in an active seismic zone where it has been suffered great losses in economy and souls. As a result of site investigations that have been conducted after earthquakes, it has been concluded that many buildings had not been designed according to codes and regulations. It was also seen that the strength of the concrete used is very low in addition to the presence of many defects in buildings which decreased the buildings' resistance to earthquakes. To avoid these risks, the issue of evaluating the performance of a building and retrofitting has received great attention in recent years. The common methods used to evaluate the performance of buildings are nonlinear static and dynamic methods.

In this study, the performance evaluation of buildings has been done by using nonlinear methods. For this purpose, nonlinear analysis and pushover analysis methods were used. Both Turkish seismic code (TSC2018) and Euro-code (EC8) rules have been considered comparatively for sample rc frames and a building. The sample building has a serious torsion problem where the stiffness center does not match with the mass center. In addition to the torsion problem, the effect of low-strength concrete on performance was also investigated.

The results have proved that implementing both codes the TSC2018 and the EC8 yield similar results. Nonetheless, the only difference between these two cases is the definition of the effective section stiffness and the definition of the plastic hinge, however, the difference remains at the minimum level. In addition, it has been determined that the building performance decreases when the concrete strength decreases. Furthermore, it was found that the decline in performance when the concrete strength decreases from C20 to C10 is much greater than the case in which the concrete strength decreases from C40 to C20. Bearing in mind that the frame that has been studied in this case was multi-storey. Therefore the effects of the weaknesses in the structure on the performance may differ according to the number of floors. Lastly, it has been aimed that the obtained results will be guides and references for the project design engineers.

Keywords: Nonlinear analysis, TSC 2018, EC8, Pushover analysis, Displacement base design

ÖZET

BETONARME BİNALARIN ŞEKİLDEĞİŞTİRMEYE DAYALI DOĞRUSAL OLMAYAN PERFORMANS DEĞERLENDİRMESİNİN TBDY2018 VE EC8 İLE KARIŞLAŞTIRMALI OLARAK GEREÇEKLEŞTİRİLMESİ

ARROVA KONAK
Yüksek Lisans, İnşaat Mühendisliği
Danışman: Doç. Dr İdris BEDİRHANOĞU
Mart 2022, 130 sayfa

Türkiye aktif bir deprem kuşağında yer almakta olup, ekonomi ve insan hayatı açısından büyük kayıplara uğramıştır. Depremlerden sonra yapılan saha incelemeleri sonucunda birçok yapının deprem kurallarına göre tasarlanmadığı sonucuna varılmıştır. Binalarda depreme karşı direnci azaltan birçok kusurun bulunmasının yanı sıra kullanılan betonun mukavemetinin çok düşük olduğu da görülmüştür. Bu risklerden kaçınmak için bir binanın performansının değerlendirilmesi ve güçlendirmesi konuları son yıllarda büyük ilgi çekmektedir. Performansı değerlendirmek için kullanılan yaygın yöntemler doğrusal olmayan statik ve dinamik metotlardır.

Bu çalışmada betonarme yapıların performans değerlendirmesi doğrusal olmayan yöntemler kullanılarak yapılmıştır. Bu amaç ile zaman tanım alanında analiz ve itme analizi yöntemleri kullanılmıştır ve örnek bir yapı üzerinde hem TSC2018 hem EC8 kuralları karşılaştırmalı olarak göz önüne alınmıştır. Yapıdaki kusurların performansa olan etkilerini incelmek amaç ile seçilen örnek yapının rijitlik merkezi ile kütle merkezi ile birbirine uzaktır ve bu şekilde yapı önemli burulma etkilerine maruz kalmaktadır. Ayrıca beton dayanımın düşük olmasının performansa etkisi de incelenmiştir.

Sonuç olarak Türkiye deprem yönetmenliği ve Eurocode ile yapılan analizlerde birbirine yakın sonuçlar elde edilmiştir. Buna karşılık TSC2018 ve EC8 kuralları karşılaştırıldığında etkin kesit rijitliği ve plastik mafsal tanımlaması arasında farklıklar olduğu görülmüştür fakat bu farklılıkların sonuçlar üzerinde az etkili olduğu görülmüştür. Beton dayanımının performansa etkisi de incelenmiştir. Beton dayanımı düştüğünde bina performansının da azaldığı tespit edilmiştir. Ayrıca beton dayanımı C20 den C10 a düşütüğündeki performans azalması beton dayanımının C40 tan C20 ye düşmesindeki performans kaybı çok daha fazla olmaktadır. Bu durum gözönüne alınan çerçevenin çok katlı olması ile ilişkilendirilmektedir. Bu durumda kat sayısına bağlı olarak yapıdaki zayıflıkların performansa etki oranları farklılık gösterebilmektedir. Elde edilen sonuçların yapıların deprem performanslarının değerlendirilmesi çalışmalarını yapan proje mühendislerine önemli bilgiler sağlayacağı edeceği düşünülmektedir.

Anahtar Kelimeler: Doğrusal olmayan analizi, TSC 2018, EC8, İtme analizi, Şekildeğiştirmeye göre tasarım.

1. INTRODUCTION

It is known that Turkey is located in a higly seismic zone and most of the existing buildings in Turkey are highly prone to earthquakes. This fact cannot be ignored in the process of designing structures. Earthquakes are natural disasters that we cannot eliminate, however, we can prevent buildings from collapsing or reducing the damage caused by earthquakes by improving the resistance of buildings. The damage to structural elements in buildings during earthquakes is most often caused by errors related to improper soil research, the lack in the quality of the building materials, and insufficient details in design or application (Bedirhanoglu et al. 2022). In addition, some buildings collapse under only vertical loads mainly due to defects that occur during the construction of the building (Bedirhanoglu 2009). Below there are some pictures of collapsed buildings (Figure 1.1, Figure 1.2, Figure 1.3).

Figure 1.1 Damage to the column under vertical load (Taken from the archive of Assoc. Prof. Dr. İdris Bedirhanoğlu, Bedirhanoglu 2011a)

Figure1.2 The collapse of the building, which had damaged (Taken from the archive of Assoc. Prof. Dr. İdris Bedirhanoğlu, Bedirhanoglu 2011a)

Figure 1.3 Building had collapsed 2011 in the earthquake (Taken from the archive of Assoc. Prof. Dr. İdris Bedirhanoğlu, Bedirhanoglu 2011b)

It is known that the linear methods have been used in the design of new buildings. However, the nonlinear methods should be used to produce more reasonable outcomes. Since the nonlinear methods play a key role in the reliability of the performance analysis of the building where a separate chapter has been devoted to the non-linear methods in the newest version of Turkish seismic code (TSC2018).

This study presents results of performance analysis of buildings by considering rules provided by both TSC2018 and EC8. Performance analysis was carried out on a simple two storey reinforced concrete frame by pushover analysis and also it was carried out on a 14-story frame considering three different types of concrete strength, in order to evaluate the effect of low-strength concrete on building performance. A non-linear time history analysis was also carried out on a sample building according to TSC2018, and EC8.

2. LITERATOR REVIEW

After publishing TSC2018 many studies appeared on evaluating existing buildings, and on evaluating existing buildings using both the new Turkish code TSC2018 and the old Turkish code TSC2007 and comparing the results. Yet there is very limited research on the use of performance analysis using the Turkish and European codes and comparing the results. Particularly those studies are summarized in the following.

Irtem and Türker (2004) conducted a research on performance analysis of reinforced concrete building that has been structured in a non-linear static manner according to ABYYHY, 1998 in two different cases. In the first case, the effect of the walls on load-bearing was taken into consideration, while in the second case, the effect of the walls on load-bearing was neglected. Accordingly, it was found that the first case performed better, in other words, when the role of walls on load-bearing was taken into account.

One of the initial works has been done by Ilki et al. (2005) to evaluate the performance of an existing building located in Istanbul by non-linear seismic analysis through implementing SAP2000 program. They found that the original building having many deficiencies like low strength concrete, lack of stirrups can not reach the performance point where the lateral displacement capacity of the building had been found to be extremely limited. In the second analysis of the retrofitted building by jacketing all the columns with FRP (fiber reinforced polymers) which built a more ductile moment-curvature for the columns (Bedirhanoglu and Ilki 2004), the performance point had been achieved.

In Esin's study (Esin 2005) the pushover analysis is explained in detail and evaluated for an existing building by using SAP2000 and EPARC analysis programs. Because the building was insufficient the performance point could not be found. The building was retrofitted by adding shear walls then the building was re-analyzed. As a result, it was found that the building's performance has improved and evaded the risk of collapse.

Buzuk (2019) focused in his research on conducting performance analysis for a 24-storey frame based on the rules of the TSC2018 and Eurocode 2004. BUZUK used a non-linear analysis and entered 11 different seismic data after the analysis. It was concluded that the results of an evaluation using TSC2018 and Eurocode rules were similar.

Şahin (2019) conducted his study on evaluating an existing building according to the TSC2018 using the non-linear time history analysis. ŞAHİN used the SAP2000 program for his analysis. It was found that the building did not reach the targeted performance level. The methods for retrofitting by steel have been suggested, and their advantages and disadvantages were also discussed.

In another study, a non-linear analysis was performed for a 4-storey workshop building retrofitted by the addition of shear walls using the time-history method. Where 11 earthquake records were applied to the building in both directions. It has been observed that with the addition of shear walls elements to the structure, the lateral stifness of the building increased and the displacements remained within the allowable limits. The column and beam elements were exposed to smaller loads and their sections were less damaged, as most of the base shear force was covered by the shear walls. Thus, it was observed that the performance level of the existing structure was maximized and the damage level was minimized as a result of the addition of the shear wall. Based on the results obtained, it was concluded that adding sufficient shear walls elements to the structures could be a practical and effective solution technique (Zolmaz, 2019).

Many experimental works have been carried out to evaluate effects of many common defects (Ilki et all., 2006, Bedirhanoglu et all., 2011). Ilki and others conducted an experiment to find out the shear behavior of short columns with low-quality concrete that does not contain enough transverse reinforcement before and after retrofitting them with GFRP. The columns showed real improvement in terms of strength and deformation and from brittle behavior to better.

3. PUSHOVER CONCEPT AND NONLINEAR PERFORMANCE ASSESSMENT ACCORDING TO TSC2018 AND EC8

3.1 Pushover Concept

Pushover analysis is a nonlinear static method used to evaluate the performance of existing structures investigating seismic design. Structure performance is evaluated under constant vertical load with the lateral load increasing monotonically. The lateral load is increased until the cracks appear in some places. Therefore the stiffness of the structure declines because of these cracks. As loading continues, the fractured parts grow until the structure reaches the required displacement or collapse. (Oğuz, 2005).

Pushover analysis can be performed in two different criteria force-controlled or displacement controlled. Displacement-controlled has been used in this study. Where the force is unknown but the displacement value is known. The lateral force has changed either by increasing or by decreasing until the point at the mass‘s center in the roof reaches the specified displacement. (Özer, 2009).

“Simplified nonlinear analysis procedures using pushover method such as the capacity spectrum method and the displacement coefficient method require determination of three primary elements capacity, demand (displacement) and performance.” (ATC-40, 1996).

The demand (displacement) represents the earthquake ground motion affecting the structure, and the capacity represents the behavior of the building under the effect of this earthquake. Performance point is the point at which the seismic capacity of the structure equals the seismic demand imposed on the structure by the specified ground motion (ATC-40, 1996).

3.1.1 Determine capacity

The capacity of the structure can be expressed by the pushover curve. The best way to define this curve is by drawing a graph of the relationship between the Base Shear and the displacement in the roof. The base shear was boosted until the roof reached the demand displacement.

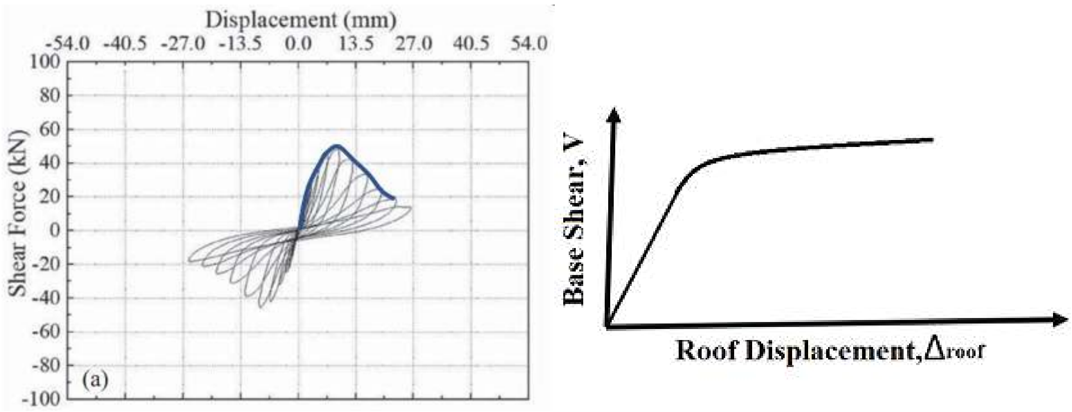

a) For column (Bedirhanoglu et al. 2022) b) For building

Figure 3.1 Pushover curve (force-displacement), a) column, b) building

3.1.2 Determine demand

A displacement on the capacity curve consistent with seismic demand should be known to determine the performance point. (Buğday, 2014). There are two methods for this determination. The first method is (Capacity Spectrum Method, ATC-40 1996) The second method is (Displacement Coefficient Method, FEMA356, ASCE 41-06) in this study, we will use the first method. Those are explained in detail in the following sections.

3.1.3 Capacity spectrum method, ATC-40(1996)

Inelastic deformations occur with increased lateral loads (earthquakes load), these deformations enlarge the damping of the structure and lessen the earthquake demand. In this method, the elastic spectrum is reduced depending on inelastic deformation. The performance point is determined at the stage when capacity and demand are equal. It has been verified that the targeted performance of the building has been achieved (Özer, 2009).

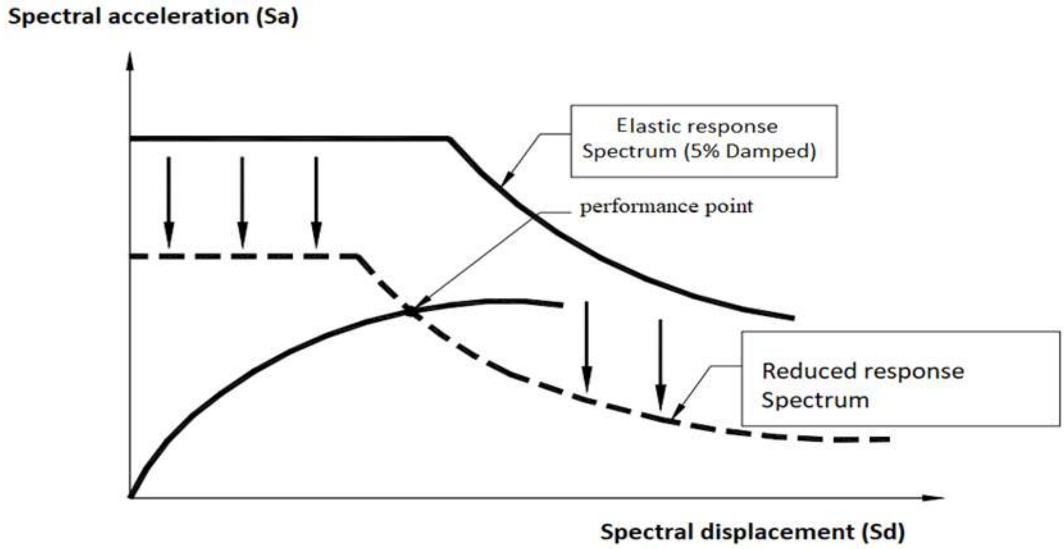

Figure 3.2 Determination of the performance point by the capacity spectrum method (Özer 2009)

3.1.4 Conversion of the capacity curve to the capacity spectrum

To compare the capacity curve with the demand spectrum, the capacity curve must be converted to a capacity spectrum.

The curve is converted by using these equations:

$$\alpha_1 = \frac{\left[\sum_{i=1}^{N}\left(\frac{w_i \emptyset_{iI}}{g}\right)\right]^2}{\left[\sum_{i=1}^{N}\left(\frac{w_i}{g}\right)\right] \cdot \left[\sum_{i=1}^{N}\left(\frac{w_i \emptyset_{iI}^2}{g}\right)\right]} \tag{3.1}$$

$$S_a = \frac{V_T/W}{a_1} \tag{3.2}$$

$$PF_1 = \left[\frac{\sum_{i=1}^{N}\left(\frac{w_i \emptyset_{iI}}{g}\right)}{\sum_{i=1}^{N}\left(\frac{w_i \emptyset_{iI}^2}{g}\right)}\right] \tag{3.3}$$

$$S_d = \frac{\Delta_{max}}{PF_1\, \emptyset_{Roof,1}} \tag{3.4}$$

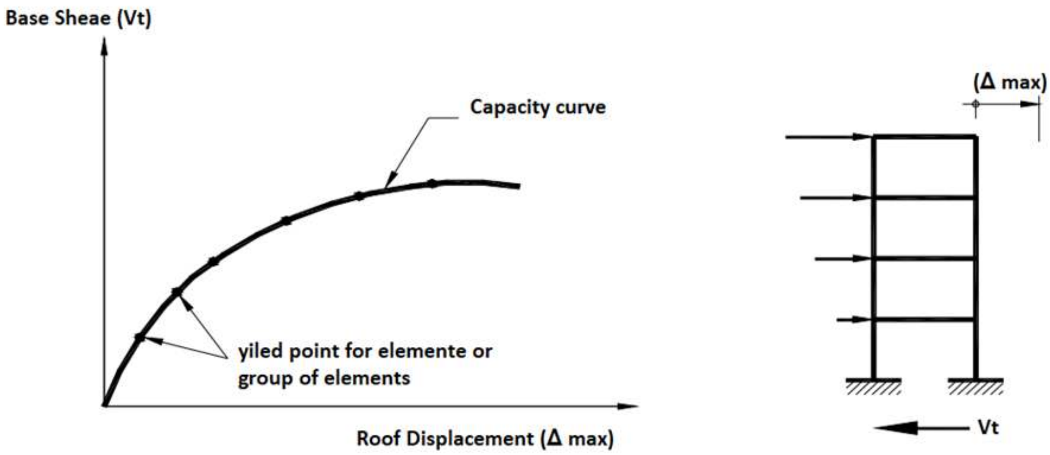

Figure 3.3 capacity curve (Özer, 2009)

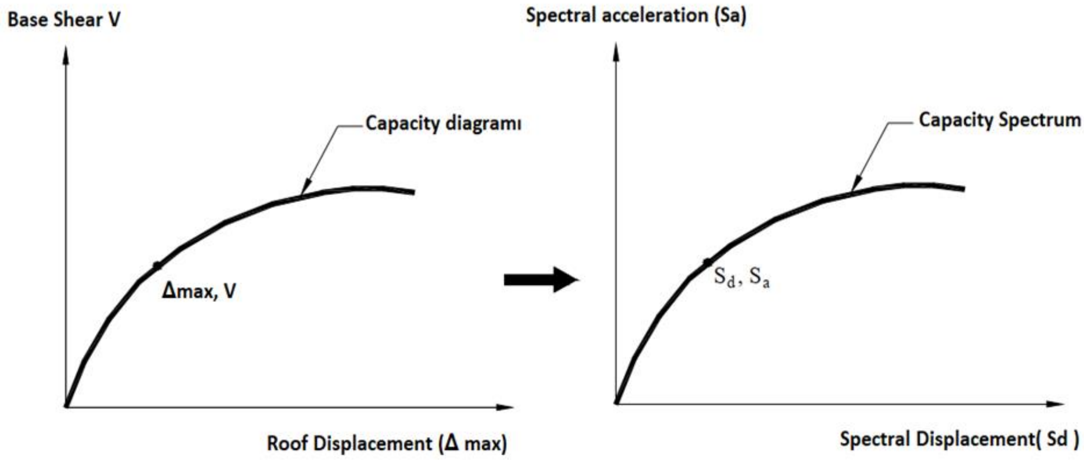

Figure 3.4 Converting the capacity curve to the capacity spectrum (Özer, 2009)

3.1.5 Conversion of the demand curve to the demand spectrum

General, Figure 3.5 represents the elastic spectrum of seismic, where the horizontal axis represents the period of the structure with a single degree of freedom and the vertical axis represents the peak of the absolute acceleration that is supposed to occur (Özuygün, 2004).

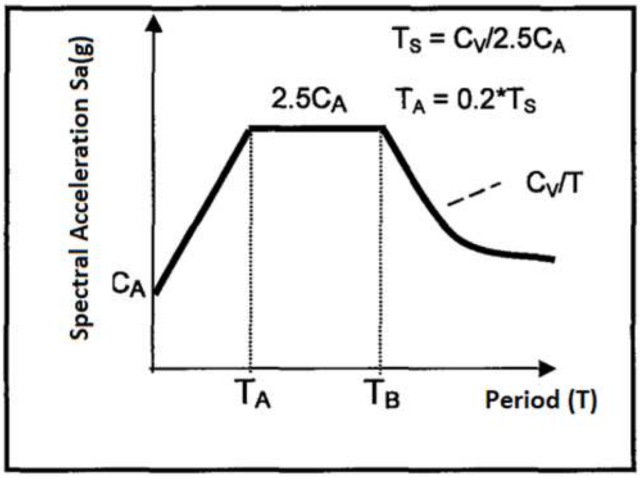

Figure 3.5 Elastic response spectrum (ATC- 40)

CA and Cv are seismic coefficients, check tables 4-7, 4-8, these tables are available in (ATC-40, 1996). For the sake of showing the demand spectrum and the capacity spectrum on the same axis; in the elastic demand spectrum, the acceleration spectrum must be converted to a displacement spectrum by using this equation:

$$S_d = \frac{1}{4\pi^2} S_a . T^2 \qquad (3.5)$$

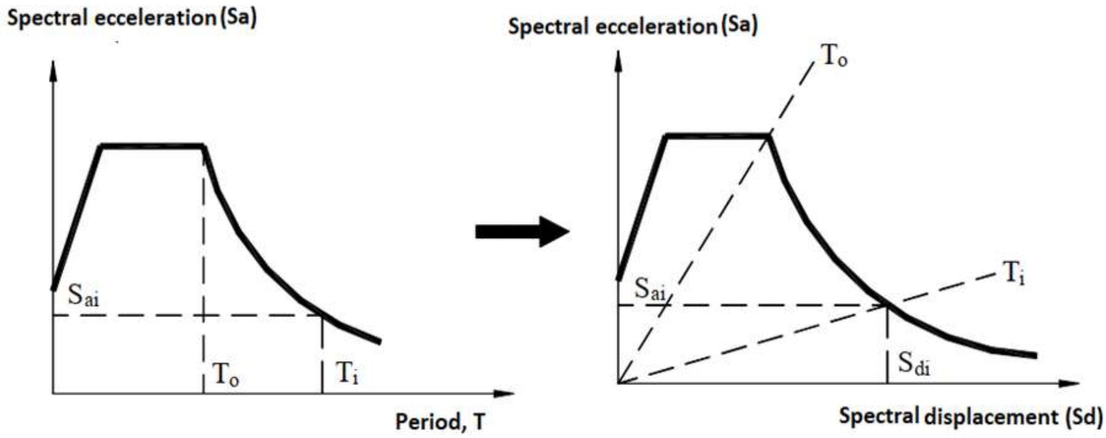

Figure3.6 Conversion Elastic Demand Spectrum (Özer, 2009)

3.1.6 Reducing the demand spectrum

The elastic demand spectrum should be reduced by increasing the damping ratio, as the damping ratio increases due to the occurrence of nonlinear deformations under the influence of earthquakes.

‘The effective damping ratio is the ratio of the sum of hysterical and viscous damping to the critical damping. Hysteretic damping is related to the area of hysteresis including the capacity spectrum and can be expressed in terms of equivalent viscous damping.' (Özer, 2009).

If the capacity spectrum is idealized effective damping ratio is defined as:

$B_{eq} = \kappa\beta_0 + 5 = \frac{63,7k(a_y d_{pi} - d_y a_{pi})}{a_y d_{pi}} + 5$

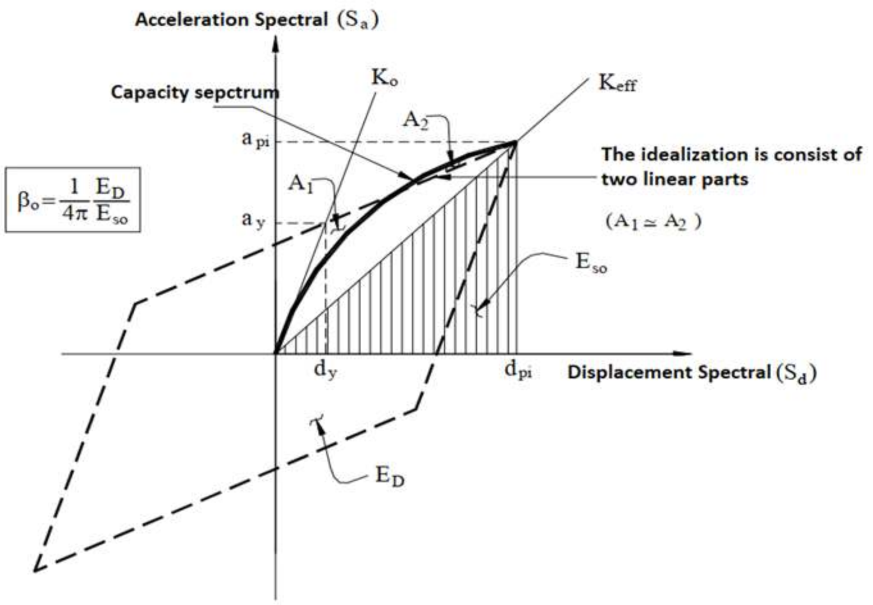

Figure 3.7 Converting the capacity curve to the capacity spectrum (Özer, 2009)

As shown in the Figure 3.7, the performance point must be known or guessed to calculate the effective damping ratio.

By using these coefficients, the demand spectrum will be reduced.

$SR_A \approx \frac{3.21-0.68\ln(\beta_{eq})}{2.12} \geq SR_A$,min =0.33 – 0.65 (3.6)

$SR_V \approx \frac{3.21-0.68\ln(\beta_{eq})}{2.12} \geq SR_V$,min =0.50 – 0.67 (3.7)

Where the minimum permissible values are in table 8-2 in ATC40

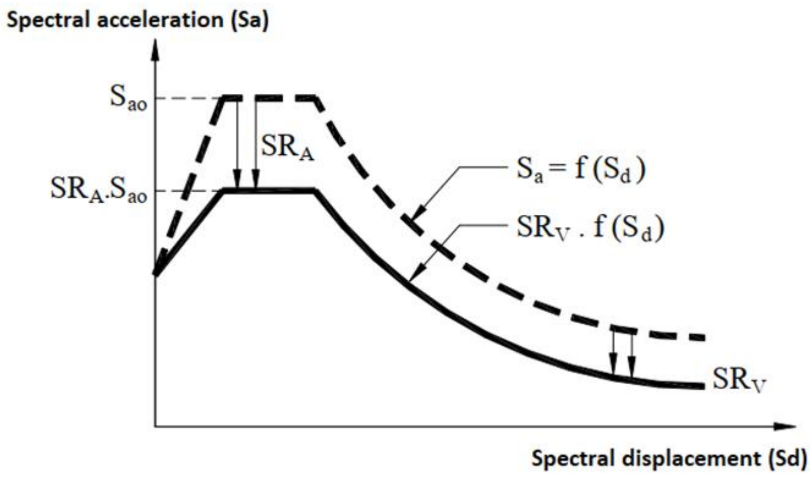

Figure3.8 Reduced demand spectrum (Özer, 2009)

3.1.7 Performance point

The performance point is the point of intersection of the capacity spectrum with the demand spectrum. To obtain a performance point, a specific sequential approach is followed. The performance point is obtained when the assumed point, in the beginning, is equal to or close enough to the resulting point of the calculations, then this approach is terminated.

‘‘After founding the performance point, the performance target must be verified whether it has been achieved or not. And that is by comparing the plastic deformations and displacement that occur at the performance point with their limit values. To achieve the expected performance level under the influence of a certain earthquake, upper limits are given to damage levels of structural or non-structural.’’ (Özer, 2009).

3.2 Performance Analysis According to TSC2018

3.2.1 Performance level for buildings according to TSC 2018

The following performance levels have been defined in TSC2018 code.

- Continuous Use (KK):

At this level of performance, there is no damage to the structural elements, and if the damage occurs, this damage can be neglected.

- Limited Damage (SH):

At this level, the damage is limited to structural elements where the nonlinear behavior is limited.

- Controlled Damage (KH):

At this level, the damage is not very large in the structural elements and can be repaired. In other words, this level is the safety live level.

- Collapse prevention (GÖ):

This level corresponds to a situation before the collapse of the structure, where significant damage occurs to the structural elements and is prevented from the complete collapse of the structure.

3.2.2 Building performance target (TSC2018)

Performance targets in TSC2018 depending on earthquake ground motion levels and earthquake design classes are given in Table 3.4 and Table 3.5. Further, the performance targets can be selected at the request of the building owner. Performance targets are prepared for existing reinforced concrete structures are given in Table 3.1. (TSC2018).

Table 3.1 Existing concrete, Precast Concrete, and Precast steel buildings (Except high building –BYS ≥ 2) (TSC2018)

S	DTS= 1, 2, 3, 3a, 4, 4a		DTS= 1a, 2a	
	Normal Performance Target	Evaluation/ Design Approach	Advanced Performance target	Evaluation/ Design Approach
DD-3	–	–	SH	ŞGDY
DD-2	KH	ŞGDT	–	–
DD-1	–	–	KH	ŞGDT

3.2.3 Determination of seismic performance of the existing building

Limited damage performance level in existing buildings:

It is the performance level where the damage to the structural elements of the building is at a minimum level and the structural elements maintain their strength. At this performance level, at most 20% of the beams in any storey of reinforced concrete buildings can pass into the Significant Damage Zone. But all other load-bearing elements must be in the Limited Damage Zone. If there is a brittle damaged element at this performance level, it must be retrofitted.

Controlled damage performance level in existing buildings:

It is the performance level in which some of the building carrier system elements are damaged, but these elements do not completely lose their horizontal rigidity and strength. In other words, it is the situation where there is no local and total collapse in the building. The criteria determined for this performance level in TSC2018 are presented below.

(a) In any storey of reinforced concrete buildings, as a result of the applied calculation made for each earthquake direction a maximum of 35% of the beams and vertical elements (columns, shears, and reinforced partition wall, excluding secondary beams) may pass into the Advanced Damage Zone as defined in paragraph (b) below.

(b) The total contribution of the vertical members in the Advanced Damage Zone to the shear force carried by the vertical members at each floor should be less than 20%. The ratio of the sum of the shear forces of the vertical elements in the Advanced Damage Zone on the top floor to the sum of the shear forces of all the vertical elements on that floor can be at most 40%.

(c) All other bearing elements are in the Limited Damage Zone, Significant Damage Zone, or Advanced Damage Zone. However, the ratio of the shear forces carried by the vertical elements of which the Significant Damage Limit is exceeded in both the lower and the upper sections of any floor to the shear force carried by all the vertical elements on that floor should not exceed 30%.

Collapse prevention performance level in existing buildings:

It is the performance level in which a significant part of the building carrier system elements is damaged and these elements lose their horizontal rigidity and strength significantly. It should be considered that these elements are damaged because the brittle at this performance level is in the Failure Zone. The criteria determined for this performance level in TSC2018 are presented below.

a) In any floor of reinforced concrete buildings, in consequence of the applied, calculations made for each earthquake direction, except for the secondary beams, a maximum of 20% of the beams may pass into the Collapse Zone.

b) The other elements are all in the Limited Damage Zone, Significant Damage Zone, or Advanced Damage Zone. However, the ratio of the shear forces carried by the vertical elements of which the Significant Damage Limit is exceeded in both the lower and upper sections of any floor should not exceed 30%.

c) The use of the building in its current state is dangerous and life-threatening.

Collapse Performance Level in Existing Buildings

It is the performance level in which the structural elements of the building reach the collapse state under the effect of the applied earthquake. If the building cannot stay at the collapse prevention Performance Level, it is in the State of Failure. In this case, occupying the building is life-threatening.

3.2.4 Damage limits and damage zone in structural elements (element level)

3.2.4.1 Damage limits for sections

In TSC2018 Three damage states and damage limits were defined for ductile sections. They are Limited Damage (SH), Controlled Damage (KH), and Collapse Prevention Damage (GÖ) and their limit values [TSC2018].

1. Limited Damage (SH): It can be defined as a limited amount of inelastic behavior in the relevant section.

2. Controlled Damage (KH): Inelastic behavior in which the section strength can be achieved safely.

3. Collapse Prevention (GÖ): It can be defined as an advanced level of inelastic behavior in the section. This classification does not apply to cross-sections of brittle damaged elements.

3.2.4.2 Damage zones for reinforced concrete cross-sections

Elements whose critical sections do not reach SH are located in the Limited Damage Zone. The elements between SH and KH are in the Significant Damage Zone, and the elements between KH and GÖ are in the Advanced Damage Zone. Eventually, the elements exceeding GÖ are in the Failure Zone. The representation of damage zones in TSC-2018

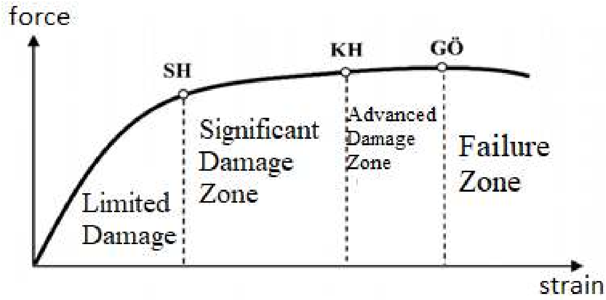

Figure 3.9 Damage zones for sections

3.2.5 Identification of section and element damage

The internal forces or deformations of the structural system elements are calculated with linear or non-linear calculation methods defined by TSC2018. By all means, the deformations are decided in which damage zone the sections are. The damage of the element will be determined according to the most damaged section.

3.2.6 Allowed strain limits and plastic rotation for reinforced concrete building elements

Strain and rotation limits are given in Table 3.2 and Table 3.3.

Table 3.2 Performance level for the strain of the beams, columns, and walls to TSC 2018

Section Damage Limits	Concrete strain	Steel strain
Limited Damage (SH)	$(\varepsilon_c)SH=0.0025$	$(\varepsilon_s)SH=0.0075$
Controlled Damage (KH)	$(\varepsilon_c)KH=0.75(\varepsilon c)GÖ$	$(\varepsilon_s)KH=0.75(\varepsilon s)GÖ$
Collapse Prevention (GÖ)	$(\varepsilon_c)GÖ=0.0035+0.04(\omega_{we})$^0.5≤0.018	$(\varepsilon_s)GÖ=0.4\varepsilon su$

Table 3.3 Performance level for plastic rotation of the beams, columns, and walls to TSC 2018

Section Damage Limits	Plastic rotation
Limited Damage (SH)	$\Theta_p^{(SH)} = 0$
Controlled Damage (KH)	$\Theta_p^{(KH)} = 0.75\ \Theta_p^{(KH)}$
Collapse Prevention (GÖ)	$\Theta_p^{(GÖ)} = \frac{2}{5}\ [(\emptyset_U - \emptyset_y]L_P\ \left(1 - 0.5\frac{L_P}{L_S}\right) + 4.5\emptyset_U\ d_b]$

3.2.7 Nonlinear modeling

We need a non-linear analysis to determine the realistic behavior of the building during an earthquake. Nonlinear analysis can be done with three different methods. These methods are respectively; They are single modal pushover analysis, multimodal pushover analysis, and nonlinear analysis in time history.

The single modal pushover analysis can be used for building that height class BYS ≥5. According to Table 3.3 mentioned in TSC2018, multimodal pushover analysis methods can be used for all buildings with BYS ≥2. Moreover, time history can be used for all buildings in the seismic calculation, above that, this method is mandatory for high-rise buildings (BYS=1).

3.2.8 Nonlinear material

In the evaluation according to deformations with Nonlinear Methods, the stress-strain relations have been defined for confined and unconfined concrete in the appendix "EK 5A" in TSC2018.

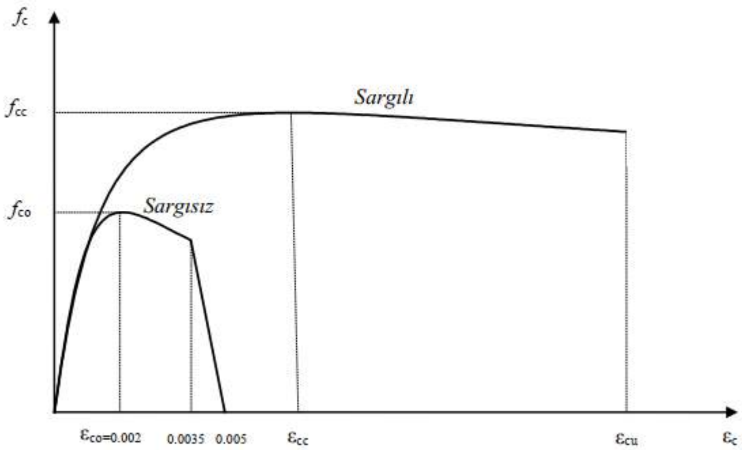

Figure 3.10 Stress-Strain relation for unconfined and confined concrete (TSC2018)

AS for reinforcement steel model, the stress-strain relations have been defined in the appendix "EK 5A" in TSC2018 as shown in Figure 3.11.

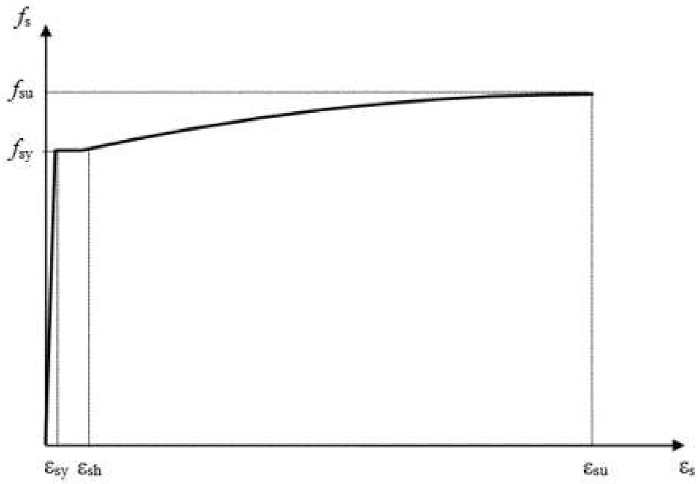

Figure 3.11 Stress-Strain relation for rebar reinforcement concrete (TSC2018)

Table 3.4 Information about reinforcement steel (TSC 2018)

Type	f_{sy} (MPa)	ε_{sy}	ε_{sh}	ε_{su}	f_{su} / f_{sy}
S220	220	0.0011	0.011	0.12	1.20
S420	420	0.0021	0.008	0.08	1.15 – 1.35
B420C	420	0.0021	0.008	0.08	1.15 – 1.35
B500C	500	0.0025	0.008	0.08	1.15 – 1.35

3.2.9 Cracked elements

As mentioned in 4.5.5. in TSC2018 the effective section of the stiffness factors for in-plane and out-of-plane behavior of linearly modeled walls and slabs will be taken from Table 3.5. While columns, beams, tie beams, and walls modeled according to the stacked plastic behavior will be determined according to the mentioned hereafter Equation. However, in this study, the table values were used for all elements. The reason will be mentioned in the next chapters (Case Study).

$$(EI)_e = \frac{M_Y}{\theta_Y}\frac{L_S}{3} \tag{3.8}$$

$$\theta_y = \frac{\emptyset_y}{3} + 0.0015\eta\left(1 + 1.5\frac{h}{L_S}\right) + \frac{\emptyset_y\, d_b\, f_{ye}}{8\sqrt{f_{ce}}} \tag{3.9}$$

Table 3.5 Structural elements effective stiffness coefficients (TSC2018)

Reinforced concrete Element	Effective Section Stiffness Coefficient	
Shear Wall-Slab System (In-plane)	Axial	Shear (kayma)
Shear Wall	0.5	0.5
Basement shear Wall	0.8	0.5
Slab	0.25	0.25
Shear Wall-Slab(Out-of-plane)	Bending	Shear
Shear Wall	0.25	1.00
Basement Shear Wall	0.50	1.00
Slab	0.25	1.00
Bar Element	**Bending**	**Shear**
Transverse Beam	0.15	1.00
Frame Beam	0.35	1.00
Frame Column	0.7	1.00
Shear Wall (Mid-Peir)	0.50	0.50

3.2.10 Plastic hinge zone and length

The plastic hinges are placed in the beams and columns at the beginning and the end of each element. But for the shear walls, they are employed at the lower end of each floor as shown in paragraph 5.4.3.1.a of the TSC2018. The length of the plastic hinge is equal to half of the length sections in the effective direction) as mentioned in paragraph 5.3.1.2 in TSC2018.

3.2.11 Earthquake ground movement levels

In the new seismic code TSC2018, four different earthquake ground motion levels are defined as given in the design of buildings under the influence of earthquakes: **Earthquake ground motion level-1 (DD-1):** The probability of exceeding the spectral magnitudes in 50 years is 2% and the corresponding recurrence period is assumed to be 2475 years. Infrequent earthquake refers to ground motion. DD-1. The largest earthquake considered is also called ground motion (TSC2018).

Earthquake ground motion level-2(DD-2): It expresses the sparse earthquake ground motion where the probability of exceeding the spectral magnitudes in 50 years is 10% and the corresponding recurrence period is assumed to be 475 years. DD-2 is also called standard design earthquake ground motion. (TSC2018).

Earthquake ground motion level-3(DD-3): Expresses frequent earthquake ground motions where the probability of exceeding the spectral magnitudes in 50 years is 50% and the corresponding recurrence period is 72 years. (TSC2018).

Earthquake ground motion level-4(DD-4): Spectral magnitudes It refers to very frequent earthquake ground motions, where the probability of exceedance is assumed to be 68% in 50 years (50% of probability of exceedance in 30 years) and the corresponding recurrence period of 43 years. DD-4 is also called service earthquake ground motion (TSC2018).

3.2.12 Standard earthquake ground motion spectra:

Earthquake ground motion spectra are defined either in standard form for a 5% damping ratio or by site-specific earthquake hazard analysis based on map spectral acceleration coefficients and local ground effect coefficients.

3.2.13 Map spectral acceleration coefficients

In the regulation, they are defined as non-dimensional coefficients, and they are the outcome of dividing the map spectral acceleration values for the 5% damping ratio by the gravity acceleration value. Taking into account that [(V)30 =760 m/s] the reference soil condition for a given earthquake motion level, which corresponds to the geometric average of the earthquake, effects in two perpendicular horizontal directions:

a) Short period map spectral acceleration coefficient S_s.
b) Map spectral acceleration coefficient Si for 1 second period.

3.2.14 Local ground effect coefficients

Depending on the local soil classes as defined in Table 3.6. the local soil effect coefficients Fs and F1 are given in Table 3.7. and Table 3.8, respectively. Linear interpolation can be made for the intermediate values of the map spectral acceleration coefficients in the tables (paragraph 2.3.3.1 in TSC2018).

Table 3.6 Soil class (TSC2018)

Local Soil Class	Soil Type	Average at the top 30 meters		
		(Vs)30 [m/s]	(N 60)30 [darbe/30 cm]	(Cu)30 [kPa]
ZA	Soild, hard rocks	>1500	_	_
ZB	Less, moderately strong rocks	760- 1500	_	_
ZC	Very hard stand, gravel and hard clay layers, weak rocks with many cracks	360 – 760	>50	>250
ZD	Meduim dense or dense sand, gravel or very solid clay	180 - 360	15-50	70 - 250
ZE	Loose sand, gravel, or soft to solid clay layers or profiles with a total thickness of more than 3 meters of soft clay layer ($C_u <$ 25 kPa) satsifying PI > 20 and w > %40	< 180	< 15	< 70
ZF	Soils that require site-specific investigation and evaluation: 1) Soils that have the risk of collapse and potential collapse under the influence of earthquakes (liquefiable soils, highly sensitive clays, collapsible weak cement soils, etc.), 2) Peat and/or organic content with a total thickness of more than 3 meters high clays, 3) High plasticity (PI>50) clays with a total thickness of more than 8 meters, 4) Very thick (> 35 m) soft or medium solid clays.			

Table 3.7 Local soil effect coefficients for short period (TSC2018)

Local Soil Category	Local soil effect coefficients for short period F_s					
	$S \leq 0.25$	$S = 0.50$	$S = 0.75$	$S = 1.00$	$S = 1.25$	$S \geq 1.50$
ZA	0.8	0.8	0.8	0.8	0.8	0.8
ZB	0.9	0.9	0.9	0.9	0.9	0.9
ZC	1.3	1.3	1.2	1.2	1.2	1.2
ZD	1.6	1.4	1.2	1.1	1.0	1.0
ZE	2.4	1.7	1.3	1.1	0.9	0.8
ZF	Special soil behavior analysis will be done					

Table 3.8 Local soil effect coefficients for 1. second period (TSC2018)

Local Soil Category	Local soil effect coefficients for 1.second period F_1					
	$S \leq 0.10$	$S = 0.20$	$S = 0.3$	$S = 0.4$	$S = 0.5$	$S \geq 0.6$
ZA	0.8	0.8	0.8	0.8	0.8	0.8
ZB	0.8	0.8	0.8	0.8	0.8	0.8
ZC	1.5	1.5	1.5	1.5	1.5	1.4
ZD	2.4	2.2	2.0	1.9	1.8	1.7
ZE	2.4	3.3	2.8	2.4	2.2	2.0
ZF	Special soil behavior analysis will be done					

The map spectral acceleration coefficients S_S and S_1, are converted to the local ground effect coefficients Fs and F1. And the design spectral acceleration coefficients S_{DS} and S_{D1}, as given in Equation 3.10. Horizontal and vertical elastic design spectra are defined using the design spectral acceleration coefficients obtained by Equation (3.10).

$S_{DS} = S_s F_s$ (3.10)

$S_{D1} = S_1 F_1$ (3.11)

3.2.15 Horizontal elastic design spectrum

The horizontal elastic design acceleration $S_e(T)$ is the ordinates of the horizontal elastic design acceleration spectrum for any earthquake ground motion level under consideration. The horizontal elastic design acceleration is defined in Equation (3.12), (3.13), (3,14), and (3.15) in terms of gravity acceleration [g] depending on the natural vibration period. Corner periods T_A and T_B are given depending on S_{DS} and S_{D1}. The horizontal elastic design spectrum graph depending on the limit values (T_A, T_B, and T_L) given in Equation 3.16 is given in Figure 3.12.

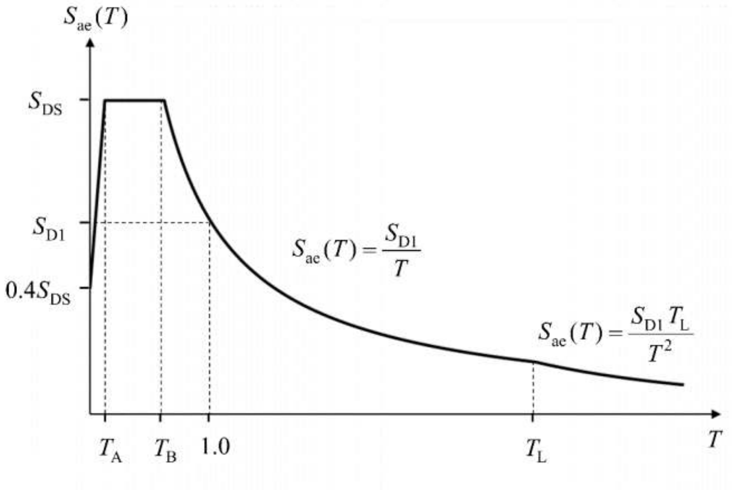

Figure 3.12 Horizontal elastic design spectrum (TSC2018)

$$S_{ae}(T) = (0.4 + 0.6\frac{T}{T_A})S_{DS} \qquad 0 \leq T \leq T_A \qquad (3.12)$$

$$S_{ae}(T) = S_{DS} \qquad T_A \leq T \leq T_B \qquad (3.13)$$

$$S_{ae}(T) = \frac{S_{D1}}{T} \qquad T_B \leq T \leq T_L \qquad (3.14)$$

$$S_{ae}(T) = \frac{S_{D1x}T_L}{T^2} \qquad T_L \leq T \qquad (3.15)$$

$$T_A = 0.2\,\frac{S_{D1}}{S_{DS}}\,;\; T_B = \frac{S_{D1}}{S_{DS}} \qquad (3.16)$$

3.2.16 Vertical elastic design spectrum

The vertical elastic spectral acceleration S(T) is the ordinates of the vertical elastic design acceleration spectrum for any earthquake ground motion level under consideration. The vertical elastic spectral acceleration is in gravity (g] depending on the short period design spectral acceleration coefficient defined for horizontal earthquake ground motion and the natural vibration period. It is defined in Equation 3.4. The vertical elastic design spectrum graph depending on the limit values (T_{AD}, T_{BD}, and T_{LD}) given in Equation 3.20 is given in Figure 3.13.

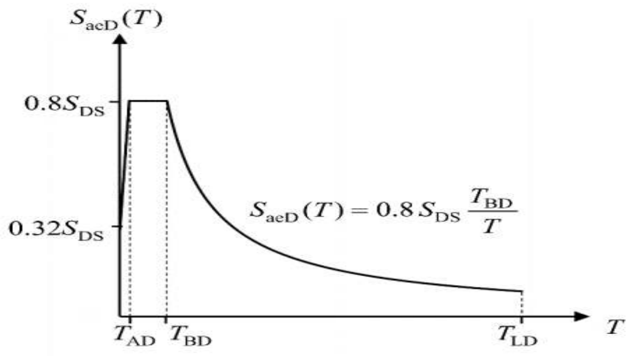

Figure 3.13 Vertical elastic design spectrum (TSC2018)

$S_{ae}(T) = (0.32 + 0.48\frac{T}{T_{AD}})S_{DS}$ $\quad 0 \leq T \leq T_{AD}$- (3.17)

$S_{ae}(T) = 0.8\,S_{DS}$ $\quad T_{AD} \leq T \leq T_{BD}$ (3.18)

$S_{ae}(T) =(0.8\,S_{DS}\frac{T_{BD}}{T})$ $\quad T_{BD} \leq T \leq T_{LD}$ (3.19)

$T_{AD} = \frac{T_A}{3}; \quad T_B = \frac{T_B}{3}; \quad T_{LD} = \frac{T_L}{3}$ (3.20)

3.3 Performance Analysis According to the EC8

The perfoemance analysis according to the EC8 has been explained in the following sections.

3.3.1 Ground type

"Ground types A, B, C, D, and E described by the stratigraphic profiles and parameters given in Table 3.9 and described hereafter, may be used to account for the influence of local ground conditions on the seismic action" (Eurocode 8, 2004).

Table 3.9 Ground type (EC8)

Ground type	Description of stratigraphic profile	Parameters		
		$v_{s,30}$ (m/s)	N_{SPT} (blows/30cm)	c_u (kPa)
A	Rock or other rock-like geological formation, including at most 5 m of weaker material at the surface.	> 800	_	_
B	Deposits of very dense sand, gravel, or very stiff clay, at least several tens of metres in thickness, characterised by a gradual increase of mechanical properties with depth.	360 – 800	> 50	> 250
C	Deep deposits of dense or medium-dense sand, gravel or stiff clay with thickness from several tens to many hundreds of metres.	180 – 360	15 - 50	70 - 250
D	Deposits of loose-to-medium cohesionless soil (with or without some soft cohesive layers), or of predominantly soft-to-firm cohesive soil.	< 180	< 15	< 70
E	A soil profile consisting of a surface alluvium layer with v_s values of type C or D and thickness varying between about 5 m and 20 m, underlain by stiffer material with v_s > 800 m/s.			
S_1	Deposits consisting, or containing a layer at least 10 m thick, of soft clays/silts with a high plasticity index (PI > 40) and high water content	< 100 (indicative)	_	10 - 20
S_2	Deposits of liquefiable soils, of sensitive clays, or any other soil profile not included in types A – E or S_1			

3.3.2 Elastic response spectrum:

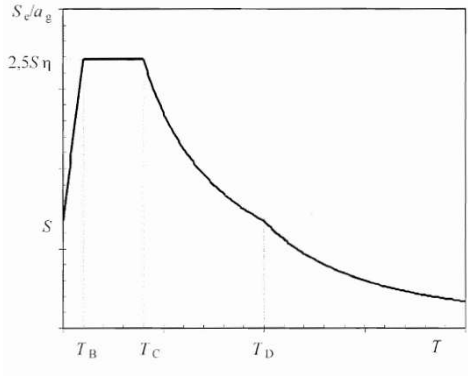

Figure 3.14 Shape of the elastic response spectrum (TSC 2018)

$0 \leq T \leq T_B$: $S_e(T) = a_g \cdot S \cdot [1+\frac{T}{T_B} \cdot (\eta . 2.5 - 1)]$ (3.21)

$T_B \leq T \leq T_C$: $S_e(T) = a_g \cdot S \cdot \eta . 2.5$ (3.22)

$T_C \leq T \leq T_D$: $S_e(T) = a_g \cdot S \cdot \eta . 2.5 . [\frac{T_C}{T}]$ (3.23)

$T_D \leq T \leq 4s$: $S_e(T) = a_g \cdot S \cdot \eta . 2.5[\frac{T_C T_D}{T^2}]$ (3.24)

Where $S_e(T)$: the elastic response spectrum, T: the vibration period T_B and T_C : the lower, upper limit of the period. S : soil factor.

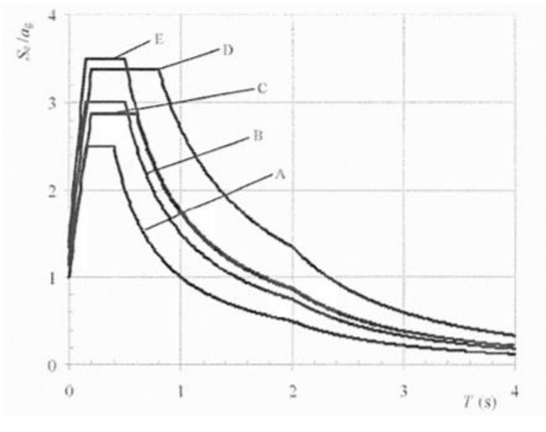

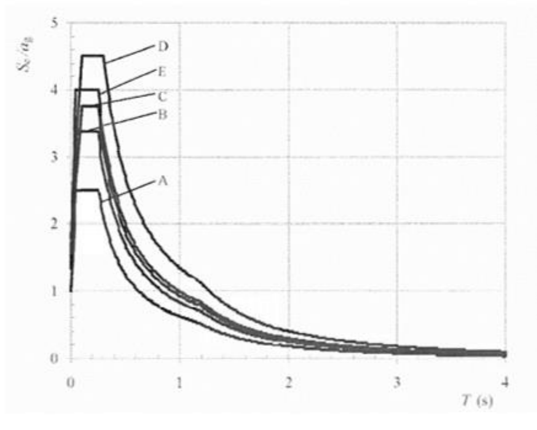

Figure 3.15 Type 1 elastic response spectra (TSC2018) Figure 3.16 Type 2 elastic response spectra (2018)

The type of 1 elastic response spectrum if large magnitude M > 5.5Hz

Table 3.10 elastic response spectra (Type1, Type2) parameters

	Elastic response spectra (Type 1)				Elastic response spectra (Type 2)			
Ground type	S	TB (s)	TC (s)	TD (s)	S	TB (s)	TC (s)	TD (s)
A	1.0	0.15	0.4	2.0	1.0	0.05	0.25	1.2
B	1.2	0.15	0.5	2.0	1.35	0.05	0.25	1.2
C	1.15	0.20	0.6	2.0	1.5	0.10	0.25	1.2
D	1.35	0.20	0.8	2.0	1.8	0.10	0.30	1.2
E	1.4	0.15	0.5	2.0	1.6	0.05	0.25	1.2

3.3.3 Nonlinear methods in Eurocode 2004

There are two methods for the nonlinear analysis according to the EC8, pushover analysis (static) and time-history analysis (dynamic).

3.3.4 Cracked elements

Because of the large number of elements, it is not practical to take the stiffness of each element equal $M_Y L_V/3\theta y$ at the two ends of the element in the SAP2000. The cracked elements took one-half of the corresponding stiffness of the uncracked elements as mentioned at EN1998-1-1, c1.4.3.1(7).

3.3.5 Plastic hinge zone and length

According to Eurocode 2004 Plastic hinges are usually fixed at the beginning and the end of the columns and beams and in the critical region of the shear walls (at the base). But in this study, plastic hinges were fixed at the base of each floor of the shear walls, due to the height of Turkish buildings, which are higher compared to European buildings.

There are two equations for calculating the length of the plastic hinge depending on the method used to obtain the ultimate curvature. (EN1998-1-1,c3.A3.2.2.(7&8)).

$$L_{p1} = 0.1\, L_V + 0.17h + 0.24\frac{d_{bL}\, f_y\,(MPA)}{\sqrt{f_c\,(MPA)}} \quad \text{……………………} \quad (3.25)$$

$$L_{p1} = 0.1\,\frac{LV}{30} + 0.2h + 0.11\,\frac{d_{bL}\, f_y\,(MPA)}{\sqrt{f_c\,(MPA)}} \quad \text{……………….} \quad (3.26)$$

3.3.6. Performance level for building according to Eurocode2004

There are three limits state (LS) in the Eurocode, Damage Limitation (DL), Significant Damage (SD), and Near Collapse (NC).

Damage limitation (DL)

At this level, there is light damage in the structure, and almost there is no damage to the structural elements, therefore, the damage can be repaired in the non-structural elements, and it is economic.

Significant damage (SD)

At this level, there is significant damage to the structure. Non-structural elements fail to occur. Therefore, repairing the structure can be uneconomical.

Near collapse (NC)

At this level, there is heavy damage to the structural elements. Most of the non-structural elements are collapsed. Therefore the structure cannot survive anymore.

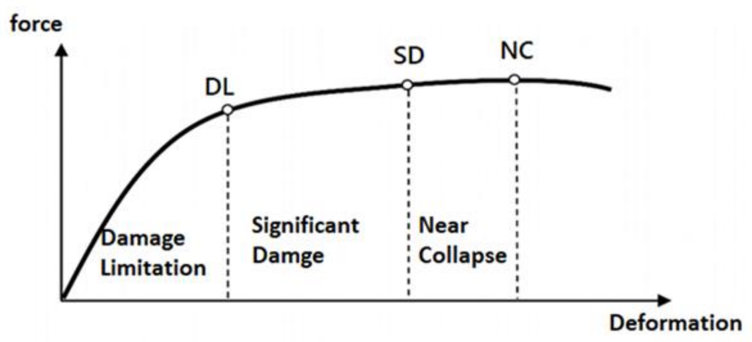

Figure 3.17 The Performance level of Eurocode 2004(modified from EC8)

Table 3.11 Limit state for elements to Eurocode 2004

Limit State (LS)(elastic+inelastic)			
Member	DL	SD	NC
Ductile primary (flexural)	$\Theta_{sd} \leq \Theta_y$	$\Theta_{sd} \leq 0.75\theta_{(um-\sigma)}$	$\Theta_{sd} \leq \theta_{(um-\sigma)}$
Ductile secondary (flexural)		$\Theta_{sd} \leq 0.75\ \theta_{(um)}$	$\Theta_{sd} \leq \theta_{(um)}$

Table 3.12 Performance level for plastic rotation of the elements (Eurocode 2004)

Limit State (LS) Plastic Part			
Member	DL	SD	NC
Ductile primary	0	$\Theta_{sd} \leq 0.75\theta^{p}_{um-\sigma}$	$\Theta_{sd} \leq \theta^{p}_{um-\sigma}$
Ductile secondary		$\Theta_{sd} \leq 0.75\ \theta^{p}_{um}$	$\Theta_{sd} \leq \theta^{p}_{um}$

For beam and column, the total chord rotation capacity (elastic plus inelastic part):

$$\theta_{(um)} = \frac{1}{\gamma_{el}}\ 0.016.(0.3^{v})[\frac{\max(0.01;\omega')}{\max(0.01;\omega)}\ f_c]\ \ (\min(9;\ \frac{L_v}{h}))^{0.35}\ \ 25^{\ (\alpha p_{sx}\frac{f_{yw}}{f_c})}\ \ (1.25^{100 p_d})$$

……………………………………………………………………….(3.27)

Where: γ_{el} = 1.5 for primary seismic elements and γ_{el} = 1 for secondary seismic elements.

For walls $\theta_{(um)}$= 0.58* $\theta_{(um)}$beam, column. (3.28)

For the plastic part of the chord rotation:

$$\theta^{p}_{um} = \frac{1}{\gamma_{el}}\ 0.0145.(0.25^{v})\left[\frac{\max(0.01;\omega')}{\max(0.01;\omega)}\right] f_c^{0.2}.\ \ (\min(9;\ \frac{L_v}{h}))^{0.35}\ 25^{\ (\alpha p_{sx}\frac{f_{yw}}{f_c})}\ \ (1.25^{100 p_d})$$

……………………………………………………………………….(3.29)

Where: γ_{el} = 1.8 for primary seismic elements and γ_{el} = 1 for secondary seismic elements

For walls, θ^{p}_{um} = 0.6* $\theta_{(um)}$beam, column. (3.30)

The chord rotation at yielding Θ_y:

For beam and column:

$$\Theta_y = \emptyset_y\frac{L_v+\alpha_v z}{3} + 0.0014(1 + 1.5\ \frac{h}{L_v}) + \frac{\varepsilon_y}{d-d'}\frac{d_{bL}\ f_y}{6\sqrt{f_c}} \qquad (3.31\ )$$

For walls of rectangular, T, or barbelled section:

$$\Theta_y = \emptyset_y\frac{L_v+\alpha_v z}{3} + 0.0013 + \frac{\varepsilon_y}{d-d'}\frac{d_{bL}\ f_y}{6\sqrt{f_c}} \qquad (3.32\ )$$

4. CASE STUDY

4.1 Pushover Analysis in SAP2000

This is an example frame of incremental pushover analysis to assess the performance of an existing reinforced concrete frame by using TSC2018 and EC8 with comparing the results. Here we aim to chek if we are doing the push-over analysis in a correct manner.

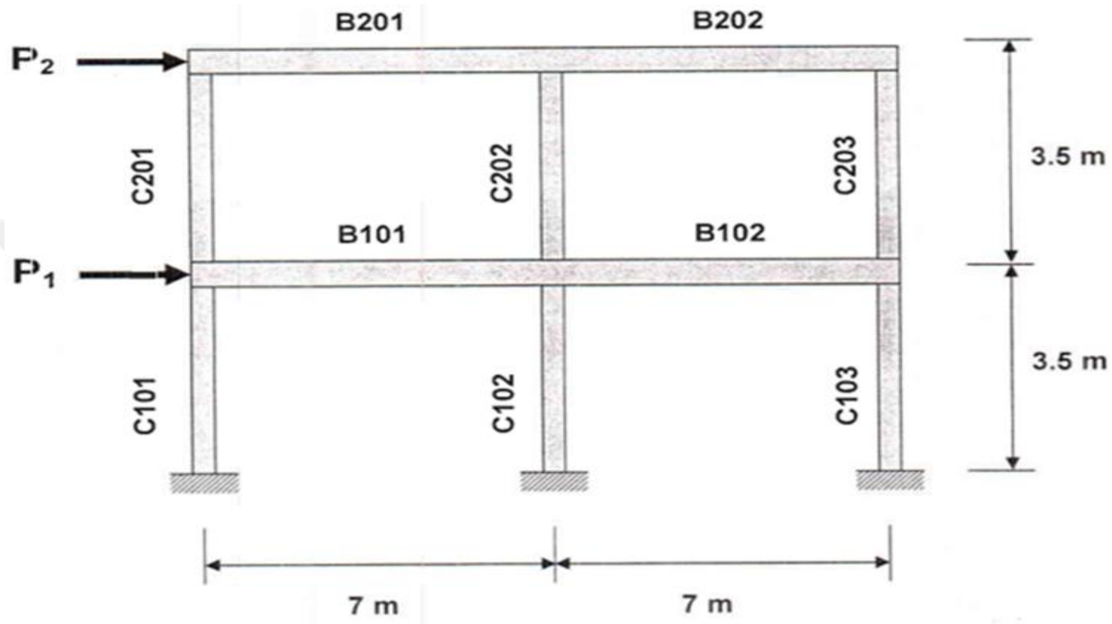

Figure 4.1 Frame Example

Table 4.1 Frame details

<table>
<tr><td rowspan="2">MATERIL</td><td colspan="2">Concrete: C2O</td></tr>
<tr><td colspan="2">Steel: S420</td></tr>
<tr><td rowspan="2">Loads</td><td colspan="2">Dead Load: G=20 KN</td></tr>
<tr><td colspan="2">Live Load: Q=10 KN</td></tr>
<tr><td>Gravity Loads</td><td colspan="2">Gravity = G+0.3Q</td></tr>
<tr><td rowspan="2">concrete cover</td><td colspan="2">Clear cover =20 mm</td></tr>
<tr><td colspan="2">Cover d'= 40 mm</td></tr>
<tr><td rowspan="2">Column Section
(450×450) mm</td><td colspan="2">Longitudinal = 8-Ø22</td></tr>
<tr><td colspan="2">Stirrups = Ø8/200 mm</td></tr>
<tr><td rowspan="2">Beam Section
(450×600) mm</td><td rowspan="2">Longitudinal =</td><td>3-Ø22 AT the top</td></tr>
<tr><td>3-Ø22 AT the Bottom</td></tr>
</table>

Table 4.1(Continue)

Beam Section (450×600) mm	Stirrups = Ø8/150 mm
Building importance coefficient	I=1
Building	Seismic zone =1
	Local soil class= Z2

4.1.1 By using TSC 2018

The data obtained from the TSC2018 is mentioned in Table 4.2.

Table 4.2 The data used in the analysis and taken from TSC 2018

The soil type	ZD	TSC2018.Tablo 16.1
The combination factor for live load	n=0.3	TSC2018. Table 4.3
Building Category	BKS=3	TSC2018. Table 3.1
The importance factor	I =1	TSC2018. Table 3.1
Seismic design class	DTS=1	TSC2018. Table 3.2
Building height class	BYS=8	TSC2018. Table 3.3
Behavior factor	R=8	TSC2018. Table 4.1
The strength increase factor	D=3	TSC2018. Table 4.1
The plastic hinge length	L_P=0.5H	TSC2018.5.3.1.2
Cracked column	0.7*stiffness	TSC2018. Table 4.1
Cracked beam	0.35* stiffness	TSC2018. Table 4.1
seismic coefficients	C_A=0.44	ATC-40 Table 4.7
seismic coefficients	C_V=0.64	ATC-40 Table 4.8
Nonlinear material	ε_{co} =0.002, ε_{cu}=0.005	TSC.Figure 5A.1
Nonlinear material	ε_{Sh} =0.008, ε_{su}=0.08	TSC.Table 5A.1

4.1.1.1 Obtaining data from the AFAD earthquake website

Figure 4.2 presents earthquake risks of different regions in Turkey.

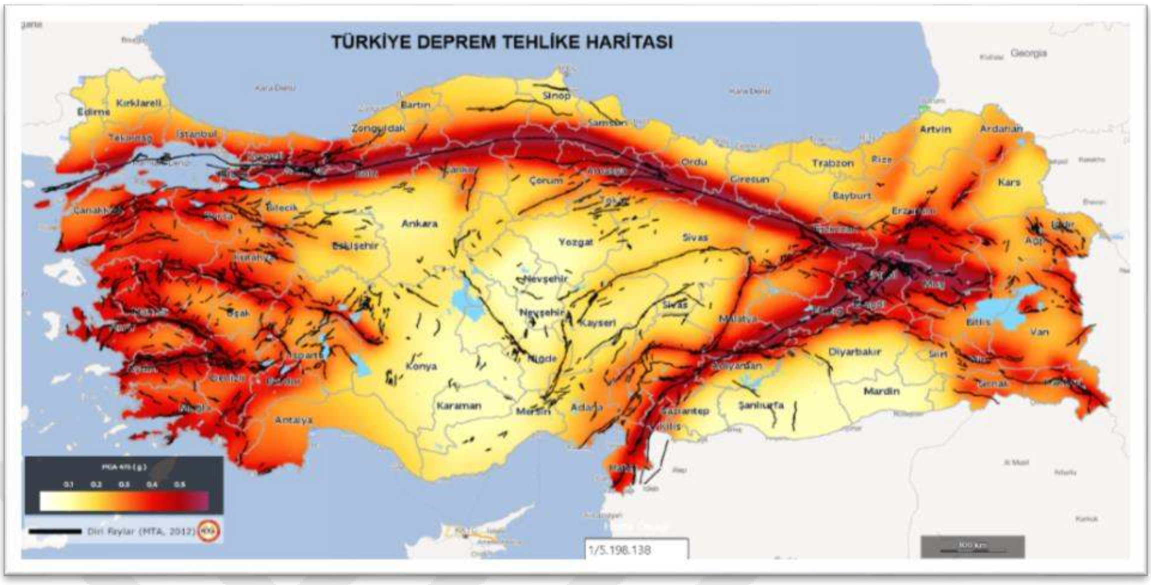

Figure 4.2 Turkey earthquake hazard map (AFAD website)

By using the seismic map on AFAD Website (Türkiye Deprem Tehlike Haritaları) and depending on the latitude, longitude, seismic zone, and soil type, the horizontal and vertical elastic spectrum was obtained.

.

Figure 4.3 Data entered in the AFAD website

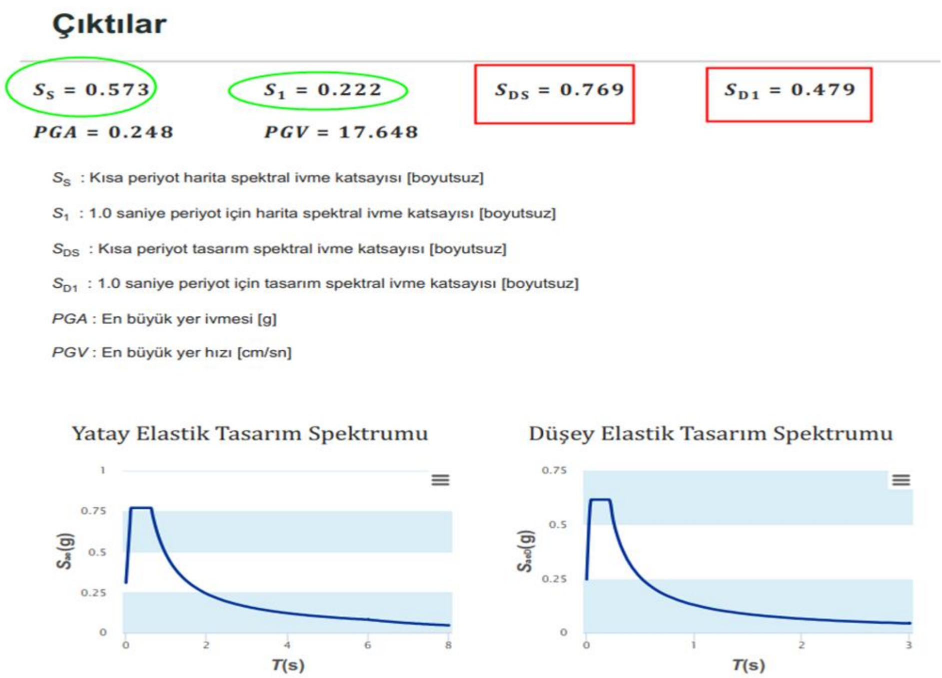

Figure 4.4 Outputs obtained from AFAD website

The values of S_{DS} and S_{D1} that are taken from the AFAD map, also important factors and soil classes are entered in the SAP2000 program.

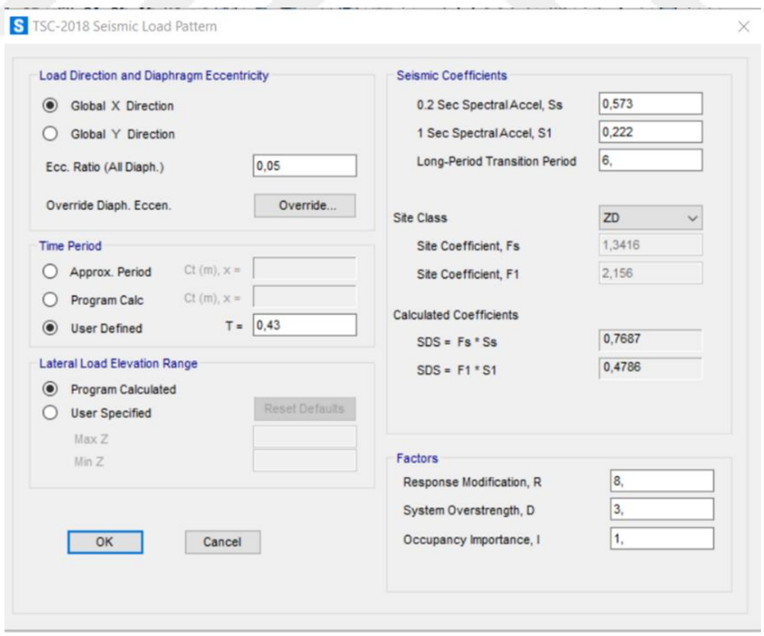

Figure 4.5 TSC-2018 seismic load pattern

4.1.1.2 Defining nonlinear material properties

C20 concrete class was used in modeling. Nonlinear material was defined in SAP2000 to be used in the plastic hinge moment calculation. After choosing the Mander model from “Stress Straing Curve Definition Options” The mander model data for unconfined concrete ε_{co} =0.002 and ε_{cu} =0.005 was entered in the “Parametric Strain Data” as shown in the Figure 4.6.

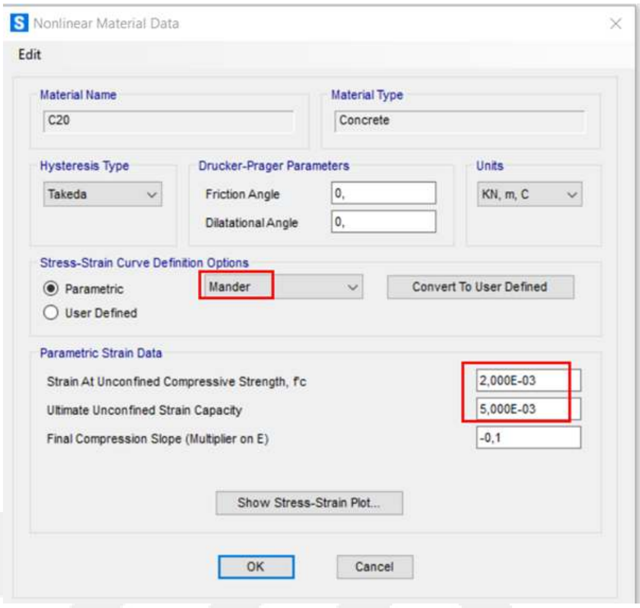

Figure 4.6 Nonlinear concrete data for TSC2018

Nonlinear material for reinforced concrete steel was defined in SAP2000 according to TSC2018. Where “Strain at Onest of Strain Hardening” is εco =0.008 and “Ultimate Strain Capacity” is εcu =0.08 for S420.

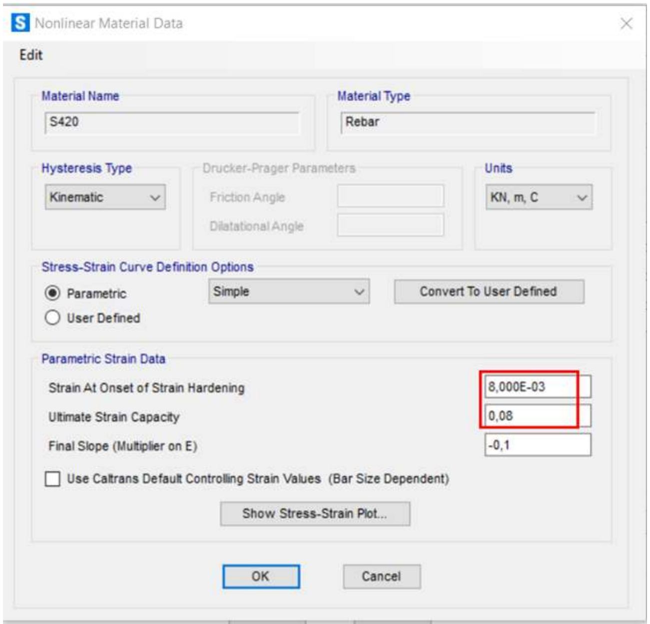

Figure 4.7 Nonlinear rebar data for TSC2018

4.1.1.3 Input cracked elements in SAP2000

The Effective section stiffness factors has been entered in SAP2000 for Column = 0.7 and Beam= 0.35

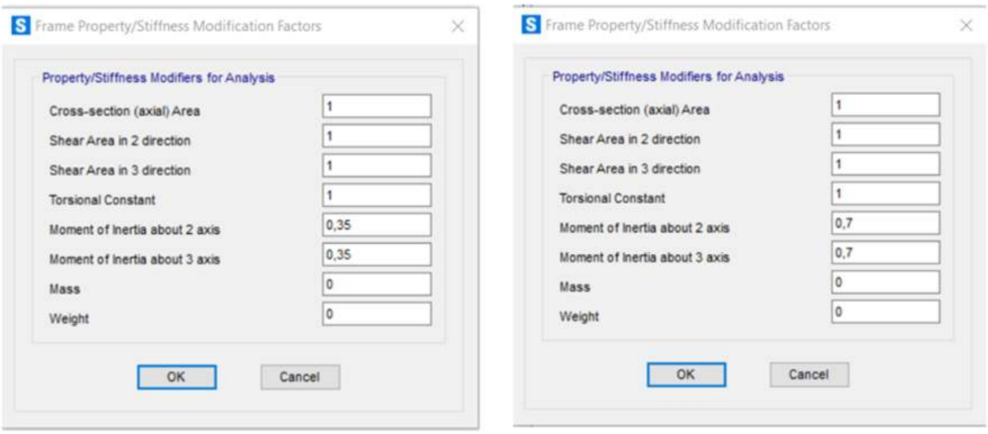

Figure 4.8 Stiffness modification factors

4.1.1.4 Moment-curvature and interaction surface in SAP2000

To calculate the moment-curvature and interaction surface of the element sections, the cross-sections for beam and column were created from the “Section Designer” menu in SAP2000. Figure 4.9 shows the calculation of moment-curvature for beam section (45-60) containing 3Ø22 rebar at the bottom and 3 Ø22 rebars at the top.

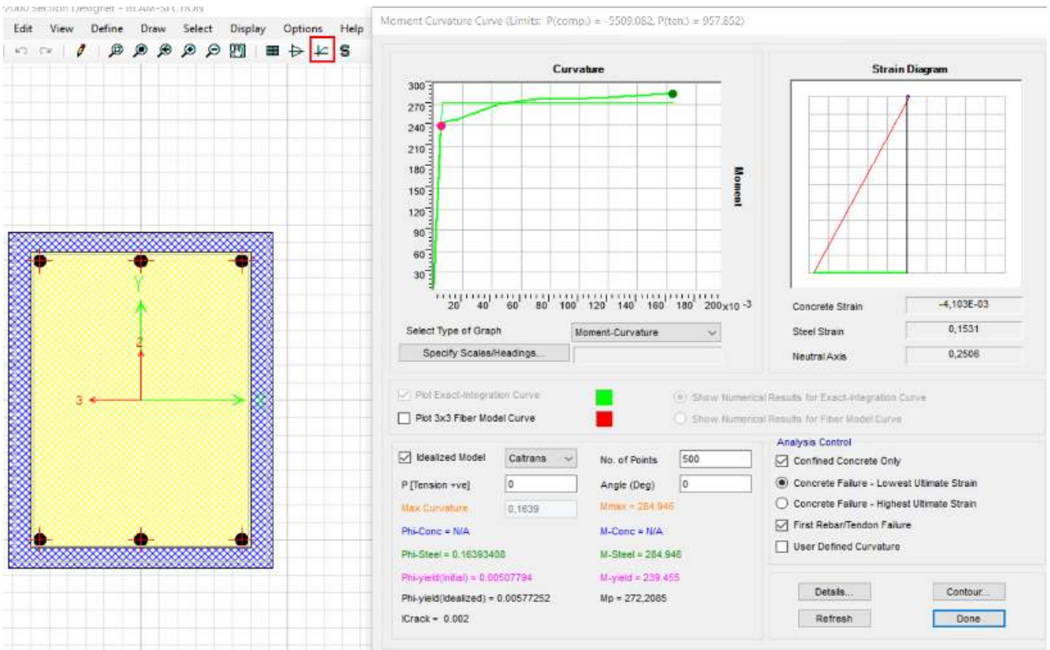

Figure 4.9 Modeling Section Beam and calculate moment-curvature

Figure 4.10 shows the calculation of moment-curvature for column section (450-450) containing 8Ø22 and axial load is P=345,5 KN. Interaction surface was also calculated for the column from the section design menu, where after defining the section, the interaction surface is obtained by clicking on the “Show Interaction Surface” button. There are 24 curves of different degrees. In this example, because the structure is a frame, one curve with angles 0 was taken for section.

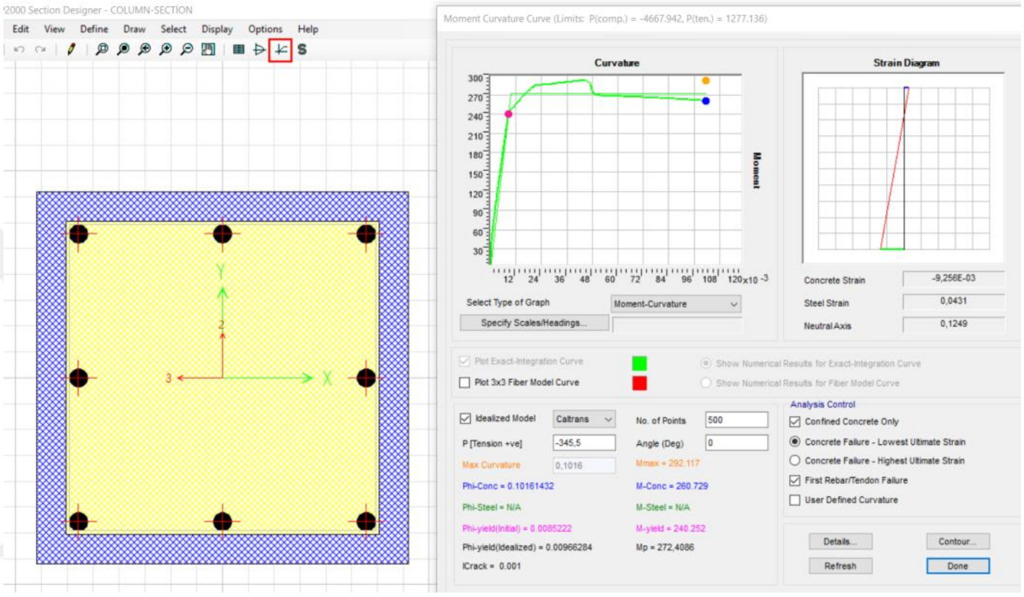

Figure 4.10 Modeling section column and calculate moment-curvature

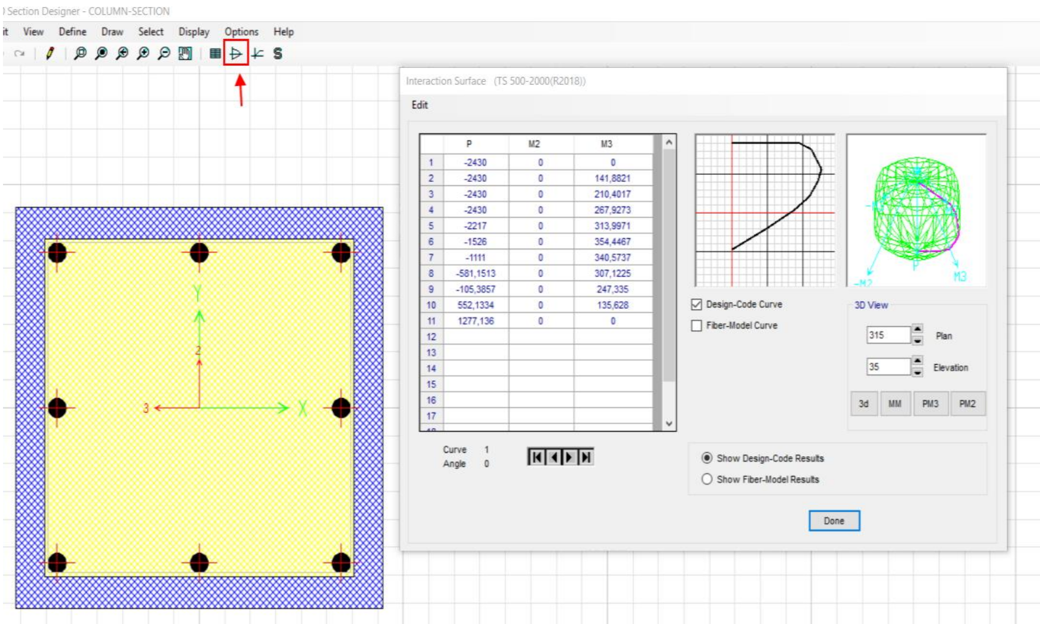

	P	M2	M3
1	-2430	0	0
2	-2430	0	141,8821
3	-2430	0	210,4017
4	-2430	0	267,9273
5	-2217	0	313,9971
6	-1526	0	354,4467
7	-1111	0	340,5737
8	-581,1513	0	307,1225
9	-105,3857	0	247,335
10	552,1334	0	135,628
11	1277,136	0	0
12			
13			
14			
15			
16			
17			

Figure 4.11 Interaction surface curve for a section column (angle= 0)

4.1.1.5 Calculating strain limits and plastic rotation for reinforced concrete building elements

The limits for beam and column were calculated according to TSC2018 as mentioned in the below tables 4.3, and 4.4.

Table 4.3 Performance level for the beam to TSC 2018

Beam				
Limate State	εc	εs	Θp	Θp/Θy
Limited Damage (SH)	0.0025	0.0075	0	0
Controlled Damage (KH)	0.00571	0.024	0.030876	20,58376
Collapse prevention (GÖ).	0.00762	0.032	0.041167	27,44501

Table 4.4 Performance level for the column to TSC 2018

Colmun			
Limate State	εc	εs	Θp
Limited Damage (SH)	0.0025	0.0075	0
Controlled Damage (KH)	0.00571	0.024	0.0147
Collapse prevention (GÖ).	0.00762	0.032	0.0196

4.1.1.6 Defined and assignments of plastic hinge for beam and column

The M3 type was used for beams hinge and P-M3 for column hinge. Determining the properties of the plastic hinge was needed to the moment-curvature that was previously calculated. Rotation is obtained by multiplying the curvature to the length of the plastic hinge.

Moments and rotation are included in the (Displacement Control Parameters) as shown in Figure 4.12 taking into account the scale factor for yield moment and yield rotation. The hinges rotation was taken from Table 4.5. to determine the performance levels for the beam, taking into account scale factors for yield rotation. and entered this data in the (Acceptance Criteria) as shown in Figure 4.12.

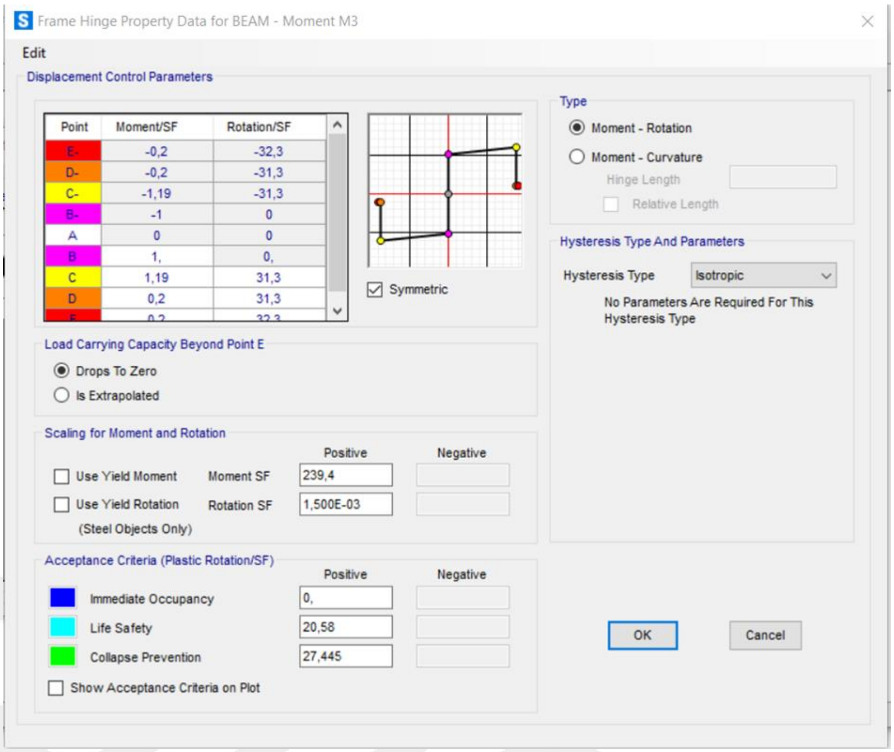

Figure 4.12 Frame hinge property data for beam

For column:

The P-M3 type was chosen, and the properties of the column hinge were defined in a similar way to beam, but by entering the axial force and considering scale factor = 1, as well as entering interaction curve data.

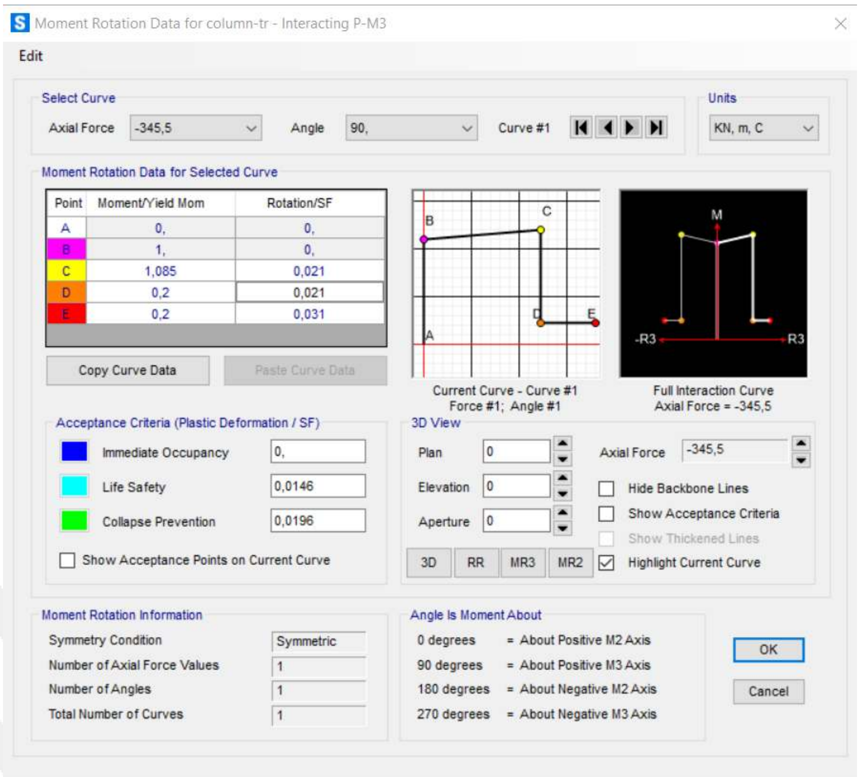

Figure 4.13 Moment rotation data for column

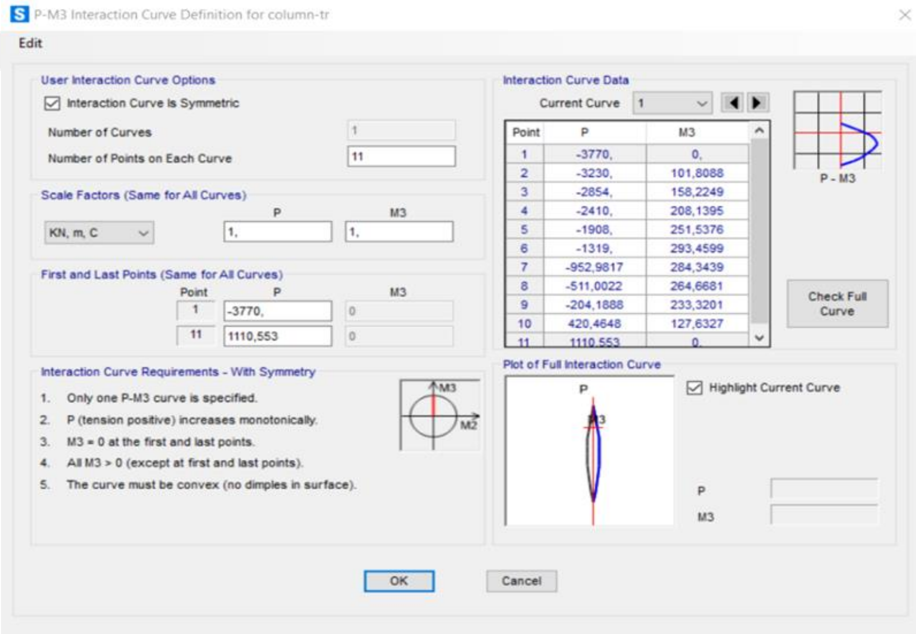

Figure 4.14 Interaction curve definition for column

The plastic hinge was assigned at the beginning and end of each beam and column as shown in Figure 4.15.

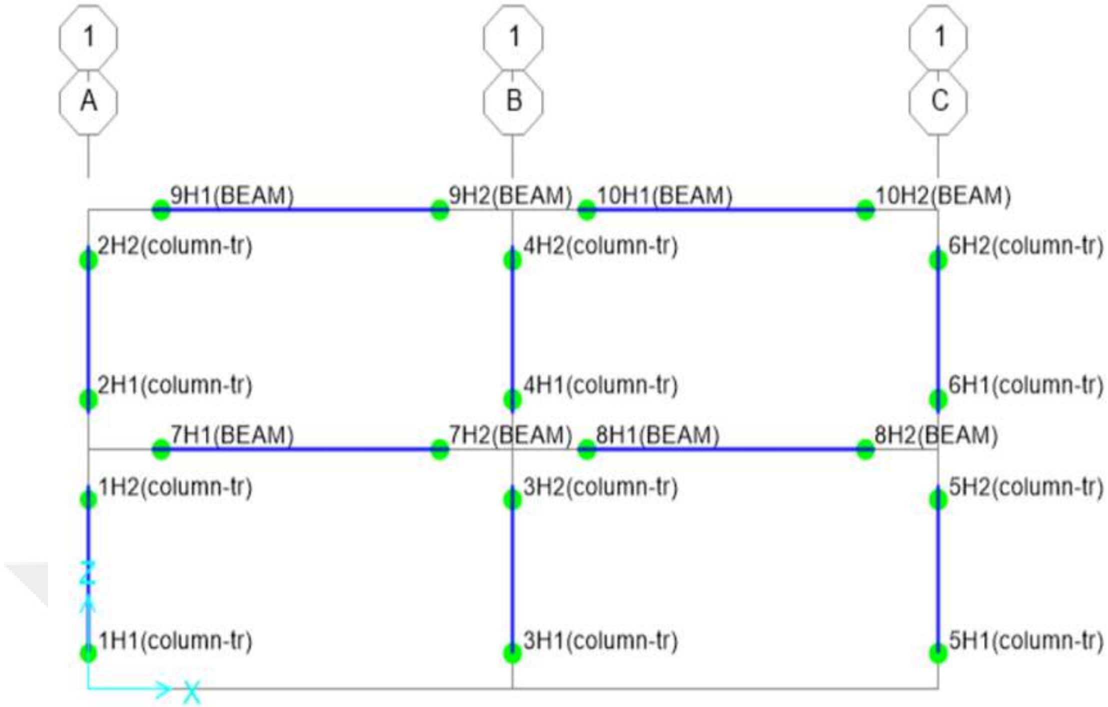

Figure 4.15 assignments of plastic hinge for beam and column

4.1.1.7 Modal analysis

The analysis has also been carried out for the building. Where the damage to the structure was determined under constant vertical loads, increased horizontal earthquake loads as shown in Figure 4.16.

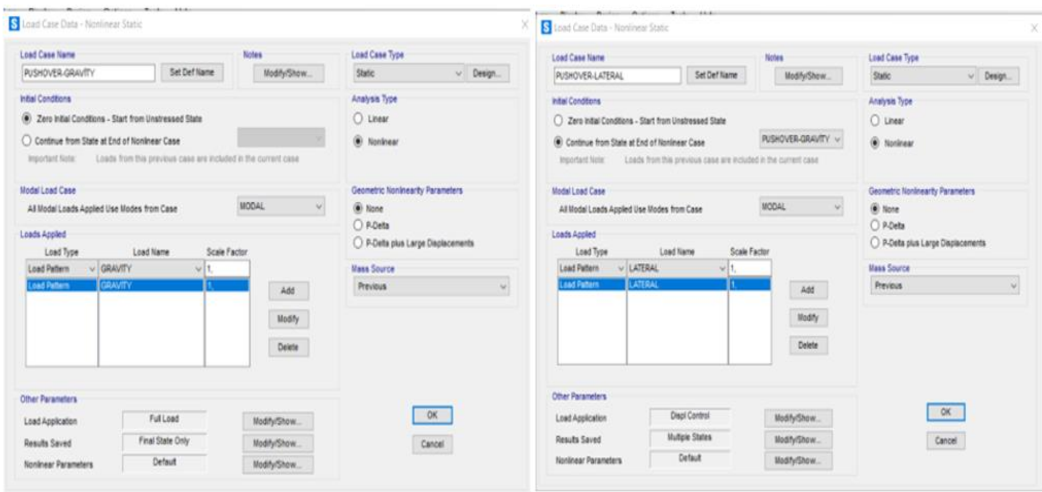

Figıre 4.16 Load case data – nonlinear static

As a result of the analysis, the pushover curve was obtained.

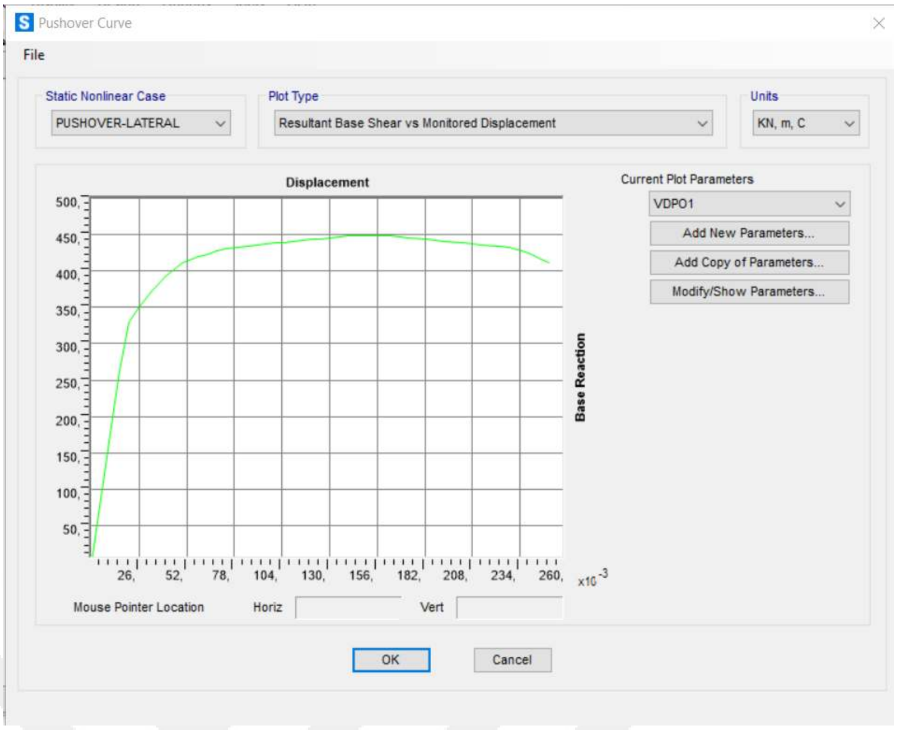

Figire 4.17 Pushover curve for TSC2018

To obtain a performance point, the seismic coefficients C_A and C_V are taken from the ATC-40 mentioned in the Table 4.2.

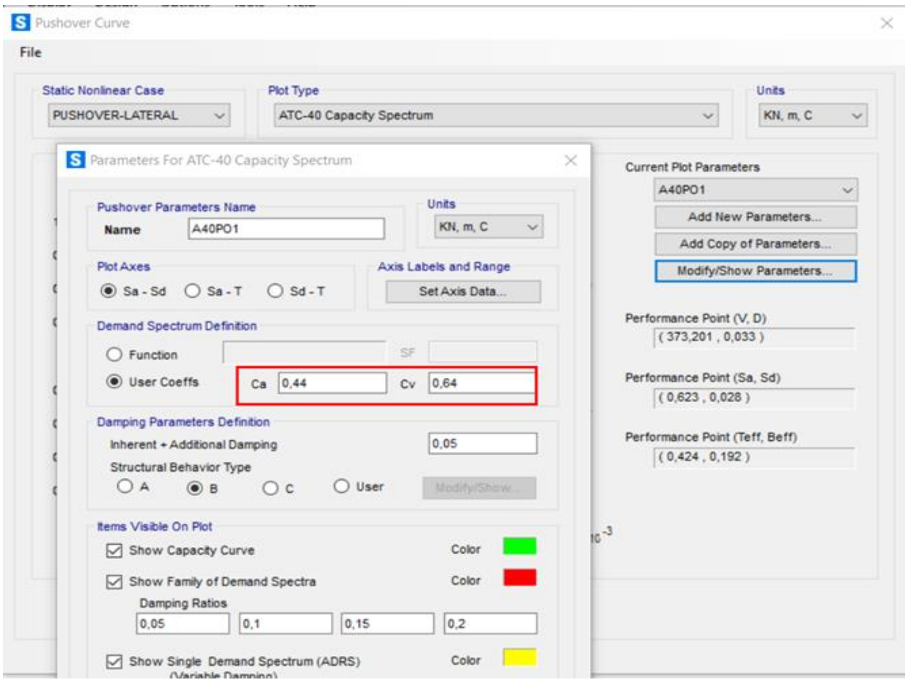

Figure 4.18 Parametres For ATC-40 Capacity Spectrum

Figure 4.19 Pushover Curve and performance point of TSC2018

4.1.2 By Eurocode 2004:

The data obtained from the Eurocode 2004 has been given in the Table 4.5.

Table 4.5 The data used in the analysis and taken from Eurocode 2004

The soil type	ZD	EN 1998-1 :2004 Table3.1
Soil factor	S= 1.15	EN 1998-1 :2004 Table3.2
The combination factor for live load	n=0.3 Live Load Participation Factor	EN 1998-1 :2004. Table A1.1
Spectrum Period	T_B=0.2 , T_C=0.6 , T_D= 2	EN 1998-1 :2004. Table 4.3
The importance factor	I =II, Ɣ1=1	EN1998-1:2004.4.2.5.5(P)
Correction factor lambda	1	
Lower Bound Factor	*B*=0.2	
Behavior factor	q=1.5	EN1998-1:2004 C3 4.2.3(P)
Ground acceleration	a_g=0.4	
The plastic hinge length	$L_P=\frac{L_V}{30}+0.2h+0.11\frac{d_{bL}f_y(Mpa)}{\sqrt{f_c(Mpa)}}$	EN 1998-1 :2004 C3 A.3.2.1(P)8
Cracked column	0.5*stiffness	EN 1998-1 :2004.4.3.1.7(p)
Cracked beam	0.5* stiffness	EN 1998-1 :2004.4.3.1.7(p)
seismic coefficients	C_A=0.44	ATC-40 Table 4.7
seismic coefficients	C_V=0.64	ATC-40 Table 4.8

The soil quality factors, spectrum period, and behavior factor were entered in the SAP 2000 program to define seismic load pattern.

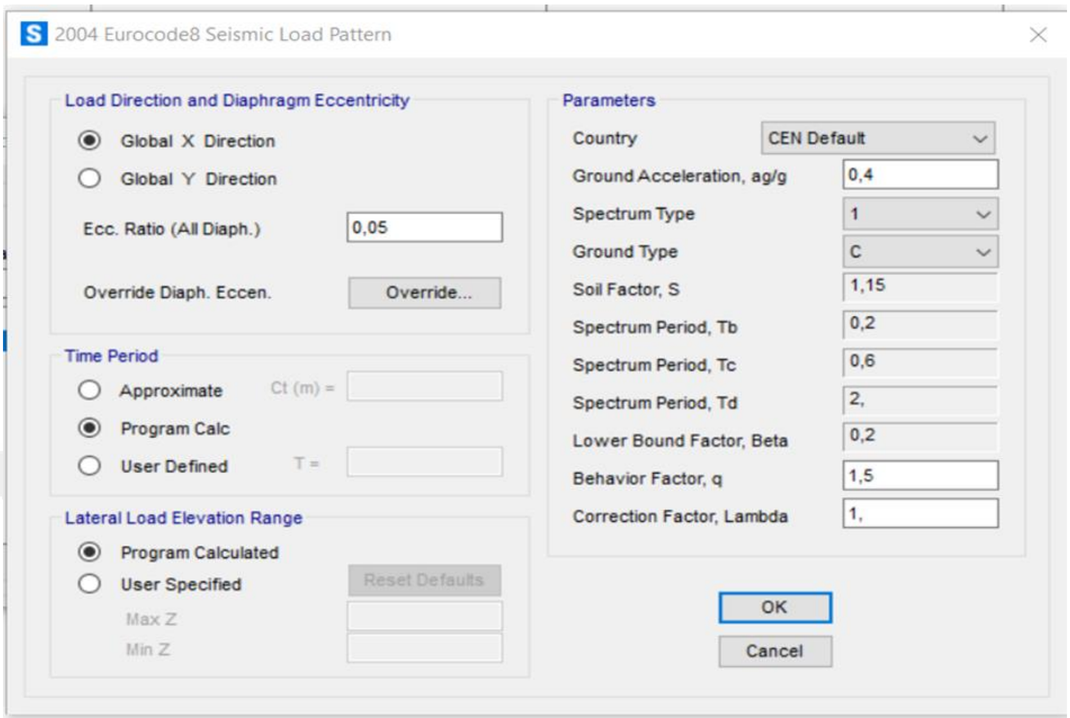

Figure 4.20 Eurocode seismic load pattern

4.1.2.1 Input cracked elements in SAP2000

The enter of effective section stiffness factors for reinforced concrete column and beam members in SAP2000.

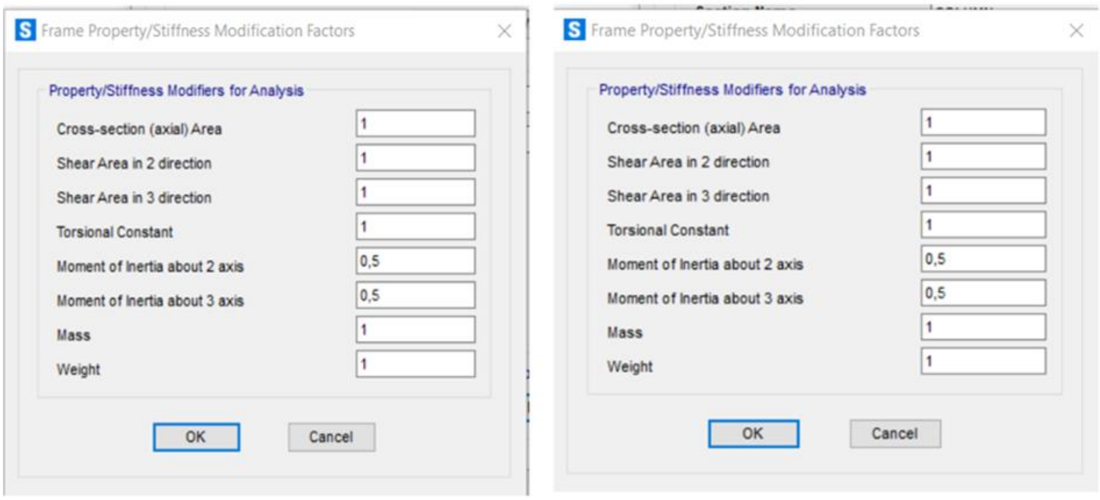

Figure 4.21 Stiffness modification factors for Eurocode

4.1.2.2 Performance level for building according to EC8

The limits for beam and column were calculated according to EC8 as mentioned in the below tables 4.6, 4.7, and 4.8.

Table 4.6 Performance level for the beam to EC8

Limit State (LS) For Beam (Plastic part)			
Member	DL	SD	NC
Ductile primary	0	0.020619	0.027492
Ductile secondary		0.037114	0.049485

Table 4.7 Performance level for the beam to EC8 to yielding rotation

Limit State (LS) For Beam (Plastic part) (ϴp/ϴy)			
Member	DL	SD	NC
Ductile primary	0	8,895064	11,86008
Ductile secondary		16,01111	21,34815

Table 4.8 Performance level for the column to EC8

Limit State (LS) for column (Plastic part)			
Member	DL	SD	NC
Ductile primary	0	0.014	0.019
Ductile secondary		0.0268	0.0358

4.1.2.3 Defined and assignments of plastic hinge for beam and column

As mentioned in 4.1.1. when the TSC2018 is used, the same steps are processed, but by considering the EC8 rules.

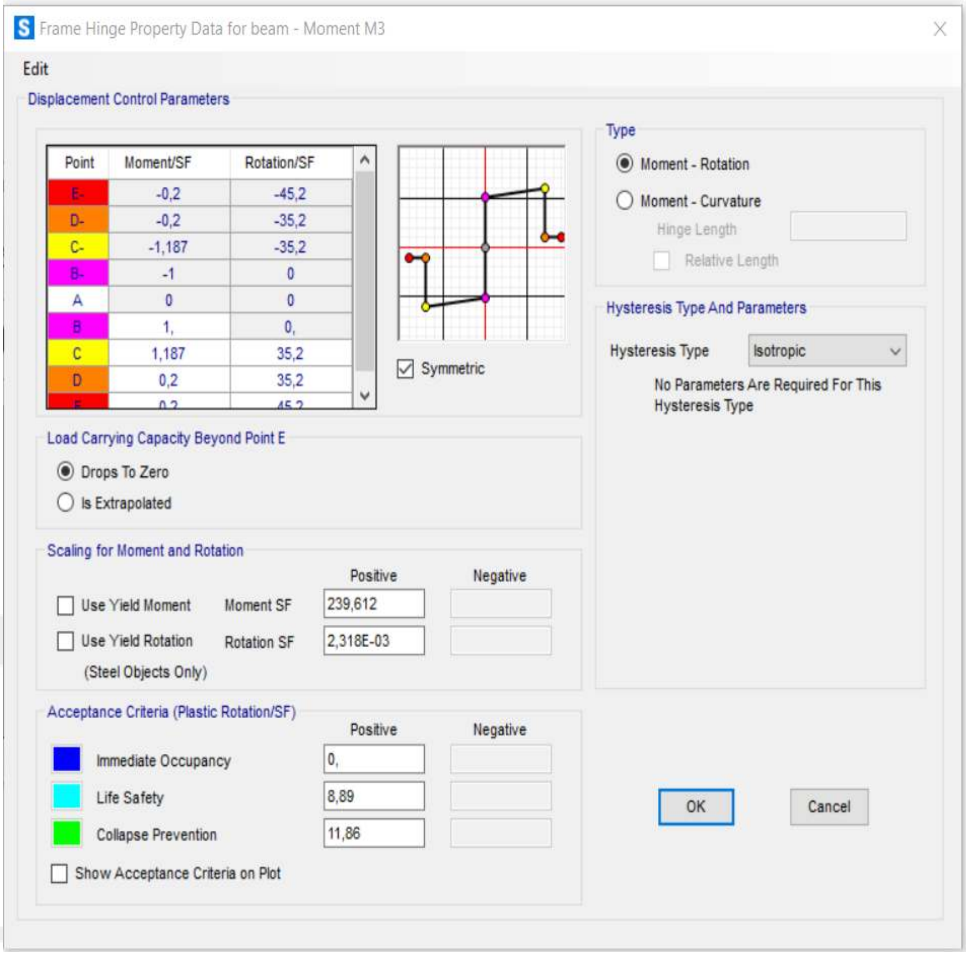

Figure 4.22 Frame hinge property data for the beam of Eurocode 2004

For column:

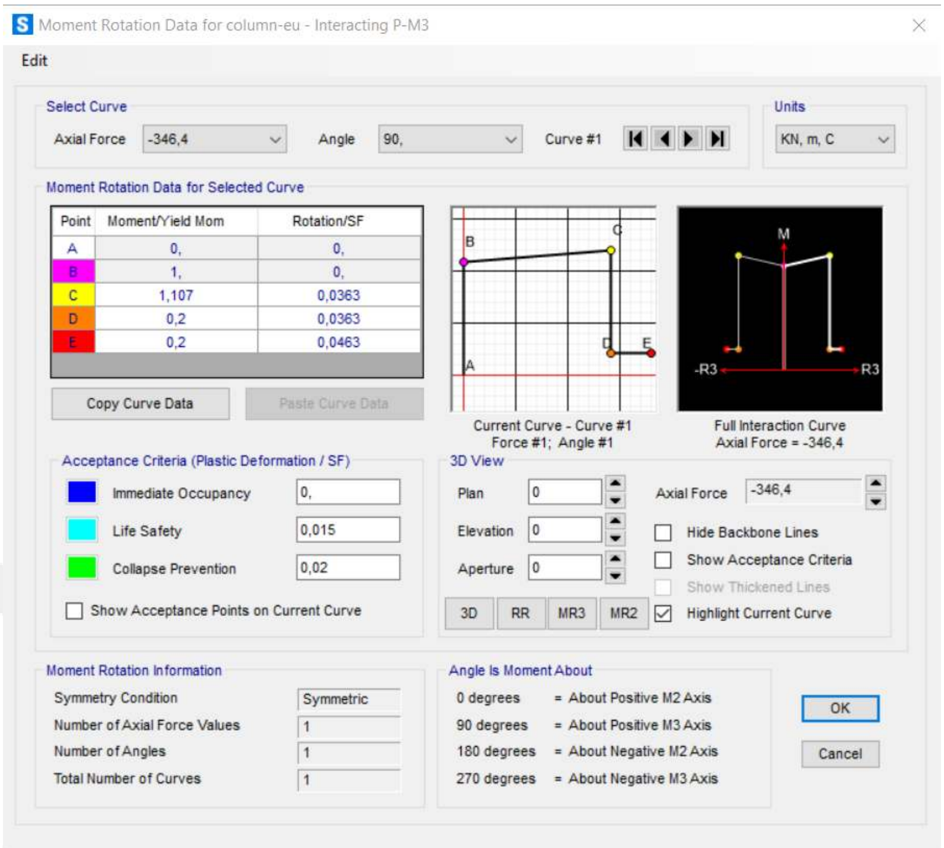

Figure 4.23 Frame hinge property data for column of Eurocode 2004

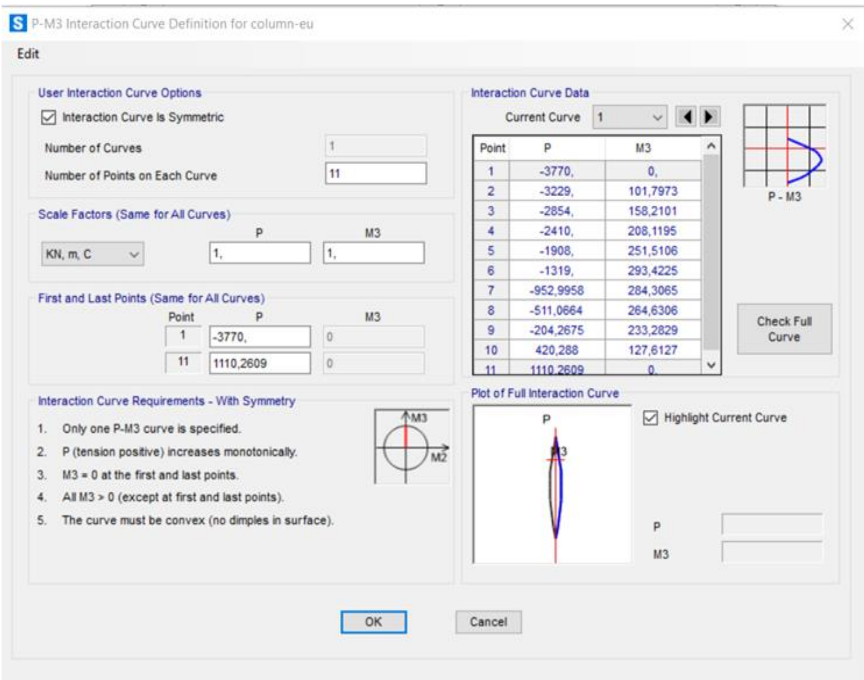

Figure 4.24 Interaction curve definition for column of Eurocode 2004

The plastic hinges are assigned at the beginning and the end of each beam and column as shown in Figure 4.36.

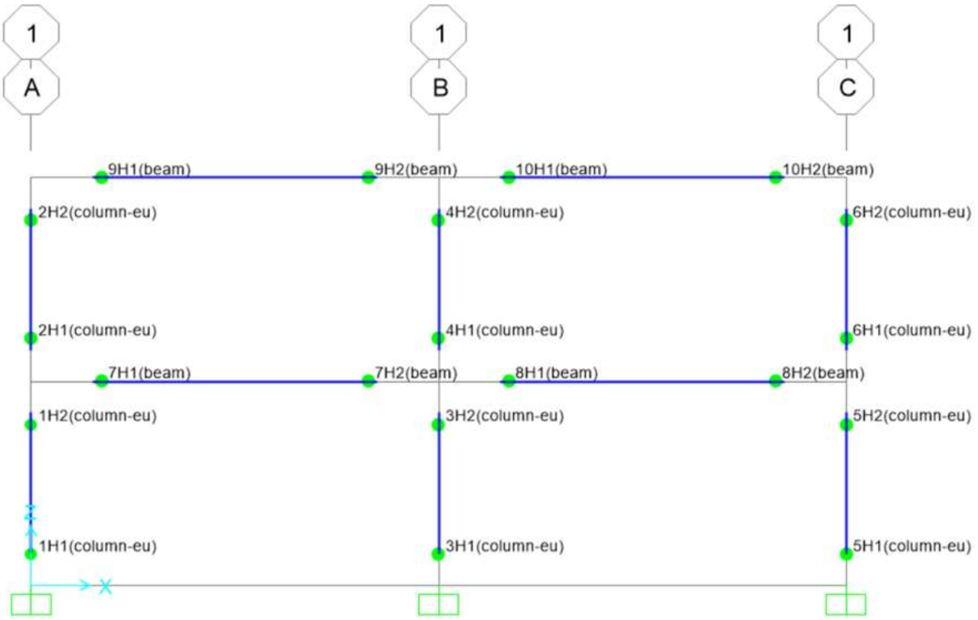

Figure 4.25 assignments of plastic hinge for beams and columns

4.1.2.4 Modal analysis

As mentioned, when the Turkish code has been implemented, the same steps were utilized for analysis, and the pushover curve and performance point were obtained.

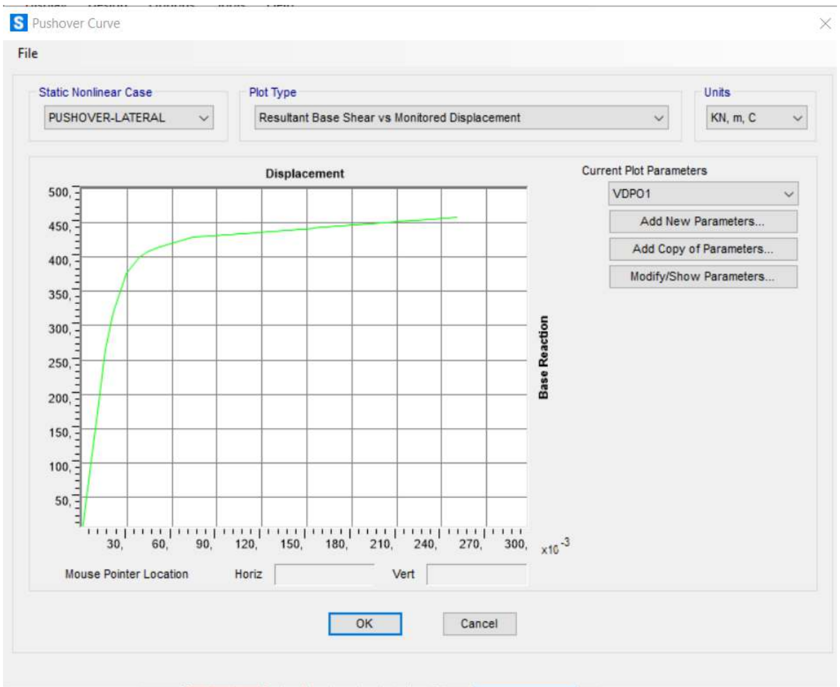

Figure 4.26 Pushover curve for Eurocode2004

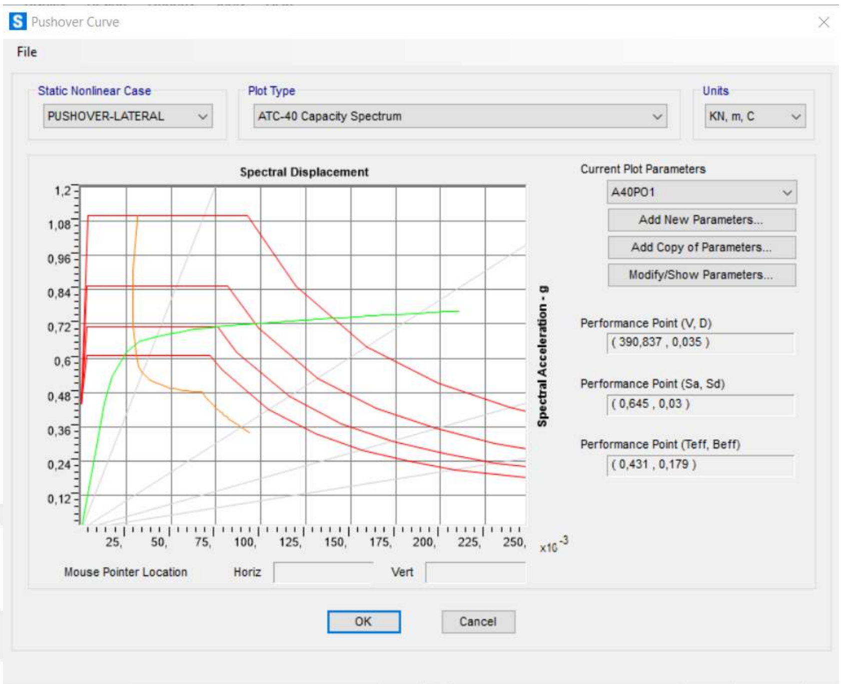

Figure 4.27 Pushover Curve and performance point for Eurocode2004

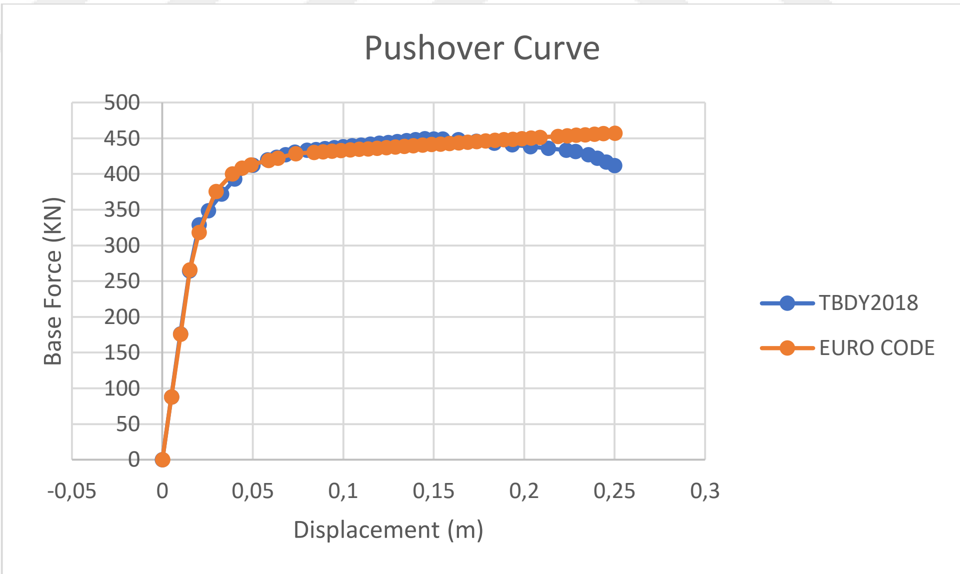

Figure 4.28 Pushover curve for C20 according to TSC2018 and Eurocode2004

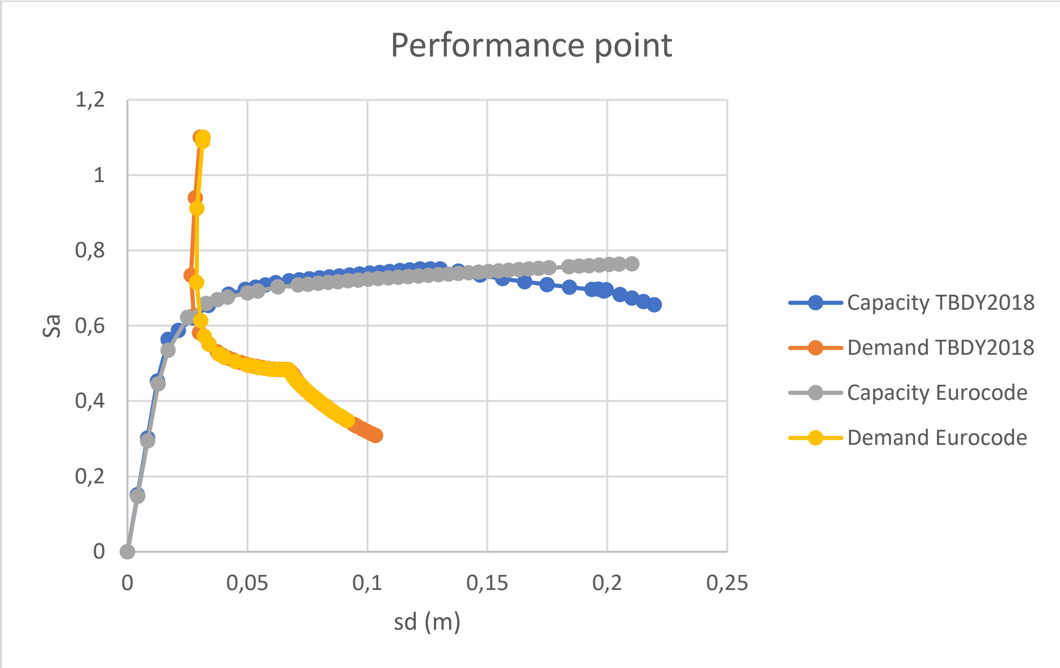

Figure 4.29 Performance point according to TSC2018 and Eurocode2004

4.1.2.5 At performance point

The plastic deformation that occurred to frame at performance point according to TSC2018 and EC8 were showed in the below Figure 4.30.

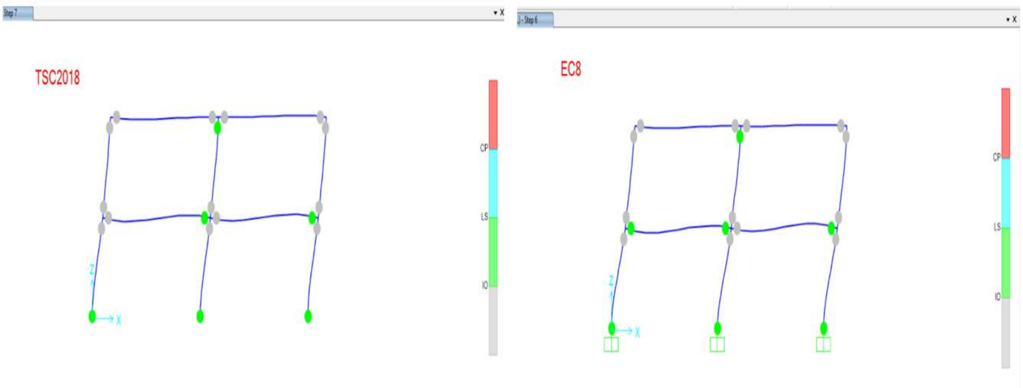

Figure 4.30 Plastic deformation to the frame at performance point (TSC2018 and EC8)

4.1.2.6 At failure:

The plastic deformation that occurred to frame at failure according to TSC2018 and EC8 were showed in the below Figure 4.31.

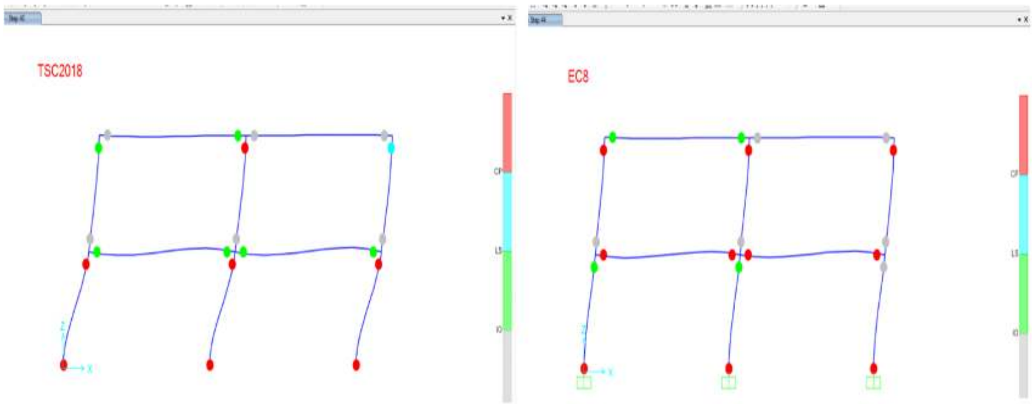

Figure 4.31 Plastic deformation to the frame at failure (TSC2018 and EC8)

Table 4.9 Plastic deformation to beams and columns at performance point and failure according to (TSC2018 and EC8)

		Beam				Column			
		B to IO	**IO to LS**	**LS to CP**	**> CP**	**B to IO**	**IO to LS**	**LS to CP**	**>CP**
At performance point	**TSC2018**	6	2	-	-	8	4	-	-
	EC8	5	3	-	-	8	4	-	-
At failure	**TSC2018**	3	5	-	-	3	1	1	7
	EC8	2	2	-	4	4	2	-	6

4.2 The Effect of low concrete strength on performance

14-Storey Frame :

In this chapter, the effect of decreasing the quality of concrete was studied by the pushover method according to TBDY2018 and EC8. Where a 14-storey frame was defined and the pushover analysis was done three times for (C10, C20, C40) by following the same steps mentioned in the last chapter, and the results were compared.

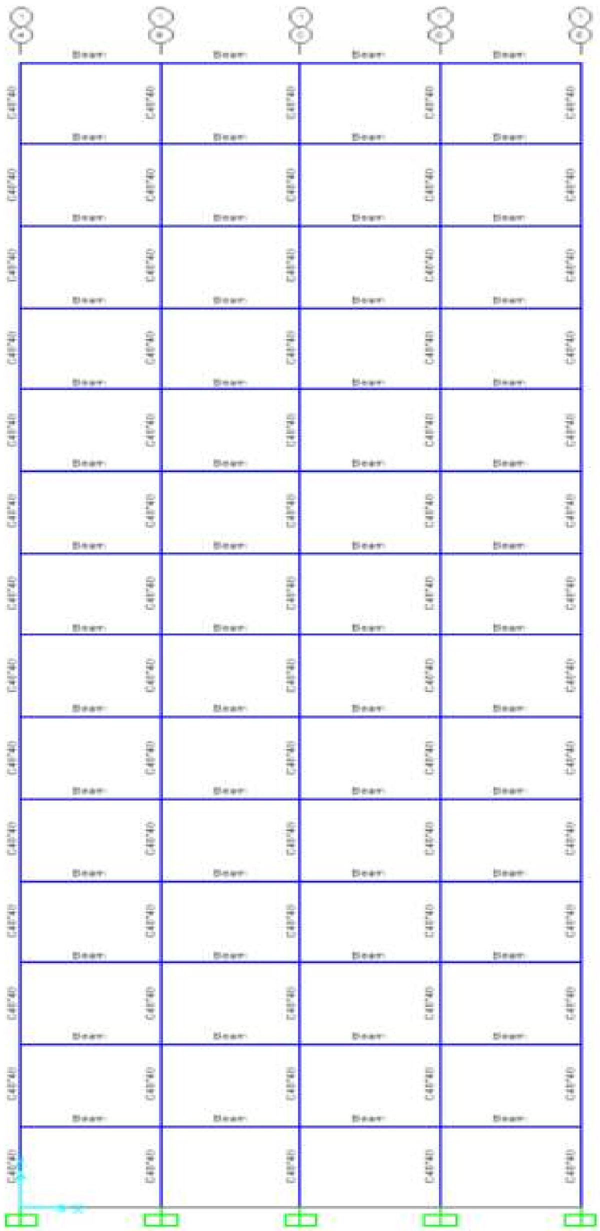

Figure 4.32 view of the frame modeled in SAP2000

Table 4.10 Frame data

Frame Information		
The Number of stories	14 story	
floor Hight	3 m	
Total Building Hight	42m	
Mterial Information		
Concrete Class	C10-C20-C40	
Concrete Elasticiy Modulus	30000 MPa	
Rebar Class	S420	
Steel Elasticity Modulus	200000 MPa	
Other Information		
Columun Section (400*400) mm	Longitudinal = 8-Ø20 Stirrups = Ø10/15 mm	
Beam Section (300*600) mm	Longitudinal	2-Ø14 AT the top
		4-Ø14 AT the Bottom
	Stirrups	Ø8/150 mm
Seismic Zone	DD2	
Spektral İvme Katsayısı	Ss=0.573, S1= 0.222	
2018 Turkish Code		
The soil type	ZD	TSC2018.Tablo 16.1
The combination factor for live load	n=0.3	TSC2018. Table 4.3
Building Category	BKS=3	TSC2018. Table 3.1
The importance factor	I =1	TSC2018. Table 3.1
Seismic design class	DTS=3	TSC2018. Table 3.2
Building height class	BYS=4	TSC2018. Table 3.3
Behavior factor	R=6	TSC2018. Table 4.1
The strength increase factor	D=2.5	TSC2018. Table 4.1
The plastic hinge length	LP=0,5H	TSC2018.5.3.1.2
Cracked column	0.7*stiffness	TSC2018. Table 4.1
Cracked beam	0.35*stiffness	TSC2018. Table 4.1
seismic coefficients	C_A=0.4	ATC-40 Table 4.7
seismic coefficients	C_V=0.56	ATC-40 Table 4.8
Nonlinear material	εco =0.002, εcu=0.05	TSC.Figure 5A.1
Nonlinear material	εsh =0.008, εsu=0.8	TSC.Table 5A.1

4.2.1 Define concrete material

As also given by Bedirhanoglu (2014) the elastic modulus equation given by Turkish Code (TS500) yields very high values then real value particularly for low strength concrete. For this reason, other equations given by Bedirhanoglu (2014) and ACI 318 has been implemented to calculate young modulus from concrete strength. The American Concrete Institute ACI 318 (2008) provides the following relationship for modulus of elasticity (Bedirhanoglu 2014).

Ec= $4.73\sqrt{F_C{}'}$

For C10 → Ec= $4.73\sqrt{10}$ = 14957573 KN

C20 → Ec= $4.73\sqrt{20}$ = 21153203 KN

C40 → Ec= $4.73\sqrt{40}$ = 29915146 KN

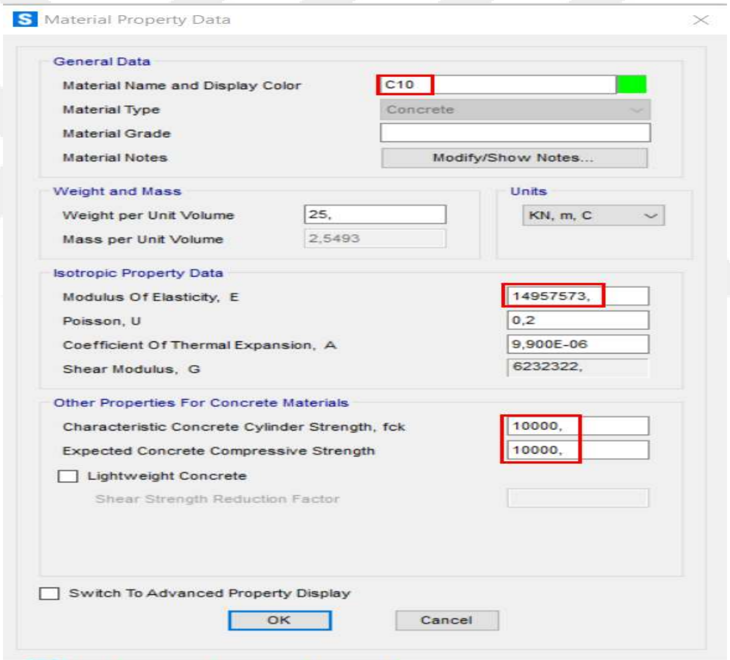

Figure 4.33 defined material concrete (C10) in SAP2000

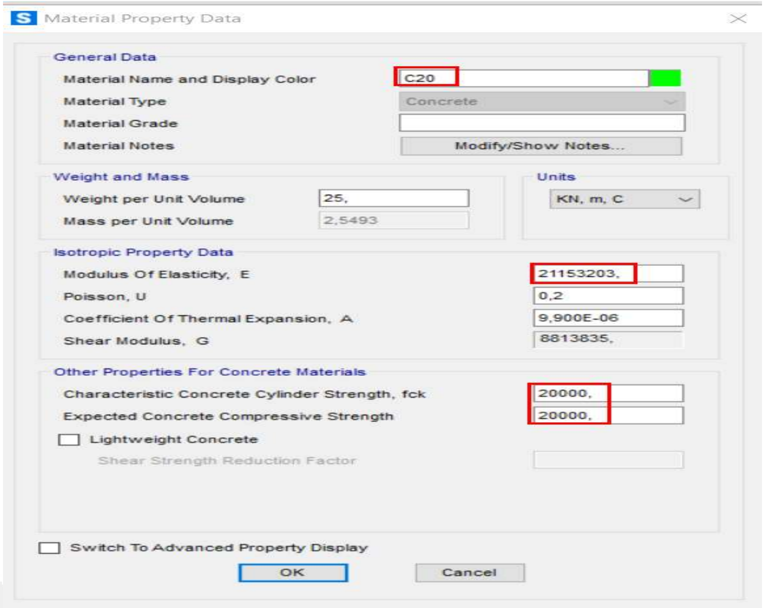

Figure 4.34 defined material concrete (C20) in SAP2000

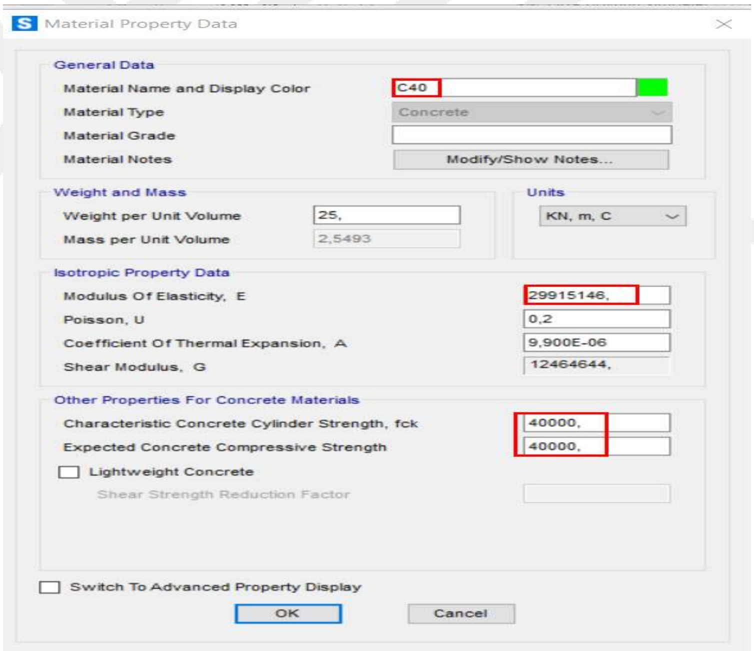

Figure 4.35 defined material concrete (C40) in SAP2000

To define the properties of the hinges, the moment-curvature and plastic rotation of all section beam and column elements were calculated for each type of concrete. The same steps were followed in the previous example of the frame that explains the method of pushover analysis. The pushover analysis was done according to the three types of concrete (C10, C20, C40), according to TSC2018 and EC8, and these results were obtained.

4.2.2 Pushover curve

Comparative push-over curves have been presented in Fig. 4.36 and Fig. 4.37.

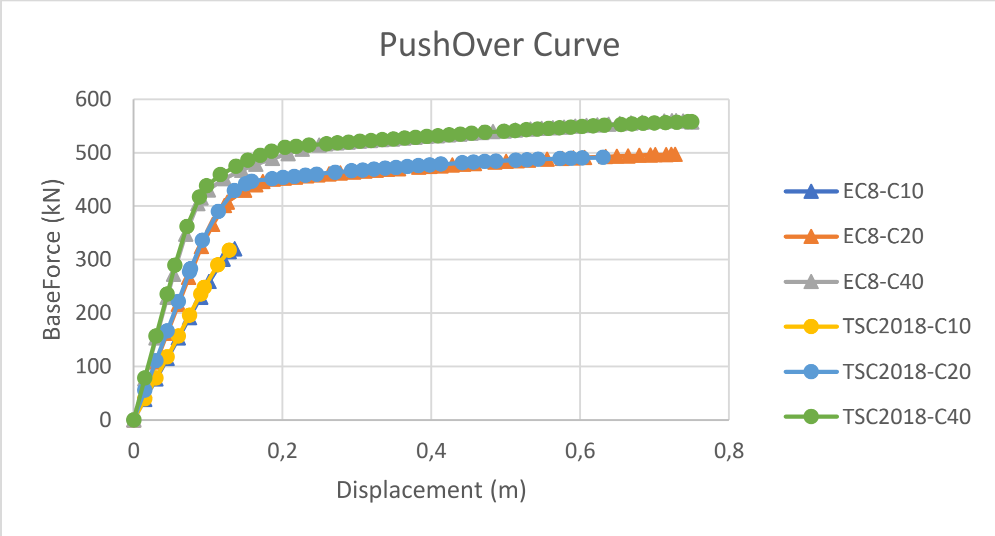

Figure 4.36 Pushover curve for C10, C20, and C40 according to TSC2018 and EC8

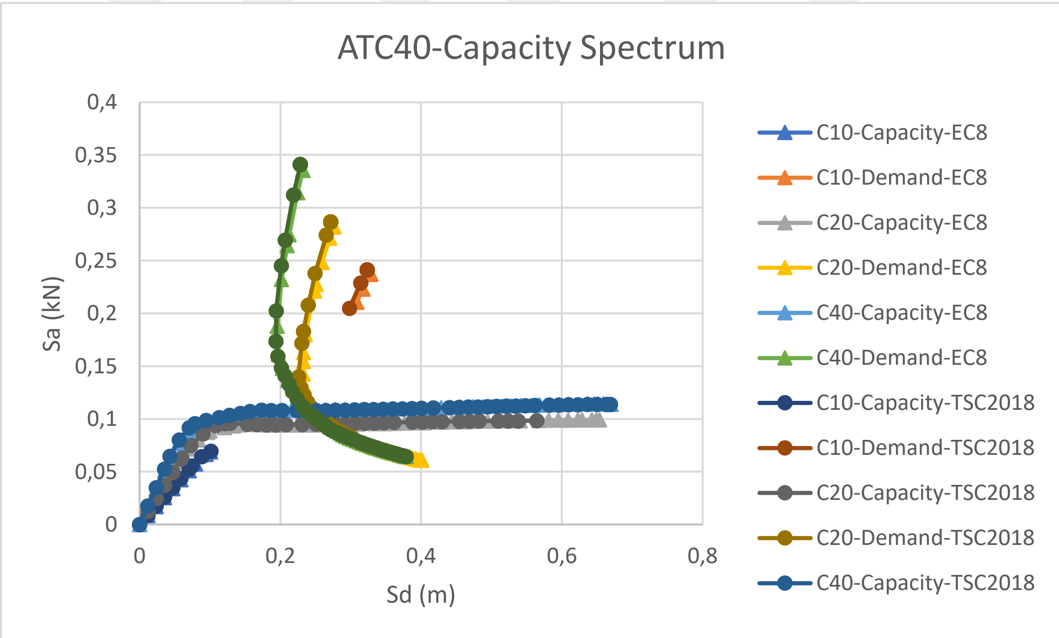

Figure 4.37 Performance point for C10, C20, and C40 according to TSC2018 and EC8

Table 4.11. The number of hinges formed in the columns and beam according to Hinge Status performance point (TSC2018 and EC8)

Beam-damage -TBDY2018-per						Beam -damage-EC8					
	Steps	B-IO	IO-LS	LS-CP	CP-C		Steps	B-IO	IO-LS	LS-CP	CP-C
C10	-----------		--	-----	----	C10	--------	---	-----	----	----
C20	20	67	45	----	------	C20	22	68	43	1	----
C40	18	60	52	---	------	C40	18	77	35	-----	----
	Column-TBDY2018-per-						Column -damage-EC8				
	Steps	B-IO	IO-LS	LS-CP	CP-C		Steps	B-IO	IO-LS	LS-CP	CP-C
C10	--------					C10	--------				
C20	20	135	--------	2	3	C20	22	135	-------	2	3
C40	18	135	5	--------	-----	C40	18	135	5	--	------

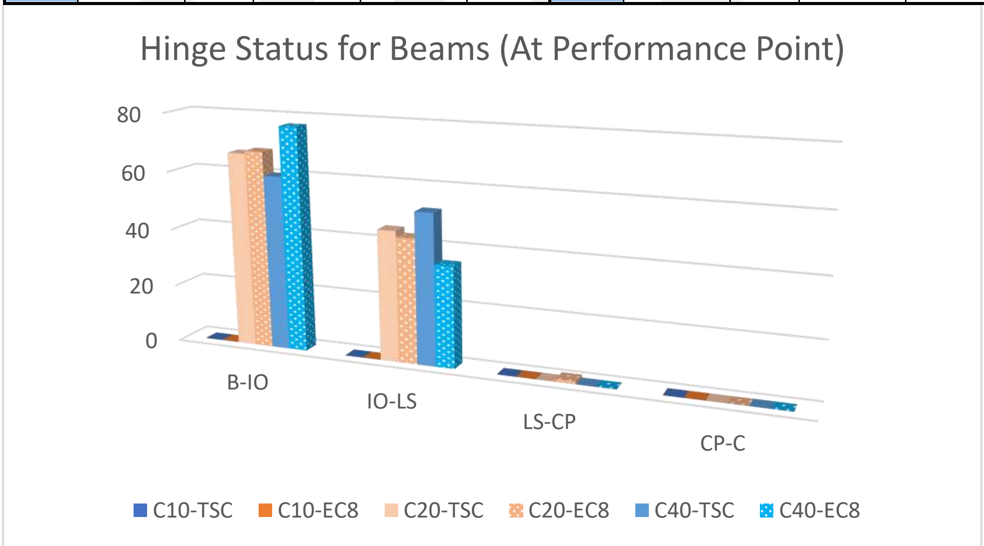

Figure 4.38 The status of beam hinges at different performance points in case of different concrete strengths according to TSC2018, and EC8 (B-IO; Continuous Use, IO-LS; Limited Damage, LS-CP; Controlled Damage, CP-C; Collapse prevention)

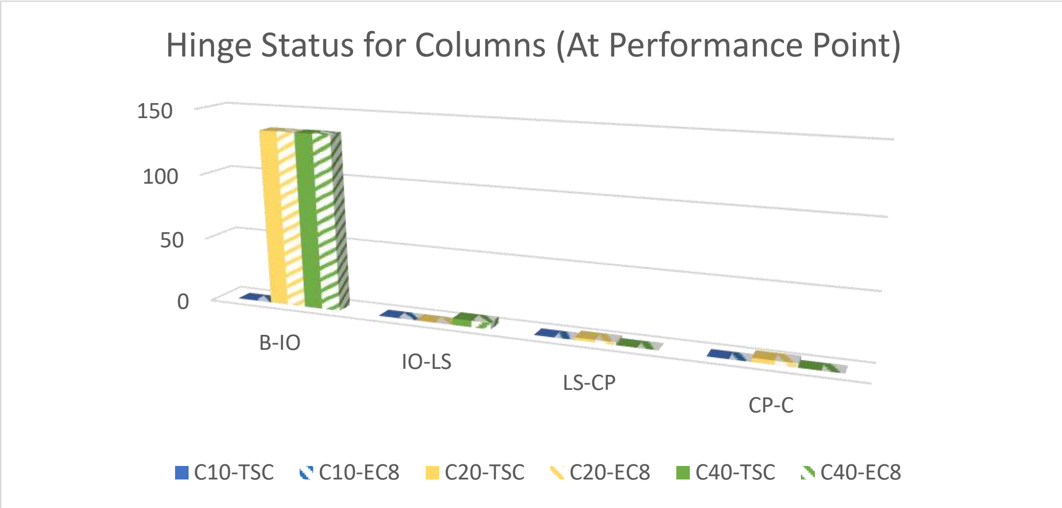

Figure 4.39 the status of formed hinges and their number to columns at performance point for (C10, C20, C40) according to (TSC2018, EC8)

Table 4.12 Plastic hinge that happened to the frame at failure point (TSC2018 and EC8)

At failure point											
Beam-damage-TBDY2018-						Beam-damage-EC8					
	Steps	B-IO	IO-LS	LS-CP	>CP		Steps	B-IO	IO-LS	LS-CP	>CP
C10	9	--	8	---------	----	C10	--------	----	---	----	---
C20	37	60	35	4	13	C20	47	60	24	4	24
C40	48	52	28	8	24	C40	48	64	16	7	25
Column-damage-TBDY2018						Column-damage-EC8					
	Steps	B-IO	IO-LS	LS-CP	>CP		Steps	B-IO	IO-LS	LS-CP	>CP
C10	9	0	11	----		C10	---------	--	---	----	----
C20	37	121	14	-----	5	C20	47	122	13	---	5
C40	48	122	13	----	5	C40	48	134	----	-------	5

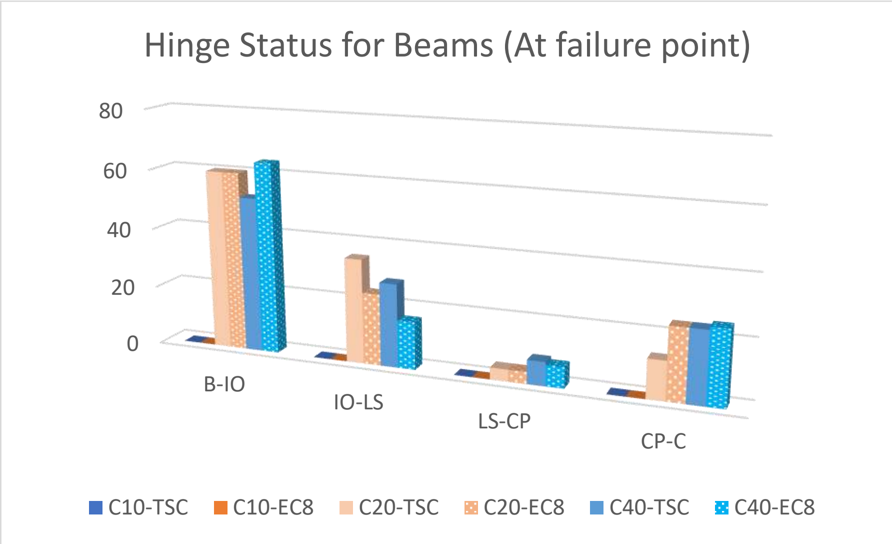

Figure 4.40 The status of formed hinges and their number to beams at failure for (C10, C20, C40) according to (TSC2018, EC8)

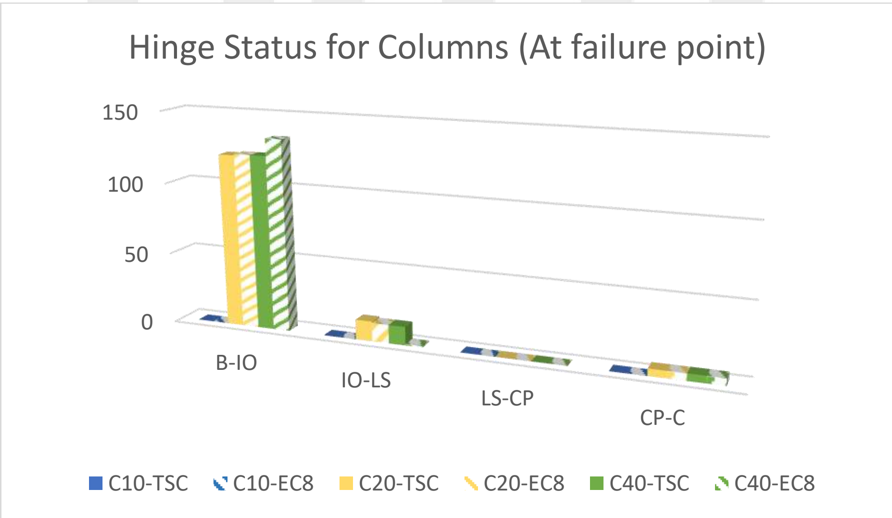

Figure 4.41 The status of formed hinges their number to columns at failure for (C10, C20, C40) according to (TSC2018, EC8)

4.3 Nonlinear static and dynamic analysis for 14 story building

In this chapter, performance analysis of a 14-storey building having a torsion-dominated behavior. The pushover procedure and time-history analysis have been applied by considering TSC2018 and EC8. Details of the analysis have been given in the following in different sections of this chapter.

4.3.1 Existing building details

The building located in Diyarbakir Province, Turkey. It consists of a basement, a ground floor, and 12 typical floors. It consists of beams, columns, shear walls, and slabs.

Table 4.13 Existing building data

Building Information	
The Number of stories	Basement, Ground floor and, 12 story
Basement Hight	3.5 m
Ground floor Hight	3 m
Typical floor Hight	3 m
Total Building Hight	42.5 m
Mterial Information	
Concrete Class	C25
Concrete Elasticiy Modulus	30000 MPa
Rebar Class	S420
Steel Elasticity Modulus	200000 MPa
Safety factor for concrete	1.50
Safety factor for steel	1.15
Unit waight for concrete	25 KN/m^3
Other Information	
Shear Wall (Number, Section Dimention)	24, (25x175, 25x180, 25x330, 25x335, 25x425)
Columun (Number, Section Dimention)	15, (30x70, 35x70, 70x30, 70x35, 40x80, 40x85, 35x80, 45x85)
Beam (Section Dimension)	(25x50) for all beams
Seismic Zone	DD2
Latitude	37,962174°
Longitude	40,184938°
The soil type	ZC
The combination factor for live load	n=0,3
The importance factor	I =1

Figure 4.42 Perspective view of the building

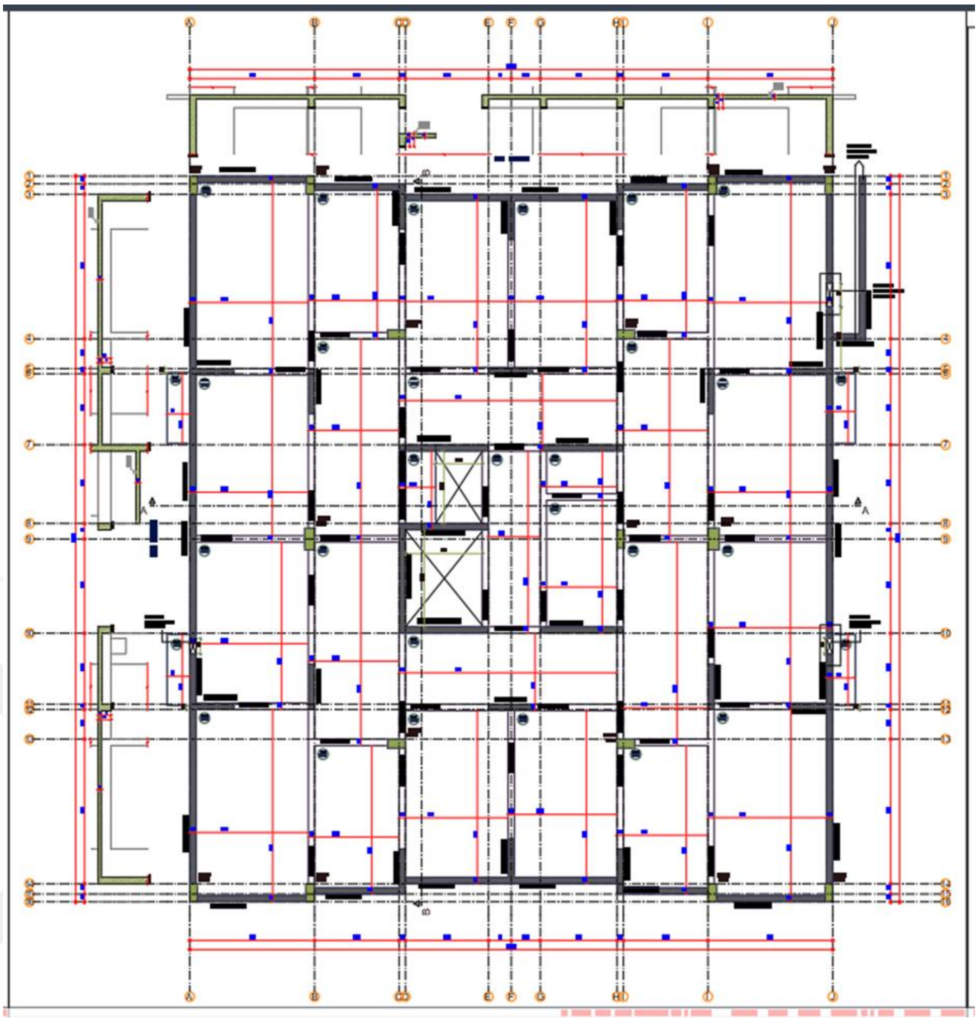

Figure 4.43 2d plan view for the basement

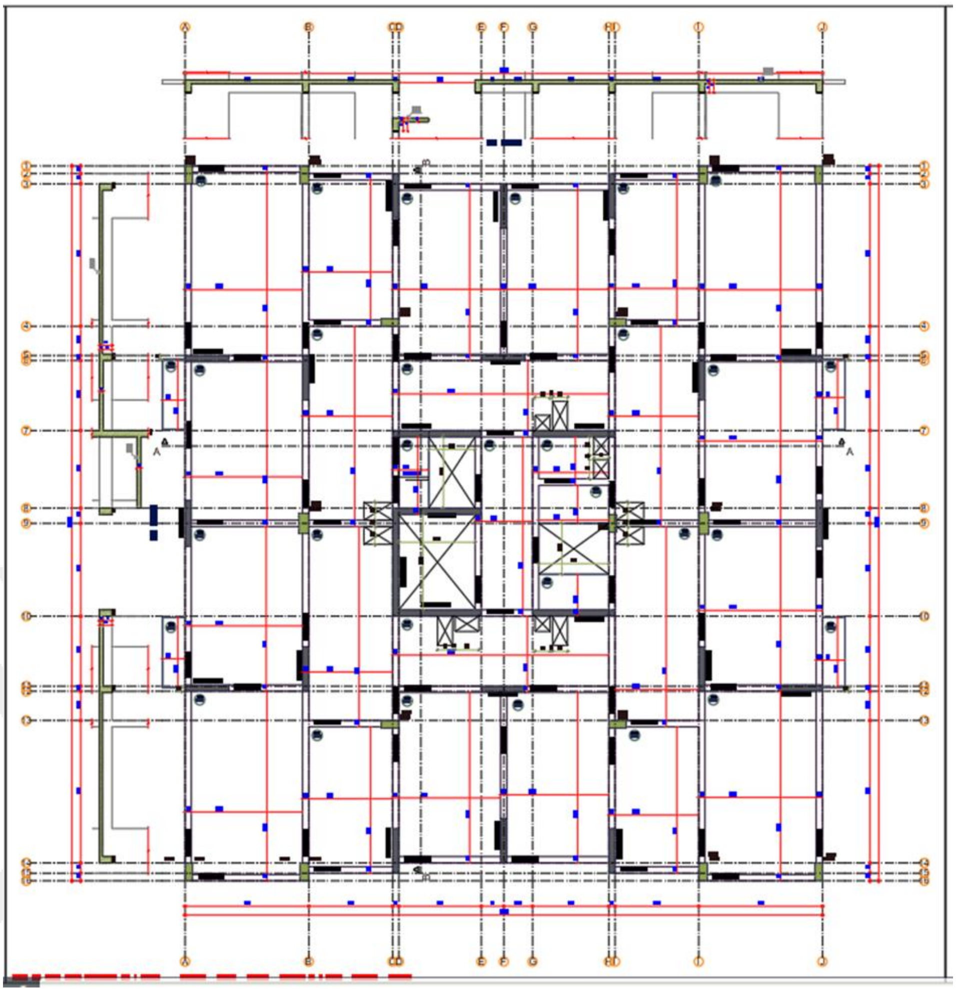

Figure 4.44 2d plane view for the ground floor

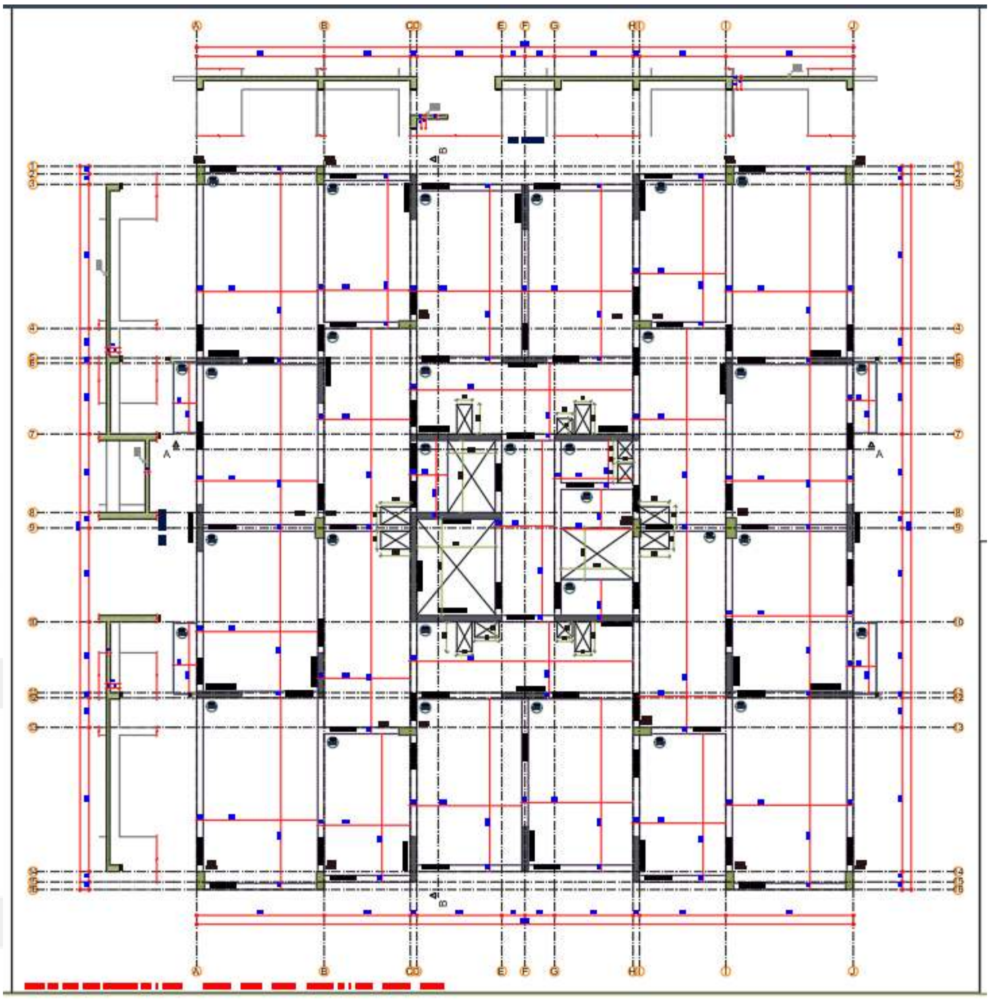

Figure 4.45 2d plane view for the typical floor

4.3.2 Building structural modeling

The building was modeled 3D in SAP 2000. To do a non-linear analysis, the diameter of the reinforcement and its quantity were defined for all sections, beams, columns, and shear walls. Shear walls were modeled as mid-pier. And that is after checking the possibility of modeling the shear walls as mid-pier according to the Turkish code “the ratio of the longest length for the shear wall in the plan to the total shear wall height does not exceed 1/2” mentioned in paragraph 4.5.3.8 in TSC2018

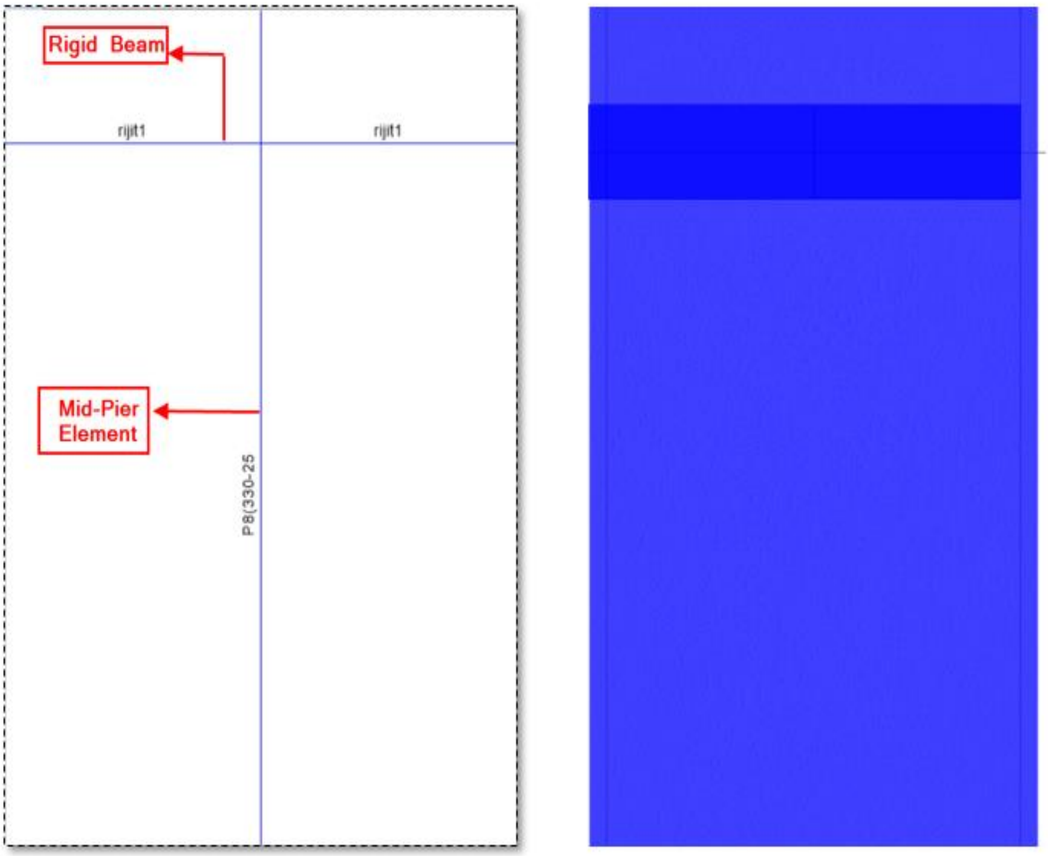

Figure 4.46 Mid Pier Model for Shear Wall

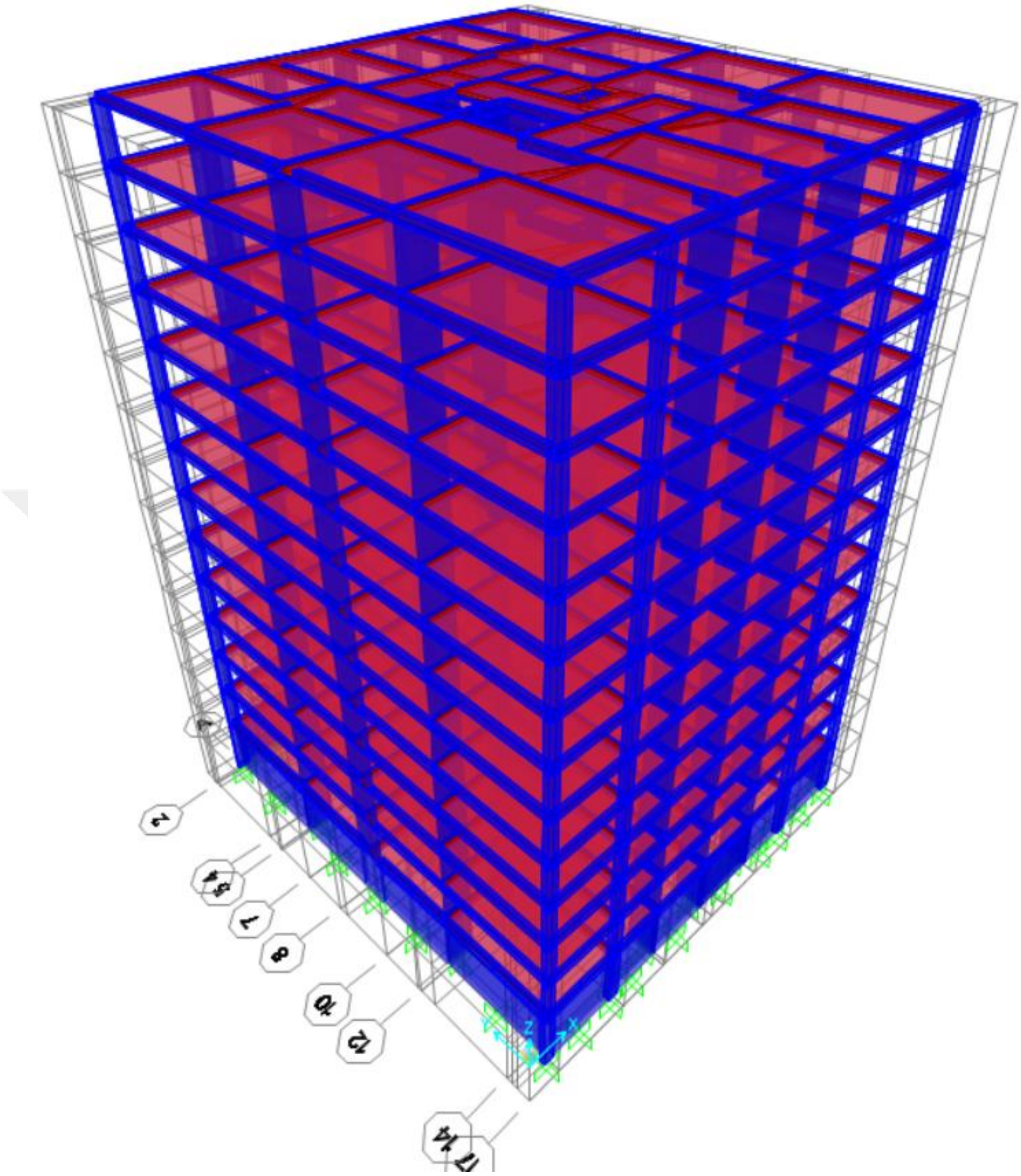

Figure 4.47 3d view of the building modeled in SAP2000

4.3.3 Nonlinear modeling

We need a non-linear analysis to determine the realistic behavior of the building during an earthquake. Nonlinear analysis can be done with three different methods. These methods are respectively, single modal pushover analysis, multimodal pushover analysis, and nonlinear analysis in time history.

4.3.3.1 Choosing a calculation method for nonlinear analysis

Nonlinear analysis in the time history was selected because the building height class is 5> BYS=4 > 2 mentioned in paragraph 5.5.2.1 in TSC2018 and it gives more real results than other methods.

4.3.3.2 Defined nonlinear material properties

C25/30 concrete class and S420 rebar were used in modeling. Nonlinear material was defined in SAP2000 to be used in the plastic hinge moment calculation. After choosing the Mander model from “Stress Straing Curve Definition Options” The mander model data for unconfined concrete ε_{co} =0.002 and ε_{cu} =0.005 As mentioned in the paragraph 5A.1 of the appendix “EK 5A” in the TSC2018 was entered in the “Parametric Strain Data” as shown in the Figure 4.48.

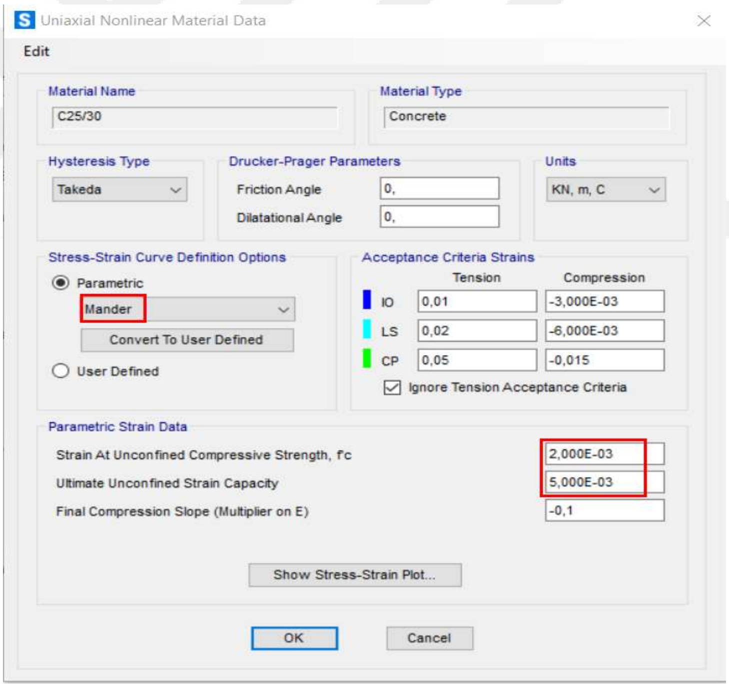

Figure 4.48 Nonlinear concrete data for TSC2018

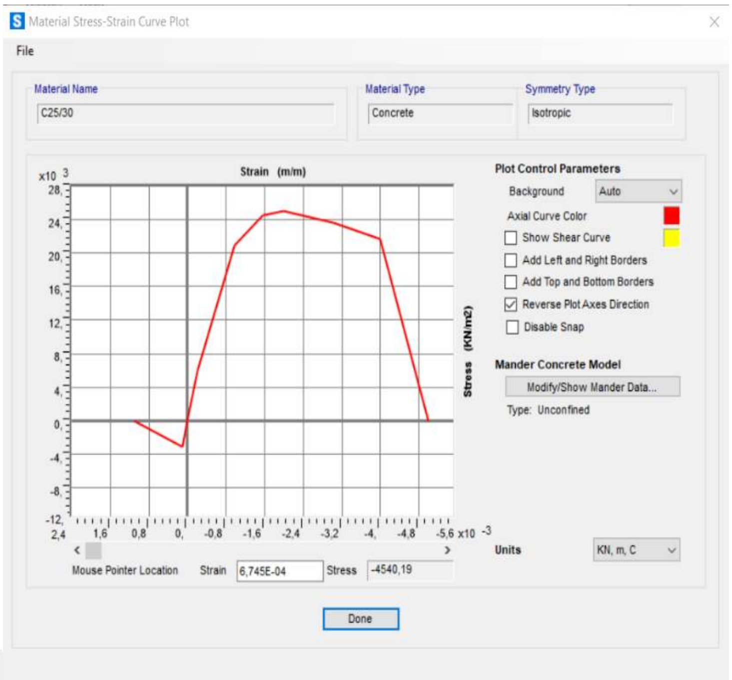

Figure 4.49 C25/30 Concrete Stress-Strain Graph

S420 rebar class was used in modeling. Nonlinear material for reinforced concrete steel was defined in SAP2000 according to TSC2018. Where “Strain At Onest of Strain Hardening” is εco =0.008 and “Ultimate Strain Capacity” is εcu =0.08 for S420 As mentioned in table 5A.1 of the appendix “EK 5A” in the TSC2018.

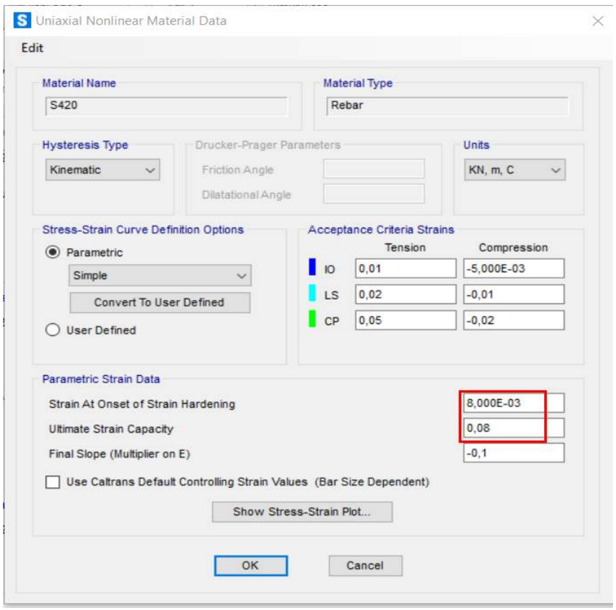

Figure 4.50 Nonlinear rebar data for TSC2018

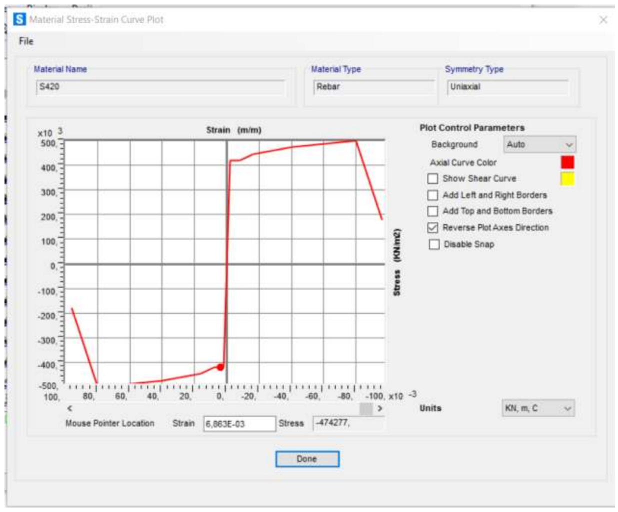

Figure 4.51 S420 rebar Stress-Strain Graph

4.3.3.3 The Relationship between Stress-Strain for unconfined and confined reinforced concrete

The Stress-Strain relationship of RC section according to Mander model were explained in figures 4.52, and 4.53.

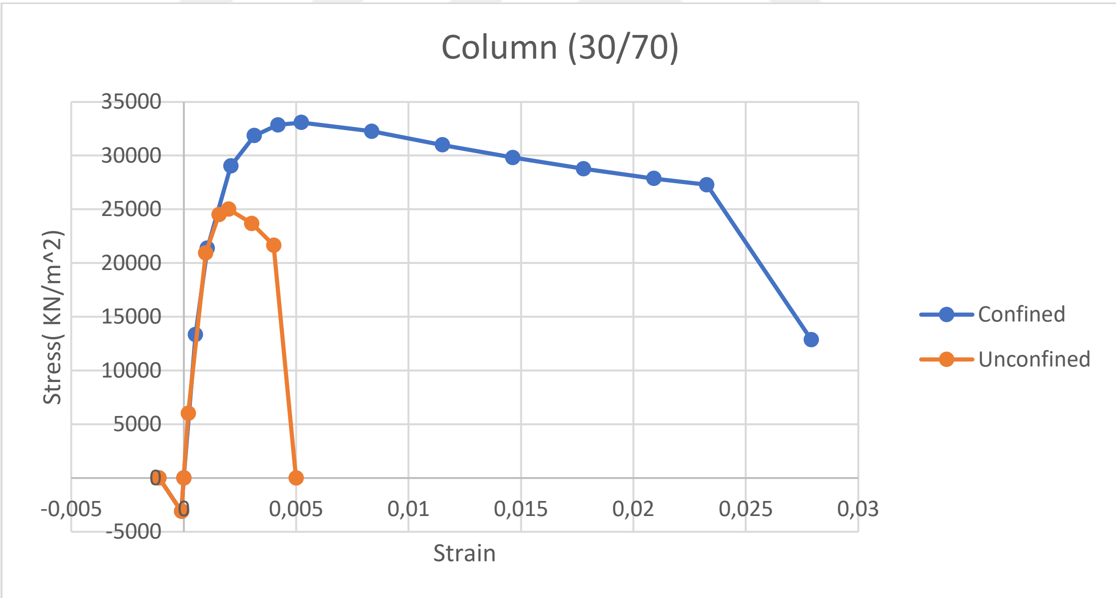

Figure 4.52 Stress-Strain relationship of a RC cross sections of a column according to Mander model

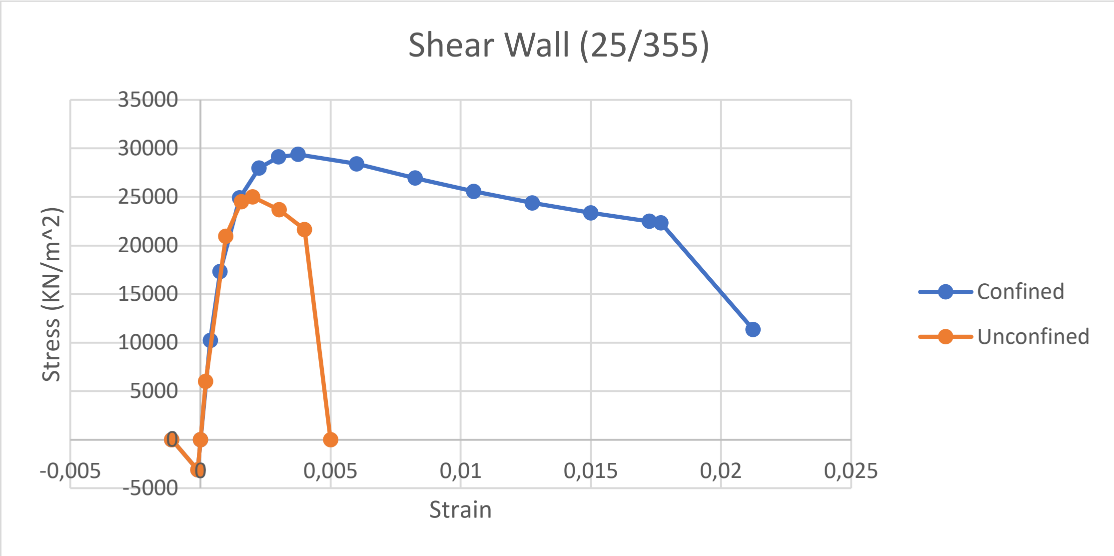

Figure 4.53 Stress-Strain relationship of a RC cross-sections of a shear wall according to Mander model

4.3.4 Cracked elements

For slabs and shear walls in the basement, according to TSC2018 “The effective section stiffness coefficient for in-plane and out-of-plane behavior of linearly modeled shear walls and slabs will be taken from Table 4.2 in 4.5.8.” as mentioned in the 5.4.5.1. in TSC2018.

For beams, columns, and shear walls with plastic hinges, the Turkish Code has been given an equation for calculating the effective stiffness coefficient. (as mentioned in paragraph 5.4.5.2.in (5.2), (5.3) equation in TSC2018).

But when we use this equation, we notice that it does not work well and gives very small values, which causes the building to weaken consequently, the pushover curve will be down. It is more logical to use this equation only in the plastic hinge zone (nonlinear zone), that is, at the beginning and end of the element. While using the table values for (linear zone) in the middle part of the element is not practical because we define an element as one part and not three parts during the modeling of the building, above that, there is a large number of elements in the building. So, in this study values that were used as in the Table 3.5, for the effective stiffness, coefficient for column flexure = 0.7, for beam flexure (bending)= 0.35, and shear wall (mid-peir) flexure= 0.5, and shear= 0.5.

Table 4.14 The effective stiffness coefficient for beam by using equation nonlinear TSC2018

	fce	b	h	η	fce	fye	E	fyw	dp(m)
	25	0.25	0.5	1	32.5	504	31000000	420	0.014
The effective stiffness coefficient (Beam)									
	Ln (net açıklık)	Ls (kesme uzunluğu	Moment	Curvature	Ɵy	Eıe	I	EI	coefficient
1	2.18	1.09	91.643	6.75E-03	0.006029	5522.87	0.002604	80729.17	0.0684123
2	2.8	1.4	91.643	6.75E-03	0.006498	6581.64	0.002604	80729.17	0.0815274
3	2.8	1.4	91.2261	0.00686	0.006566	6483.498	0.002604	80729.17	0.0803117
4	3.75	1.875	91.2261	0.00686	0.007449	7654.397	0.002604	80729.17	0.0948158
5	2.9	1.45	119.6914	0.00712	0.006819	8484.081	0.002604	80729.17	0.1050931
6	4.35	2.175	119.6914	0.00712	0.008281	10479.22	0.002604	80729.17	0.1298071
7	4.07	2.035	120.8425	0.00703	0.005871	13962.7	0.002604	80729.17	0.1729573
8	4.08	2.04	120.8425	0.00703	0.00792	10376.02	0.002604	80729.17	0.1285287
9	4.42	2.21	202.0181	0.00796	0.009104	16345.88	0.002604	80729.17	0.2024781
10	4.43	2.215	202.0181	0.00796	0.009117	16361.09	0.002604	80729.17	0.2026664

Table 4.15 The effective stiffness coefficient for the column by using equation nonlinear TSC2018

30/70	K(S1,2,3,4,12,13,14,15)				TSC2018 (Nonlinear)			
Fc	b	h	dp(m)	η	fce	fye	E	fy
25	0.3	0.7	0.016	1	32.5	504	31000000	420
The effective stiffness coefficient (column)								
KAT	ɸy	MY	LS	Ɵy	Eıe	I	EI	coefficient
1.Story	0.00725	612.847	1.25	0.00706274	36154.9297	0.008575	265825	0.1360
2.Story	0.007128	597.95	1.25	0.00699034	35641.4645	0.008575	265825	0.1340
3.Story	0.00699	581.0285	1.25	0.00690844	35043.417	0.008575	265825	0.1318
4.Story	0.00688	562.546	1.25	0.00684315	34252.3631	0.008575	265825	0.1288
5.Story	0.00674	540.418	1.25	0.00676007	33309.4641	0.008575	265825	0.1253
6.Story	0.00664	518.8913	1.25	0.00670072	32265.9037	0.008575	265825	0.1213
7.Story	0.00655	495.1922	1.25	0.0066473	31039.663	0.008575	265825	0.1167
8.Story	0.00648	471.0039	1.25	0.00660576	29709.1643	0.008575	265825	0.1117
9.Story	0.00623	414.859	1.25	0.00645739	26769.0062	0.008575	265825	0.1007
10.Story	0.00644	421.4294	1.25	0.00658202	26678.0638	0.008575	265825	0.1003
11.Story	0.0063	389.7521	1.25	0.00649893	24988.2076	0.008575	265825	0.0940
12.Story	0.00635	357.9029	1.25	0.00652861	22841.9611	0.008575	265825	0.0859

4.3.5 Moment-curvature and interaction surface in SAP2000

To calculate the moment-curvature and interaction surface of the element sections all cross-sections of the elements were created, beams, columns, and shear walls from the "Section Designer" menu in SAP2000.

For beams, all beams have the same cross-section dimension of (25-50). But the quantity of its rebar is different, so sections were defined according to its rebar and moment-curvature was calculated. The figure shows the calculation of moment-curvature for a beam section containing 4Ø14 rebar at the bottom and 3 Ø14 rebars at the top.

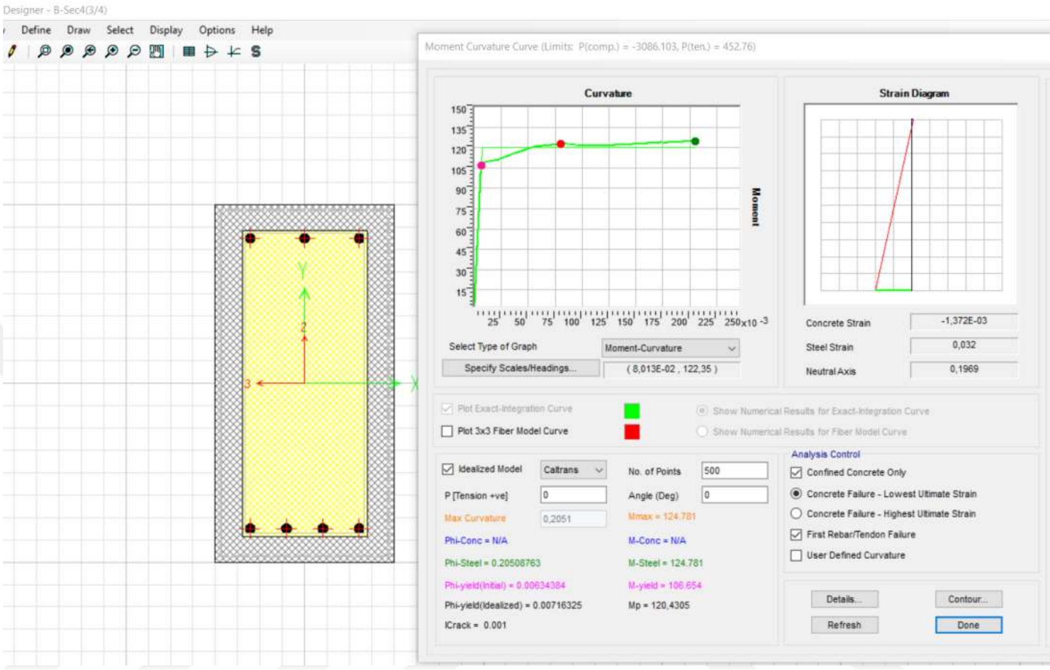

Figure 4.54 Modeling Section Beam and calculate moment-curvature

As for the shear walls and columns, the moment-curvature was calculated for all sections for M2, M3 changing angle (0-90) as shown in the Figure 4.55 and according to the axial load P that differs from section to section and from floor to floor. Interaction surface was also calculated for all sections of columns and shear walls from the section design menu, where after defining the section, the interaction surface is obtained by clicking on the “Show Interaction Surface” button. There are 24 curves of different degrees. In this study, three curves with angles 0, 45, 90 were taken for each section.

The Figure 4.55 shows the calculation of moment-curvature for a column section (30/70), 12 Ø16 and axial load is P=1680.47 KN.

The Figure 4.56 shows the interaction surface for the same column that sections (30/70).

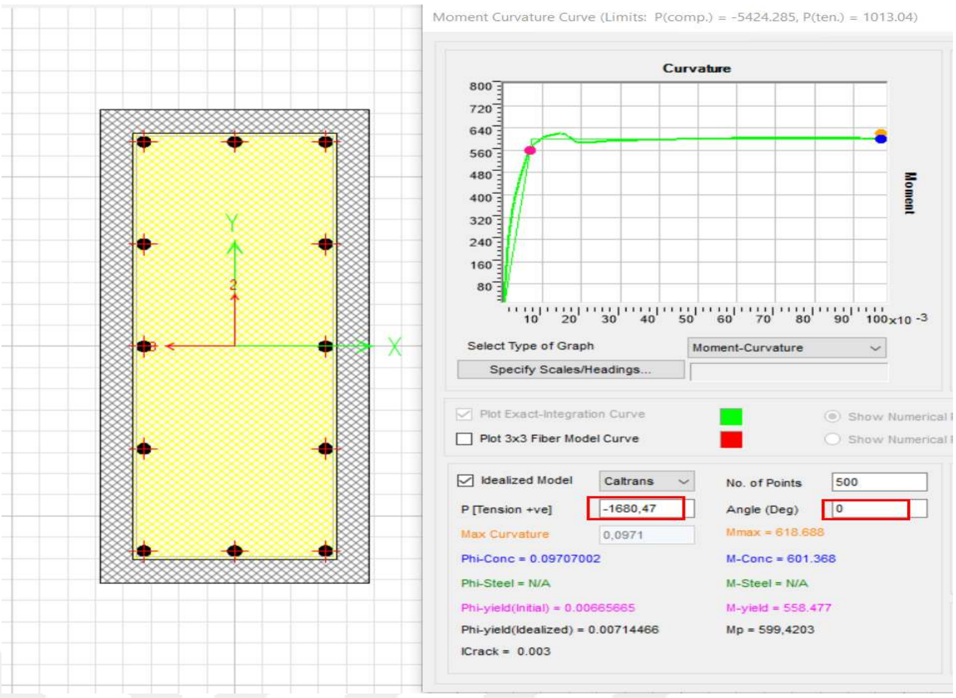

Figure 4.55 Modeling Section Column and calculate moment-curvature

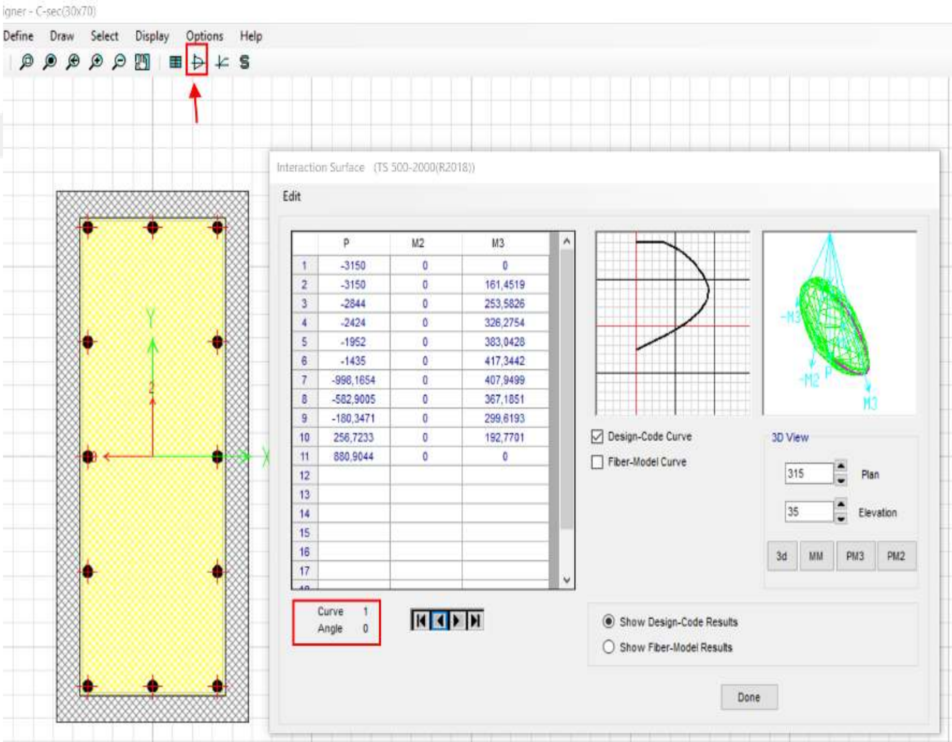

Figure 4.56 Interaction Surface curve for a section column (angle= 0)

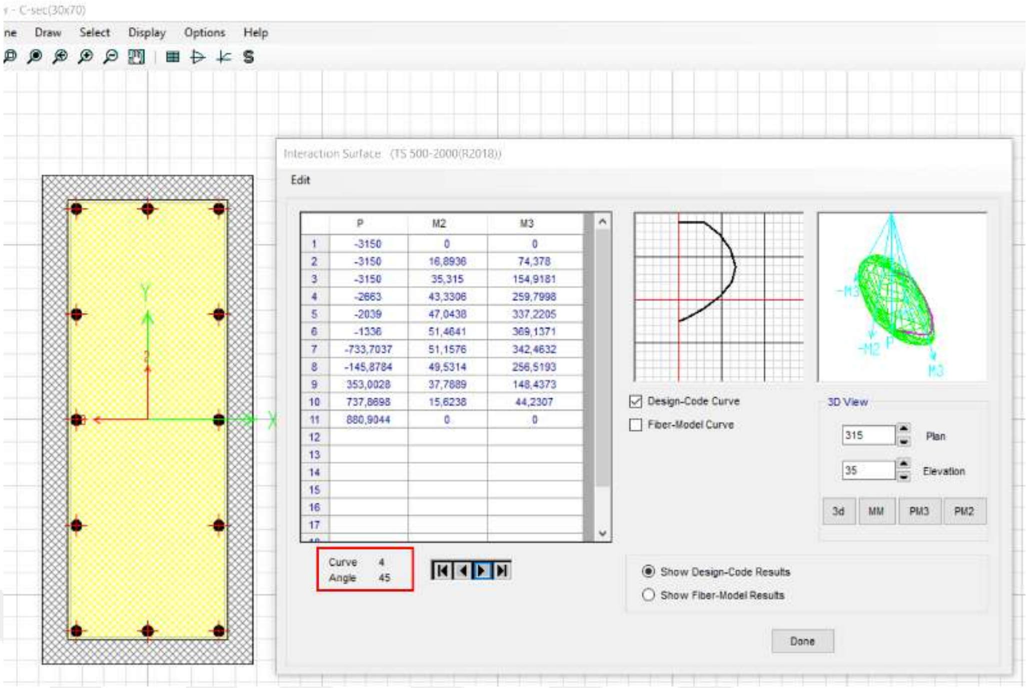

Figure 4.57 Interaction Surface curve for a section column (angle= 45)

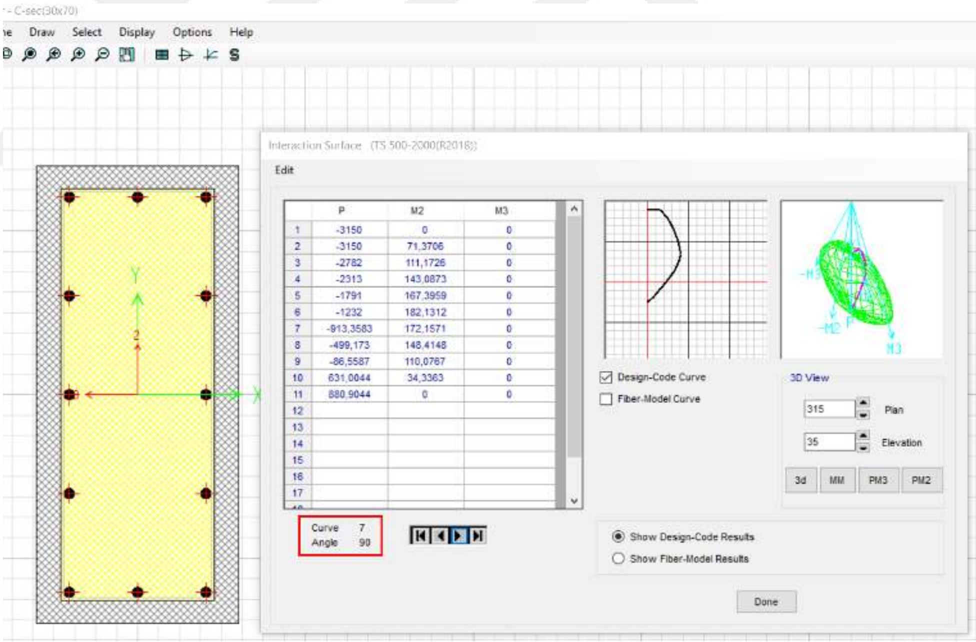

Figure 4.58 Interaction Surface curve for a section column (angle= 90)

4.3.6 Define and assignment of plastic hinges to sections

It is possible to assign automatically the plastic hinges for all elements in SAP2000, but in order to obtain more realistic solutions, plastic hinges properties are defined manually for all sections and then assign it. The M3 type was used for the beam hinge. The figure shows the definition of the hinge properties of a beam section. The idealized moment-rotation of the section beam has been entered in “Displacement Control Parameters”. The rotation is obtained by multiplying the curvature by plastic hinge length ($\theta = L_p * Ø$), Lp=0.5 h (where the length of plastic hinge is equal to the half of the section’s length in the effective direction) as mentioned in paragraph 5.3.1.2 in TSC2018. The plastic deformation was calculated for three levels (Immediate Occupancy, Life Safety, and Collapse Prevention according to the TSC2018 of all beam sections. And this data has been entered into the " Acceptance Criteria (plastic rotation/SF)" part from “Frame Hinge Property”.

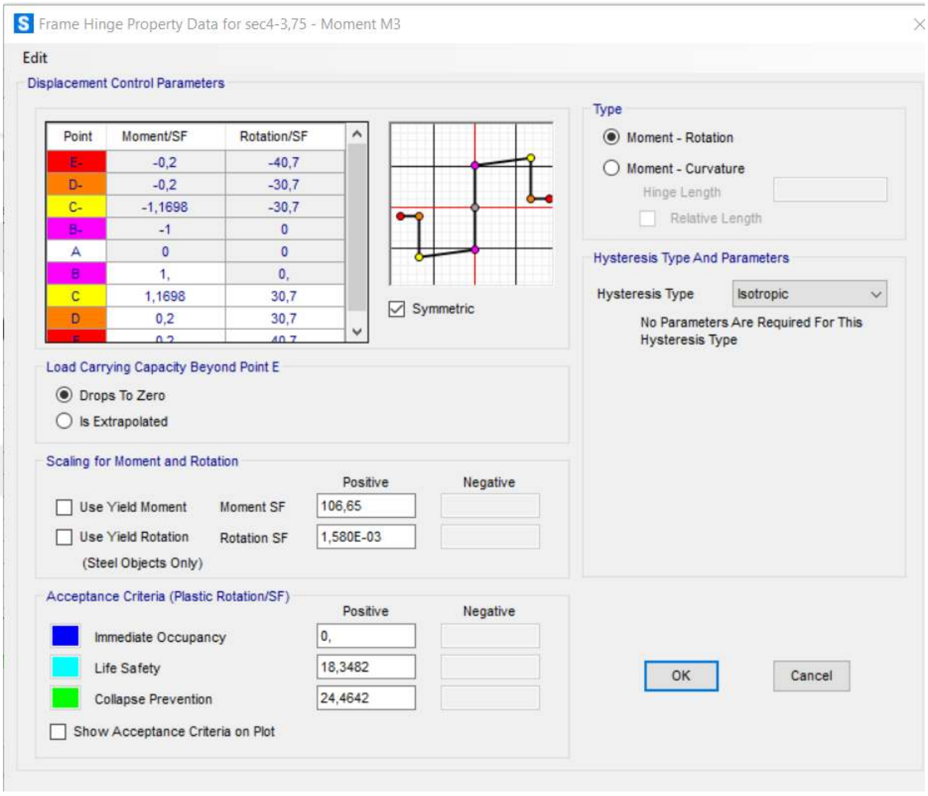

Figure 4.59 Frame hinge property data for beam

The P-M2-M3 type was used for columns and shear walls hinge. The Figures below show the definition of the hinge properties of a column section. Where the same method was followed to define all hinge properties of the sections of columns and walls. To define the 3D interaction curve for column 3 curve “Number of Curves” 3 curves were selected (P-M2, P-M3, P-M2-M3), As previously calculated in the section design in SAP2000 for (0, 45, 90) degrees. As for “Moment Rotation Data” Windows, it has been defined as previously mentioned for the beams, but the difference in the columns was defined for the x, y directions by changing the angle 0 and 90.

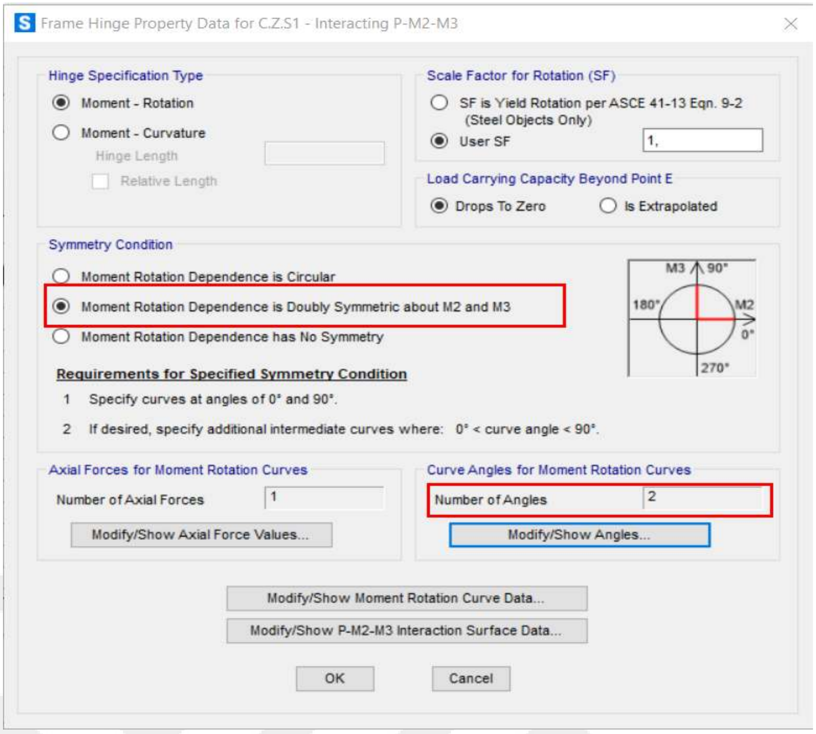

Figure 4.60 Modeling Section Beam and calculate moment – curvature

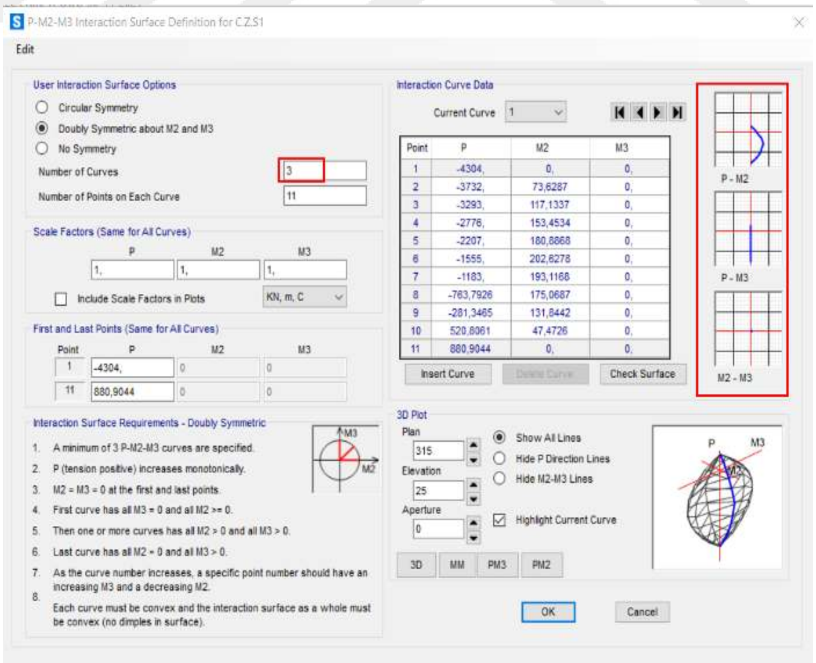

Figure 4.61 Interaction curve definition for column

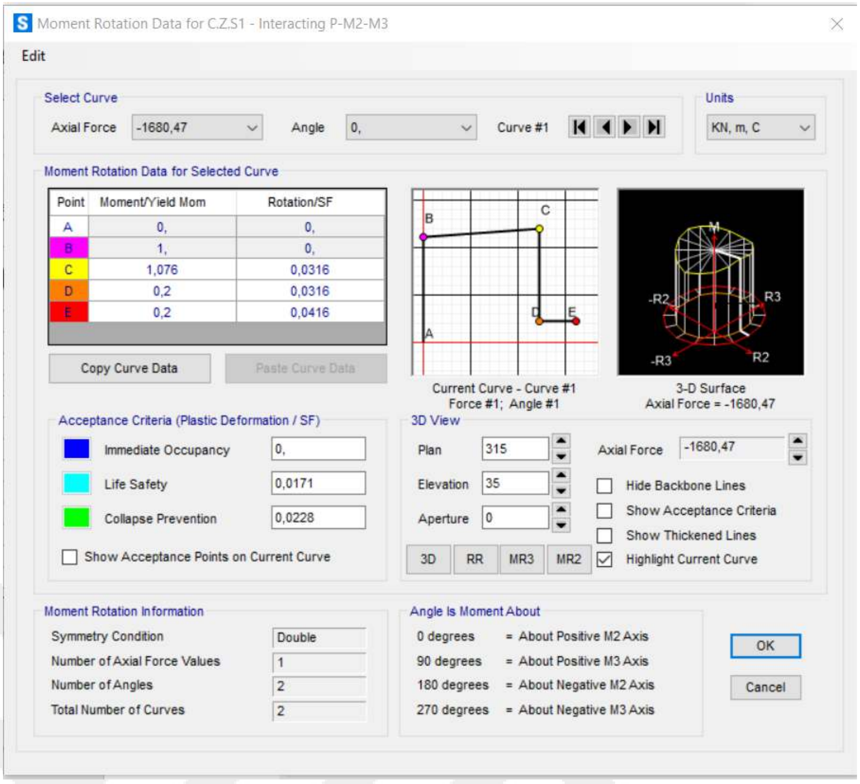

Figure 4.62 Moment rotation data for column

The plastic hinges are assigned in the beams and columns at the beginning and end of each element, as for the shear walls, they were assigned at the lower end of each floor in accordance with paragraph 5.4.3.1.a of the TSC2018.

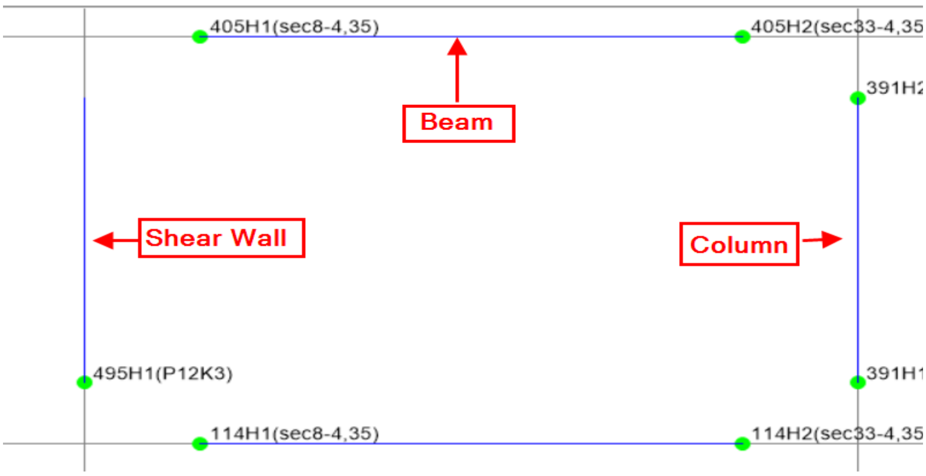

Figure 4.63 Assignments of plastic hinge for beam, column, and shear wall

4.3.7 Identification of nonlinear loads

Nonlinear loads were defined according to pushover and time history analysis.

4.3.7.1 For pushover analysis

The response spectrum was defined according to the TSC2018, where soil type and spectrum parameters were entered. Spectrum factors were obtained from the AFAD site, which depends on soil type, seismic zone, latitudinal, and longitudinal.

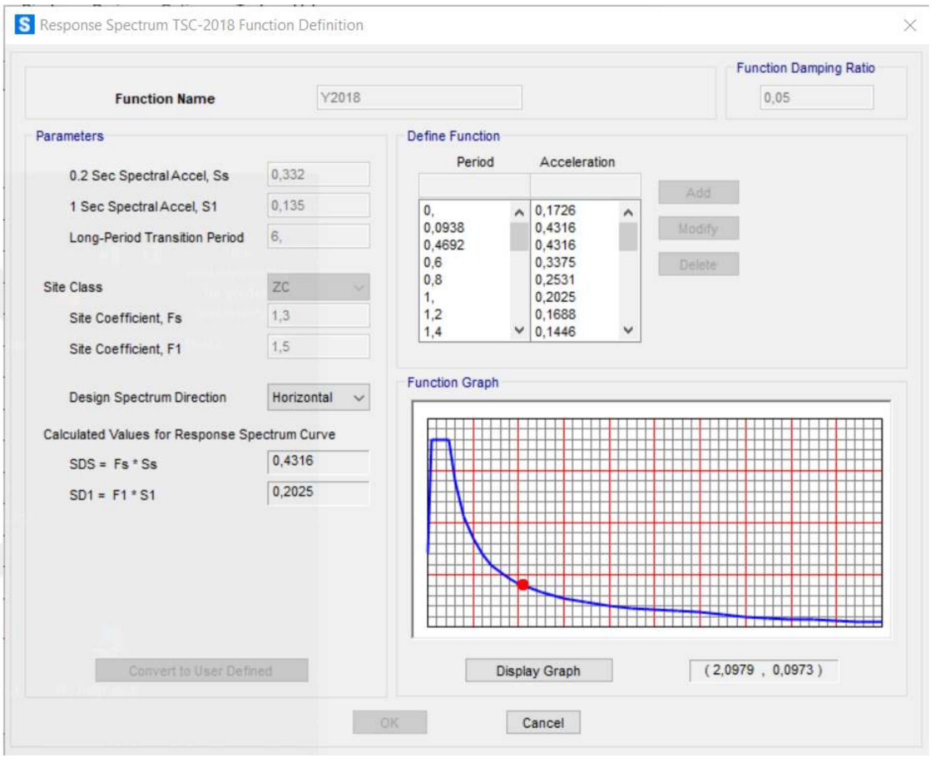

Figure 4.64 Response spectrum TSC-2018 function definition

The loads to be used in the vertical analysis are entered as a total load for dead load and 0.3 of the live loads as specified in TSC- 2018. Where pushover analysis was applied under constant vertical load and seismic load.

4.3.7.2 For time-history

The building was modeled and analyzed to be compatible with TSC-2018. During modeling and analysis, some idealizations were made so that the analysis time would not be prolonged. According to TSC-2018, at least 11 ground motions must be applied to the structure. These ground movements should be rotated 90 degrees and effected on the structure again (TSC2018). However, since this process will prolong the analysis time, only 3 earthquake ground motion record (Bingol, Duzce, and Erzincan) has been applied to the building.

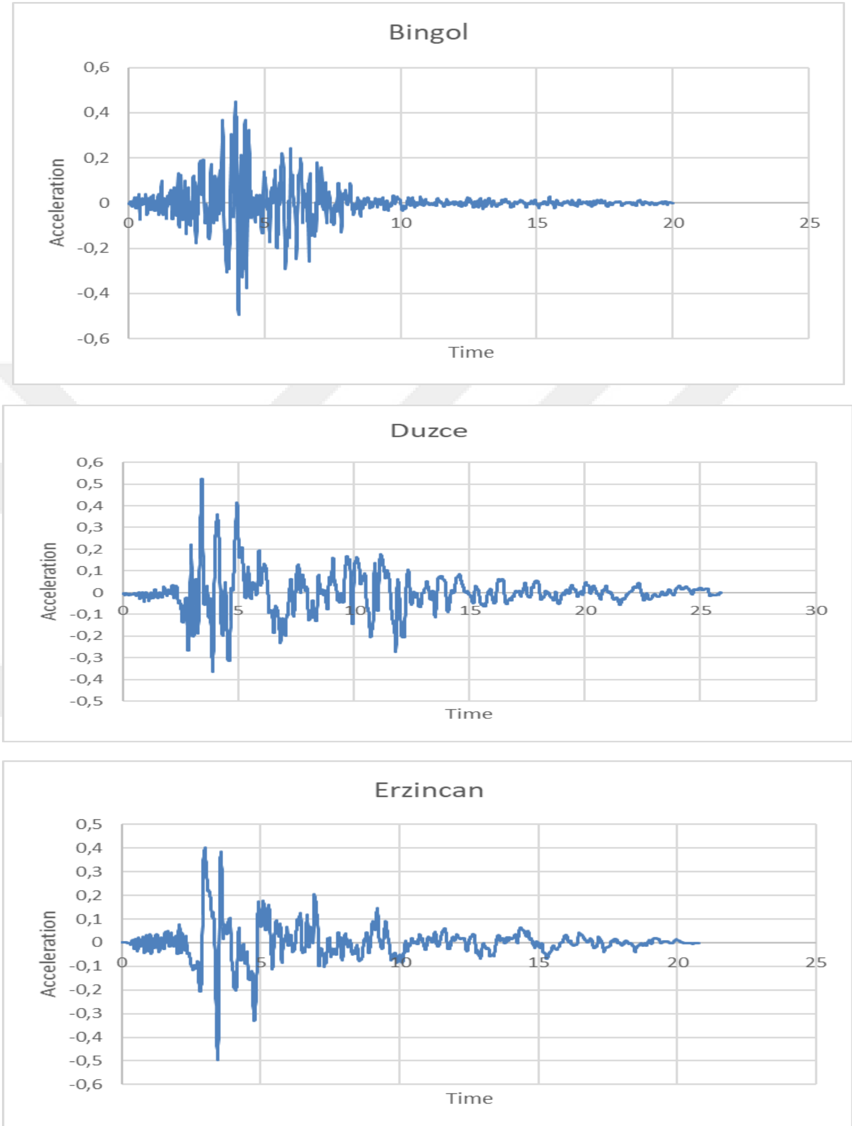

Figure 4.65 Earthquake data used in the analysis

It is very important to assign the earthquake data correctly to the SAP2000 program. The data was transmitted From (Define→ Functions →Time history menu→Choose Function Type to Add→ “from file”). Earthquake records are loaded into the SAP2000 program in two columns as time and acceleration values, and the " Time and Function Values" option is activated from the "Values are:" menu. In the "Function File" section the value "2" was written in the "Head Lines to Skip" part and, the value "1" was entered in the "Number of Points Per Line" section.

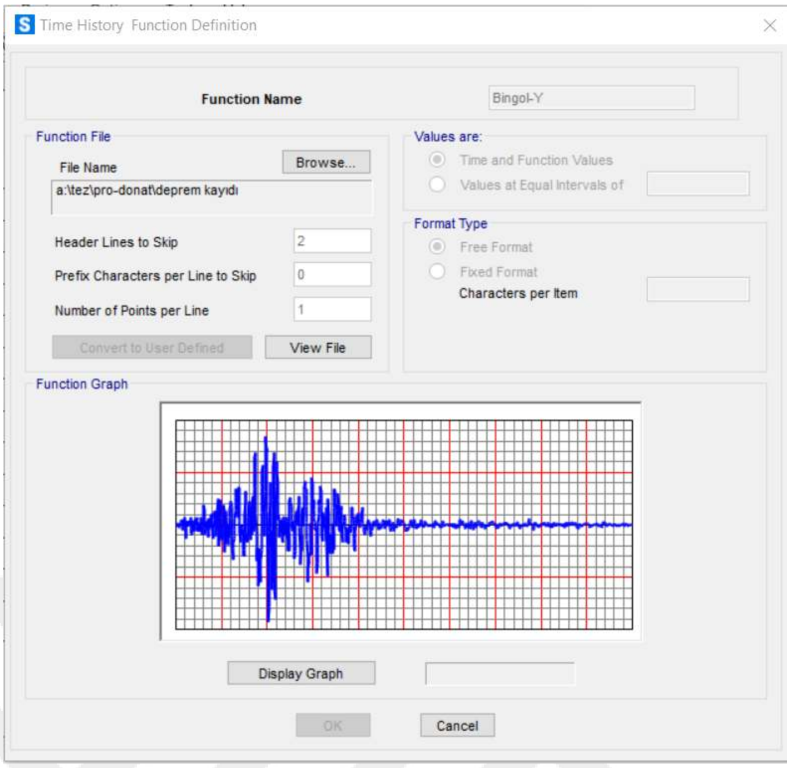

Figure 4.66 Assignment Earthquake data to SAP2000

It is necessary to define the analysis in the time history as the continuation of the nonlinear static analysis of the vertical loads acting on the structure. After the initial loading is defined, the "Load Case Type" as time history, and "Analysis Type" as Nonlinear has been selected. The value of 9,81 has been entered in "Scale Factor" because the acceleration values in the selected records are in terms of "g", that is, gravitational acceleration, they are multiplied by the coefficient of 9.81 m/s².

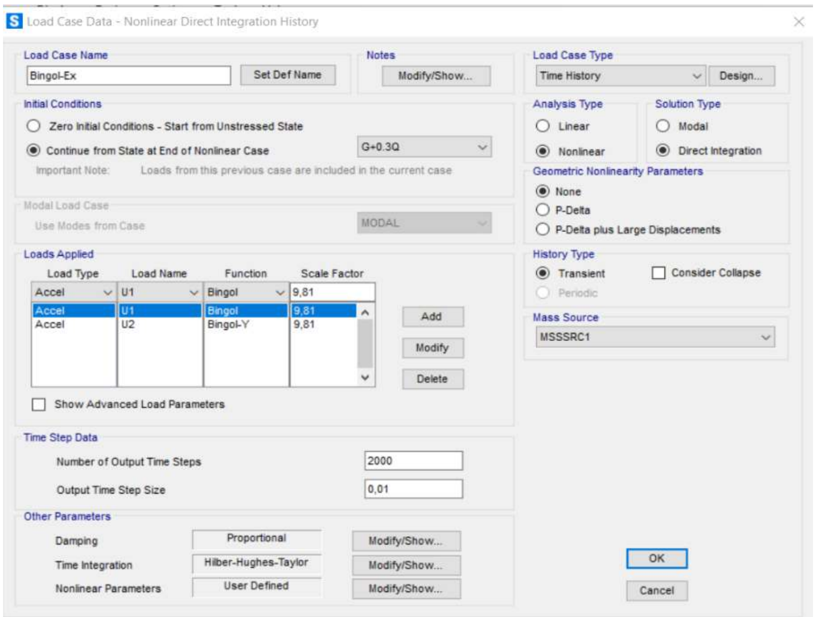

Figure 4.67 Nonlinear load-case in SAP2000

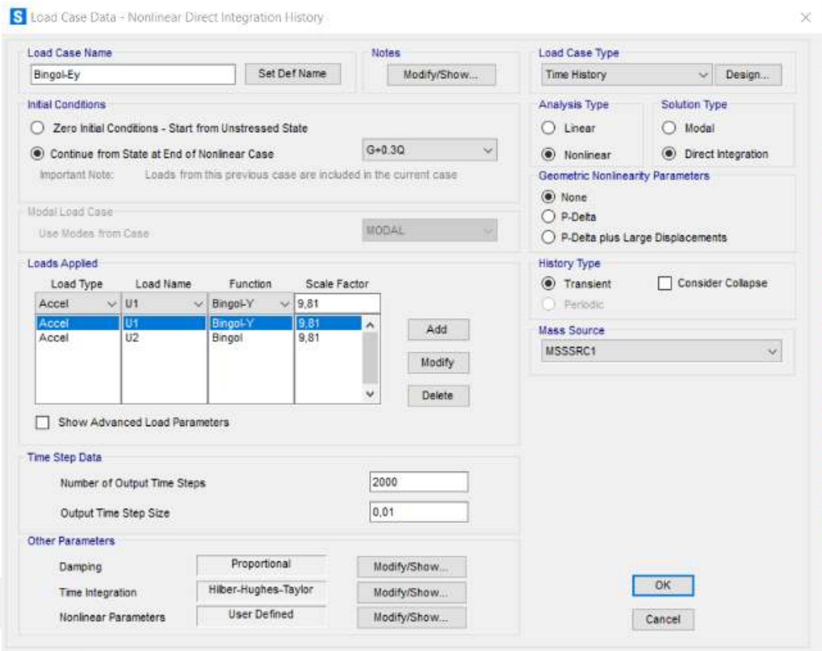

Figure 4.68 Nonlinear load-case in SAP2000 by rotating the axes by 90º

4.3.8 Performance analysis for building according to EC8:

The building was re-analyzed according to EC8. Where the cracked elements and properties of hinges are defined according to EC8. Table 4.16 shows some differences in the calculation between TSC2018, and EC8 codes.

Table 4.16 The differences in the calculation between TSC2018

	Beam (25/50)		Column (40/80)		Perde (25/425)	
	TSC-2018	EC8	TSC-2018	EC8	TSC-2018	EC8
Ѳp (SH, DL)	0	0	0	0	0	0
Ѳp (KH, LS)	0.027587	0.015548	0.016485	0.012132	0.005978	0.004561
Ѳp (GÖ, NC)	0.036783	0.020731	0.02198	0.016176	0.007971	0.006082
Lp	0.25	0.263	0.4	0.349	2.125	1.029
Stiffness factor	0.35	0.5	0.7	0.5	0.5	0.5

4.3.9 Analysis results

The analysis was done and the results obtained as mentioned in below.

4.3.9.1 Pushover curve

Fig 4.68 and Fig 4.69 shows pushover curve for x and y direction

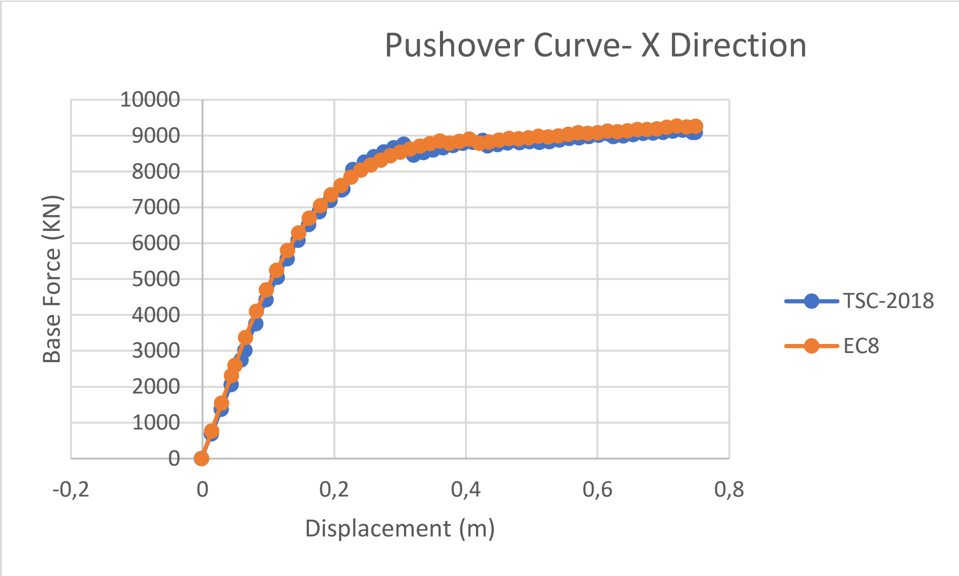

Figure 4.69 Pushover curve for x-direction

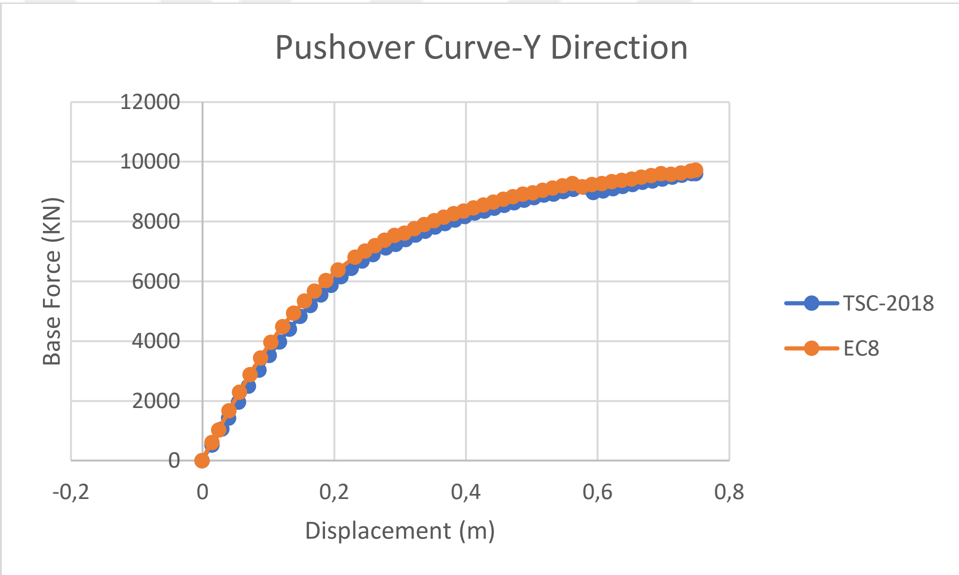

Figure 4.70 Pushover curve for y-direction

4.3.9.2 The plastic deformation that occurred to the elements according to pushover analysis (TSC-2018, EC8)

Table 4.17 The plastic deformation of beams according to pushover in the x-direction

Pushover-x							
Beam		TSC2018			Euro2004		
	Number of beam	IO-LS	LS- CP	> CP	IO-LS	LS- CP	> CP
Basement	43	0	0	0	3	0	0
Ground floor	63	14	0	0	21	0	0
1. Story	63	20	0	0	23	0	0
2. Story	63	20	0	0	24	0	0
3. Story	63	22	0	0	24	0	0
4. Story	63	20	0	0	24	0	0
5. Story	63	19	0	0	24	0	0
6. Story	63	19	0	0	22	0	0
7. Story	63	19	0	0	19	0	0
8. Story	63	16	0	0	19	0	0
9. Story	63	14	0	0	17	0	0
10. Story	63	13	0	0	15	0	0
11. Story	63	11	0	0	13	0	0
12. Story	63	6	0	0	10	0	0
Total	862	213	0	0	258	0	0

Table 4.18 The plastic deformation of shear walls according to pushover in the x-direction

Pushover-x							
ShearWall		TSC2018			Euro2004		
	Number of shear wall	IO-LS	LS- CP	> CP	IO-LS	LS- CP	> CP
Basement	24	1	0	0	1	0	0
Ground floor	24	2	0	0	2	0	0
1. Story	24	0	0	0	0	0	0
2. Story	24	0	0	0	0	0	0
3. Story	24	0	0	0	0	0	0
4. Story	24	0	0	0	0	0	0
5. Story	24	0	0	0	0	0	0
6. Story	24	0	0	0	0	0	0
7. Story	24	0	0	0	0	0	0
8. Story	24	0	0	0	0	0	0
9. Story	24	0	0	0	0	0	0
10. Story	24	0	0	0	0	0	0
11. Story	24	0	0	0	0	0	0
12. Story	24	0	0	0	0	0	0
Total	336	3	0	0	3	0	0

Table 4.19 The plastic deformation of beams according to pushover in the y-direction

Pushover-y							
Beam		TSC2018			Euro2004		
	Number of beams	IO-LS	LS- CP	> CP	IO-LS	LS- CP	> CP
Basement	43	1	0	0	1	0	0
Ground floor	63	11	0	0	13	0	0
1. Story	63	16	0	0	19	0	0
2. Story	63	19	0	0	19	0	0
3. Story	63	20	0	0	20	0	0
4. Story	63	19	0	0	20	0	0
5. Story	63	18	0	0	20	0	0
6. Story	63	16	0	0	16	0	0
7. Story	63	12	0	0	14	0	0
8. Story	63	8	0	0	10	0	0
9. Story	63	7	0	0	8	0	0
10. Story	63	5	0	0	5	0	0
11. Story	63	5	0	0	5	0	0
12. Story	63	3	0	0	4	0	0
Total	862	160	0	0	174	0	0

Table 4.20 The plastic deformation of shear walls according to pushover in the y-direction

Pushover-y							
ShearWall		TSC2018			Euro2004		
	Number of shear wall	IO-LS	LS- CP	> CP	IO-LS	LS- CP	> CP
Basement	24	1	0	0	1	0	0
Ground floor	24	2	0	0	2	0	0
1. Story	24	1	0	0	1	0	0
2. Story	24	0	0	0	0	0	0
3. Story	24	0	0	0	0	0	0
4. Story	24	0	0	0	0	0	0
5. Story	24	0	0	0	0	0	0
6. Story	24	0	0	0	0	0	0
7. Story	24	0	0	0	0	0	0
8. Story	24	0	0	0	0	0	0
9. Story	24	0	0	0	0	0	0
10. Story	24	0	0	0	0	0	0
11. Story	24	0	0	0	0	0	0
12. Story	24	0	0	0	0	0	0
Total	336	4	0	0	4	0	0

4.3.9.3 The plastic deformation that occurred to the elements according to time history analysis (TSC-2018, EC8)

Table 4.21 The plastic deformation of beams according to time history (Bingol-1)

Bingol-1								
Beam		TSC2018			Euro2004			
	Number of beams	IO-LS	LS- CP	> CP	IO-LS	LS- CP	> CP
Basement	43	1	0	0	1	0	0
Ground floor	63	6	0	0	13	0	0
1. Story	63	3	0	0	10	0	0
2. Story	63	4	0	0	14	0	0
3. Story	63	3	0	0	9	0	0
4. Story	63	0	0	0	5	0	0
5. Story	63	0	0	0	1	0	0
6. Story	63	0	0	0	5	0	0
7. Story	63	1	0	0	16	0	0
8. Story	63	10	0	0	22	0	0
9. Story	63	22	0	0	24	0	0
10. Story	63	24	0	0	25	0	0
11. Story	63	23	0	0	25	0	0
12. Story	63	22	0	0	23	0	0
Total	862	119	0	0	193	0	0

Table 4.22 The plastic deformation of shear walls according to time history (Bingol-1)

Bingol-1							
Shear Wall		TSC2018			Euro2004		
	Number of shear wall	IO-LS	LS- CP	> CP	IO-LS	LS- CP	> CP
Basement	43	1	0	0	1	0	0
Ground floor	63	0	0	0	0	0	0
1. Story	63	0	0	0	0	0	0
2. Story	63	0	0	0	0	0	0
3. Story	63	0	0	0	0	0	0
4. Story	63	0	0	0	0	0	0
5. Story	63	0	0	0	0	0	0
6. Story	63	0	0	0	0	0	0
7. Story	63	1	0	0	1	0	0
8. Story	63	1	0	0	1	0	0
9. Story	63	0	0	0	0	0	0
10. Story	63	0	0	0	0	0	0
11. Story	63	0	0	0	0	0	0
12. Story	63	0	0	0	0	0	0
Total	862	3	0	0	3	0	0

Table 4.23 The plastic deformation of beams according to time history (Bingol-2)

Bingol-2							
Beam		TSC2018			Euro2004		
	Number of beams	IO-LS	LS- CP	> CP	IO-LS	LS- CP	> CP
Basement	43	1	0	0	1	0	0
Ground floor	63	1	0	0	6	0	0
1. Story	63	4	0	0	6	0	0
2. Story	63	5	0	0	6	0	0
3. Story	63	5	0	0	6	0	0
4. Story	63	3	0	0	6	0	0
5. Story	63	0	0	0	4	0	0
6. Story	63	0	0	0	5	0	0
7. Story	63	6	0	0	8	0	0
8. Story	63	7	0	0	8	0	0
9. Story	63	7	0	0	8	0	0
10. Story	63	8	0	0	9	0	0
11. Story	63	8	0	0	10	0	0
12. Story	63	8	0	0	7	0	0
Total	862	63	0	0	90	0	0

Table 4.24 The plastic deformation of shear walls according to time history (Bingol-2)

Bingol-2							
Shear Wall		TSC2018			Euro2004		
	Number of shear wall	IO-LS	LS- CP	> CP	IO-LS	LS- CP	> CP
Basement	43	0	0	0	0	0	0
Ground floor	63	0	0	0	0	0	0
1. Story	63	0	0	0	0	0	0
2. Story	63	0	0	0	0	0	0
3. Story	63	0	0	0	0	0	0
4. Story	63	0	0	0	0	0	0
5. Story	63	0	0	0	0	0	0
6. Story	63	0	0	0	0	0	0
7. Story	63	1	0	0	1	0	0
8. Story	63	1	0	0	1	0	0
9. Story	63	1	0	0	1	0	0
10. Story	63	0	0	0	0	0	0
11. Story	63	0	0	0	0	0	0
12. Story	63	0	0	0	0	0	0
Total	862	3	0	0	3	0	0

Table 4.25 The plastic deformation of beams according to time history (Duzce-1)

Duzce-1								
Beam		TSC2018			Euro2004		
	Number of beams	IO-LS	LS- CP	> CP	IO-LS	LS- CP	> CP
Basement	43	17	0	0	21	0	0
Ground floor	63	37	0	0	36	1	1
1. Story	63	38	0	0	30	9	2
2. Story	63	38	1	0	29	10	2
3. Story	63	38	1	0	31	10	2
4. Story	63	37	1	0	31	10	2
5. Story	63	38	1	0	31	9	2
6. Story	63	39	1	0	32	9	1
7. Story	63	41	1	0	35	6	1
8. Story	63	41	0	0	35	6	1
9. Story	63	41	0	0	37	5	1
10. Story	63	41	0	0	40	0	1
11. Story	63	41	0	0	40	0	1
12. Story	63	39	0	0	39	0	1
Total	862	526	6	0	467	75	18

Table 4.26 The plastic deformation of columns according to time history (Duzce-1)

Duzce-1							
Column		TSC2018			Euro2004		
	Number of columns	IO-LS	LS- CP	> CP	IO-LS	LS- CP	> CP
Basement	15	1	0	0	0	0	0
Ground floor	15	15	0	0	15	0	0
1. Story	15	11	0	0	7	0	0
2. Story	15	1	0	0	0	0	0
3. Story	15	0	0	0	0	0	0
4. Story	15	0	0	0	0	0	0
5. Story	15	0	0	0	0	0	0
6. Story	15	0	0	0	0	0	0
7. Story	15	0	0	0	0	0	0
8. Story	15	0	0	0	0	0	0
9. Story	15	0	0	0	0	0	0
10. Story	15	0	0	0	1	0	0
11. Story	15	1	0	0	2	0	0
12. Story	15	4	0	0	5	0	0
Total	210	33	0	0	30	0	0

Table 4.27 The plastic deformation of shear walls according to time history (Duzce-1)

Duzce-1							
ShearWall		TSC2018			Euro2004		
	Number of shear wall	IO-LS	LS- CP	> CP	IO-LS	LS- CP	> CP
Basement	24	7	0	0	6	0	0
Ground floor	24	19	0	0	19	0	0
1. Story	24	12	0	0	12	0	0
2. Story	24	7	0	0	6	0	0
3. Story	24	6	0	0	6	0	0
4. Story	24	6	0	0	7	0	0
5. Story	24	6	0	0	6	0	0
6. Story	24	7	0	0	6	0	0
7. Story	24	6	0	0	5	0	0
8. Story	24	6	0	0	6	0	0
9. Story	24	4	0	0	4	0	0
10. Story	24	2	0	0	3	0	0
11. Story	24	0	0	0	0	0	0
12. Story	24	0	0	0	0	0	0
Total	336	88	0	0	86	0	0

Table 4.28 The plastic deformation of beams according to time history (Duzce-2)

Duzce-2							
Beam		TSC2018			Euro2004		
	Number of beams	IO-LS	LS- CP	> CP	IO-LS	LS- CP	> CP
Basement	43	17	0	0	17	0	0
Ground floor	63	47	0	0	39	9	0
1. Story	63	50	0	0	40	10	5
2. Story	63	51	0	0	39	10	6
3. Story	63	50	0	0	39	9	6
4. Story	63	49	0	0	40	9	4
5. Story	63	49	0	0	40	10	2
6. Story	63	51	0	0	43	9	0
7. Story	63	62	0	0	43	7	0
8. Story	63	49	0	0	45	5	0
9. Story	63	50	0	0	46	0	0
10. Story	63	46	0	0	47	0	0
11. Story	63	42	0	0	44	0	0
12. Story	63	32	0	0	34	0	0
Total	862	645	0	0	556	78	23

Table 4.29 The plastic deformation of columns according to time history (Duzce-2)

Duzce-2							
Column		TSC2018			Euro2004		
	Number of columns	IO-LS	LS- CP	> CP	IO-LS	LS- CP	> CP
Basement	15	0	0	0	13	0	0
Ground floor	15	15	0	0	10	0	0
1. Story	15	12	0	0	1	0	0
2. Story	15	5	0	0	1	0	0
3. Story	15	1	0	0	1	0	0
4. Story	15	1	0	0	1	0	0
5. Story	15	1	0	0	1	0	0
6. Story	15	1	0	0	1	0	0
7. Story	15	1	0	0	1	0	0
8. Story	15	1	0	0	1	0	0
9. Story	15	1	0	0	1	0	0
10. Story	15	1	0	0	1	0	0
11. Story	15	1	0	0	1	0	0
12. Story	15	15	0	0	15	0	0
Total	210	56	0	0	49	0	0

Table 4.30 The plastic deformation of shear walls according to time history (Duzce-2)

Duzce-2							
ShearWall		TSC2018			Euro2004		
	Number of shear wall	IO-LS	LS- CP	> CP	IO-LS	LS- CP	> CP
Basement	24	3	0	0	3		0
Ground floor	24	19	5	1	14	6	5
1. Story	24	15	1	1	13	0	1
2. Story	24	6	0	1	3	0	2
3. Story	24	3	0	0	1	0	2
4. Story	24	3	0	0	2	0	1
5. Story	24	3	0	0	2	1	0
6. Story	24	6	0	0	4	0	0
7. Story	24	6	0	0	4	0	0
8. Story	24	4	0	0	3	0	0
9. Story	24	2	0	0	2	0	0
10. Story	24	2	0	0	2	0	0
11. Story	24	3	0	0	2	0	0
12. Story	24	3	0	0	3	0	0
Total	336	78	6	3	58	7	11

Table 4.31 The plastic deformation of beams according to time history (Erzincan-1)

Erzincan-1							
Beam		TSC2018			Euro2004		
	Number of beams	IO-LS	LS- CP	> CP	IO-LS	LS- CP	> CP
Basement	43	17	0	0	21	0	0
Ground floor	63	36	0	0	37	0	0
1. Story	63	37	0	0	38	0	0
2. Story	63	38	0	0	38	0	0
3. Story	63	37	0	0	38	0	0
4. Story	63	37	0	0	38	0	0
5. Story	63	37	0	0	38	0	0
6. Story	63	37	0	0	38	0	0
7. Story	63	36	0	0	38	0	0
8. Story	63	36	0	0	38	0	0
9. Story	63	38	0	0	38	0	0
10. Story	63	38	0	0	38	0	0
11. Story	63	38	0	0	38	0	0
12. Story	63	37	0	0	38	0	0
Total	862	499	0	0	514	0	0

Table 4.32 The plastic deformation of columns according to time history (Erzincan-1)

Erzincan-1							
Column		TSC2018			Euro2004		
	Number of columns	IO-LS	LS- CP	> CP	IO-LS	LS- CP	> CP
Basement	15	0	0	0	0	0	0
Ground floor	15	14	0	0	10	0	0
1. Story	15	1	0	0	1	0	0
2. Story	15	0	0	0	0	0	0
3. Story	15	0	0	0	0	0	0
4. Story	15	0	0	0	0	0	0
5. Story	15	0	0	0	0	0	0
6. Story	15	0	0	0	0	0	0
7. Story	15	0	0	0	0	0	0
8. Story	15	0	0	0	0	0	0
9. Story	15	0	0	0	0	0	0
10. Story	15	1	0	0	1	0	0
11. Story	15	1	0	0	1	0	0
12. Story	15	4	0	0	4	0	0
Total	210	21	0	0	17	0	0

Table 4.33 The plastic deformation of shear walls according to time history (Erzincan-1)

Erzincan-1							
ShearWall		TSC2018			Euro2004		
	Number of shear wall	IO-LS	LS- CP	> CP	IO-LS	LS- CP	> CP
Basement	24	7	0	0	7	0	0
Ground floor	24	12	0	0	12	1	0
1. Story	24	7	0	0	7	0	0
2. Story	24	4	0	0	4	0	0
3. Story	24	5	0	0	5	0	0
4. Story	24	6	0	0	6	0	0
5. Story	24	6	0	0	6	0	0
6. Story	24	6	0	0	6	0	0
7. Story	24	6	0	0	6	0	0
8. Story	24	5	0	0	5	0	0
9. Story	24	4	0	0	4	0	0
10. Story	24	3	0	0	3	0	0
11. Story	24	0	0	0	0	0	0
12. Story	24	0	0	0	0	0	0
Total	336	71	0	0	71	1	0

Table 4.34 The plastic deformation of beams according to time history (Erzincan-2)

Erzincan-2							
Beam		TSC2018			Euro2004		
	Number of beams	IO-LS	LS- CP	> CP	IO-LS	LS- CP	> CP
Basement	43	9	0	0	11	0	0
Ground floor	63	30	0	0	38	0	0
1. Story	63	41	0	0	45	0	0
2. Story	63	48	0	0	48	0	0
3. Story	63	48	0	0	48	0	0
4. Story	63	49	0	0	47	1	0
5. Story	63	46	0	0	46	1	0
6. Story	63	46	0	0	44	1	0
7. Story	63	43	0	0	44	1	0
8. Story	63	44	0	0	43	1	0
9. Story	63	43	0	0	43	0	0
10. Story	63	42	0	0	41	0	0
11. Story	63	38	0	0	39	0	0
12. Story	63	28	0	0	29	0	0
Total	862	555	0	0	566	5	0

Table 4.35 The plastic deformation of columns according to time history (Erzincan-2)

Erzincan-2							
Column		TSC2018			Euro2004		
	Number of columns	IO-LS	**LS- CP**	> CP	IO-LS	**LS- CP**	> CP
Basement	15	0	0	0	0	0	0
Ground floor	15	15	0	0	6	0	0
1. Story	15	3	0	0	0	0	0
2. Story	15	0	0	0	1	0	0
3. Story	15	0	0	0	1	0	0
4. Story	15	1	0	0	1	0	0
5. Story	15	1	0	0	1	0	0
6. Story	15	1	0	0	1	0	0
7. Story	15	1	0	0	1	0	0
8. Story	15	1	0	0	1	0	0
9. Story	15	1	0	0	1	0	0
10. Story	15	1	0	0	1	0	0
11. Story	15	1	0	0	1	0	0
12. Story	15	15	0	0	15	0	0
Total	210	41	0	0	31	0	0

Table 4.36 The plastic deformation of shear walls according to time history (Erzincan-2)

Erzincan-2							
ShearWall		TSC2018			Euro2004		
	Number of shear wall	IO-LS	LS- CP	> CP	IO-LS	LS- CP	> CP
Basement	24	2	0	0	2	0	0
Ground floor	24	16	0	0	15	0	0
1. Story	24	11	0	0	11	0	0
2. Story	24	3	0	0	3	0	0
3. Story	24	3	0	0	3	0	0
4. Story	24	3	0	0	2	0	0
5. Story	24	3	0	0	2	0	0
6. Story	24	2	0	0	2	0	0
7. Story	24	2	0	0	2	0	0
8. Story	24	2	0	0	2	0	0
9. Story	24	1	0	0	1	0	0
10. Story	24	1	0	0	1	0	0
11. Story	24	1	0	0	1	0	0
12. Story	24	2	0	0	1	0	0
Total	336	52	0	0	48	0	0

4.3.10 Investigate the structural performance according to concrete strain and steel strain by using Erzincan earthquake record (TSC-2018)

4.3.10.1 Check to brittle behavior in columns and shear walls

An examination on the columns and shear walls was applied to find out if there is brittleness or not, however, no brittle behavior was confirmed.

Table 4.37 Checking the brittle behavior of columns

N	O	P	Q	R	S	T	U	V	W	X	Y	Z	AA	AB	AC	AD
	x-doğ								y - döğ							
UserProp	Vmax	Vcr	Vc	Vw	Vr	V3			Vmax	Vcr	Vc	Vw	Vr	V2		
Text	0,22*fcd *b*d	0.65.fctd .b.d	0,8 Vcr	(Ash/s)*f ywd*d	Vr=Vc+V w	KN	Vmax > V3	Vr > V3	0,22*fcd *b*d	0.65.fctd .b.d	0,8 Vcr	(Ash/s)*f ywd*d	Vr=Vc+V w	KN	Vmax > V2	Vr > V2
C.B.S1	680,68	136,045	108,836	372,483	481,319	1,63	OK	OK	740,52	148,005	118,404	378,213	496,617	109,586	OK	OK
C.B.S1	680,68	136,045	108,836	372,483	481,319	1,63	OK	OK	740,52	148,005	118,404	378,213	496,617	109,586	OK	OK
C.B.S1	680,68	136,045	108,836	372,483	481,319	1,63	OK	OK	740,52	148,005	118,404	378,213	496,617	109,586	OK	OK
C.B.S1	680,68	136,045	108,836	372,483	481,319	4,43	OK	OK	740,52	148,005	118,404	378,213	496,617	85,874	OK	OK
C.B.S1	680,68	136,045	108,836	372,483	481,319	4,43	OK	OK	740,52	148,005	118,404	378,213	496,617	85,874	OK	OK
C.B.S1	680,68	136,045	108,836	372,483	481,319	4,43	OK	OK	740,52	148,005	118,404	378,213	496,617	85,874	OK	OK
C.B.S2	811,58	162,208	129,766	355,291	485,057	12,228	OK	OK	863,94	172,673	138,138	567,32	705,458	79,197	OK	OK
C.B.S2	811,58	162,208	129,766	355,291	485,057	12,228	OK	OK	863,94	172,673	138,138	567,32	705,458	79,197	OK	OK
C.B.S2	811,58	162,208	129,766	355,291	485,057	12,228	OK	OK	863,94	172,673	138,138	567,32	705,458	79,197	OK	OK
C.B.S2	811,58	162,208	129,766	355,291	485,057	4,45	OK	OK	863,94	172,673	138,138	567,32	705,458	58,126	OK	OK
C.B.S2	811,58	162,208	129,766	355,291	485,057	4,45	OK	OK	863,94	172,673	138,138	567,32	705,458	58,126	OK	OK
C.B.S2	811,58	162,208	129,766	355,291	485,057	4,45	OK	OK	863,94	172,673	138,138	567,32	705,458	58,126	OK	OK
C.B.S4	680,68	136,045	108,836	372,483	481,319	0,943	OK	OK	740,52	148,005	118,404	378,213	496,617	83,218	OK	OK
C.B.S4	680,68	136,045	108,836	372,483	481,319	0,943	OK	OK	740,52	148,005	118,404	378,213	496,617	83,218	OK	OK
C.B.S4	680,68	136,045	108,836	372,483	481,319	0,943	OK	OK	740,52	148,005	118,404	378,213	496,617	83,218	OK	OK
C.B.S4	680,68	136,045	108,836	372,483	481,319	6,375	OK	OK	740,52	148,005	118,404	378,213	496,617	116,461	OK	OK
C.B.S4	680,68	136,045	108,836	372,483	481,319	6,375	OK	OK	740,52	148,005	118,404	378,213	496,617	116,461	OK	OK
C.B.S4	680,68	136,045	108,836	372,483	481,319	6,375	OK	OK	740,52	148,005	118,404	378,213	496,617	116,461	OK	OK
C.B.S3	811,58	162,208	129,766	355,291	485,057	13,845	OK	OK	863,94	172,673	138,138	756,426	894,564	69,227	OK	OK
C.B.S3	811,58	162,208	129,766	355,291	485,057	13,845	OK	OK	863,94	172,673	138,138	756,426	894,564	69,227	OK	OK
C.B.S3	811,58	162,208	129,766	355,291	485,057	13,845	OK	OK	863,94	172,673	138,138	756,426	894,564	69,227	OK	OK
C.B.S3	811,58	162,208	129,766	355,291	485,057	3,847	OK	OK	863,94	172,673	138,138	756,426	894,564	82,728	OK	OK
C.B.S3	811,58	162,208	129,766	355,291	485,057	3,847	OK	OK	863,94	172,673	138,138	756,426	894,564	82,728	OK	OK
C.B.S3	811,58	162,208	129,766	355,291	485,057	3,847	OK	OK	863,94	172,673	138,138	756,426	894,564	82,728	OK	OK
C.B.S12	680,68	136,045	108,836	372,483	481,319	5,726	OK	OK	740,52	148,005	118,404	378,213	496,617	113,556	OK	OK
C.B.S12	680,68	136,045	108,836	372,483	481,319	5,726	OK	OK	740,52	148,005	118,404	378,213	496,617	113,556	OK	OK
C.B.S12	680,68	136,045	108,836	372,483	481,319	5,726	OK	OK	740,52	148,005	118,404	378,213	496,617	113,556	OK	OK
C.B.S12	680,68	136,045	108,836	372,483	481,319	3,343	OK	OK	740,52	148,005	118,404	378,213	496,617	92,538	OK	OK
C.B.S12	680,68	136,045	108,836	372,483	481,319	3,343	OK	OK	740,52	148,005	118,404	378,213	496,617	92,538	OK	OK
C.B.S12	680,68	136,045	108,836	372,483	481,319	3,343	OK	OK	740,52	148,005	118,404	378,213	496,617	92,538	OK	OK
C.B.S13	811,58	162,208	129,766	355,291	485,057	3,76	OK	OK	863,94	172,673	138,138	567,32	705,458	83,194	OK	OK
C.B.S13	811,58	162,208	129,766	355,291	485,057	3,76	OK	OK	863,94	172,673	138,138	567,32	705,458	83,194	OK	OK
C.B.S13	811,58	162,208	129,766	355,291	485,057	3,76	OK	OK	863,94	172,673	138,138	567,32	705,458	83,194	OK	OK
C.B.S13	811,58	162,208	129,766	355,291	485,057	14,083	OK	OK	863,94	172,673	138,138	567,32	705,458	63,156	OK	OK
C.B.S13	811,58	162,208	129,766	355,291	485,057	14,083	OK	OK	863,94	172,673	138,138	567,32	705,458	63,156	OK	OK

4.3.10.2 The damage of elements base on strain

Table 4.38 shows how the damage was determined based on strain to beams, as the damage to the columns and the shear walls was determined in the same way. The first value in Table 4.38 was explained in detail for a section beam 250/500.

Plastic rotation Θ_p =0.00537 rad.

Plastic curvature $Ø_p = \frac{\theta p}{Lp} = \frac{0.00537}{0.25}$= 0.02149 rad.

Yiled curvature $Ø_y$= 0.00605 rad.

Total curvature $\text{Ø}_t = \text{Ø}_y + \text{Ø}_p = 0.0275$ rad. From the results of the moment-curvature analysis from the section designer in SAP2000. The strain of concrete and steel was obtained (Figure 4.70).

$\varepsilon_c = 0.00048$, $\varepsilon_s = 0.011$. Compare these results of strain with damage limits Table 4.38.

$\varepsilon_c = 0.00048 < \varepsilon_c^{(SH)} = 0.0025$. (SHB)

$\varepsilon_S^{(SH)} = 0.0075 < \varepsilon_s = 0.011 < \varepsilon_S^{(KH)} = 0.024$. (KHB)

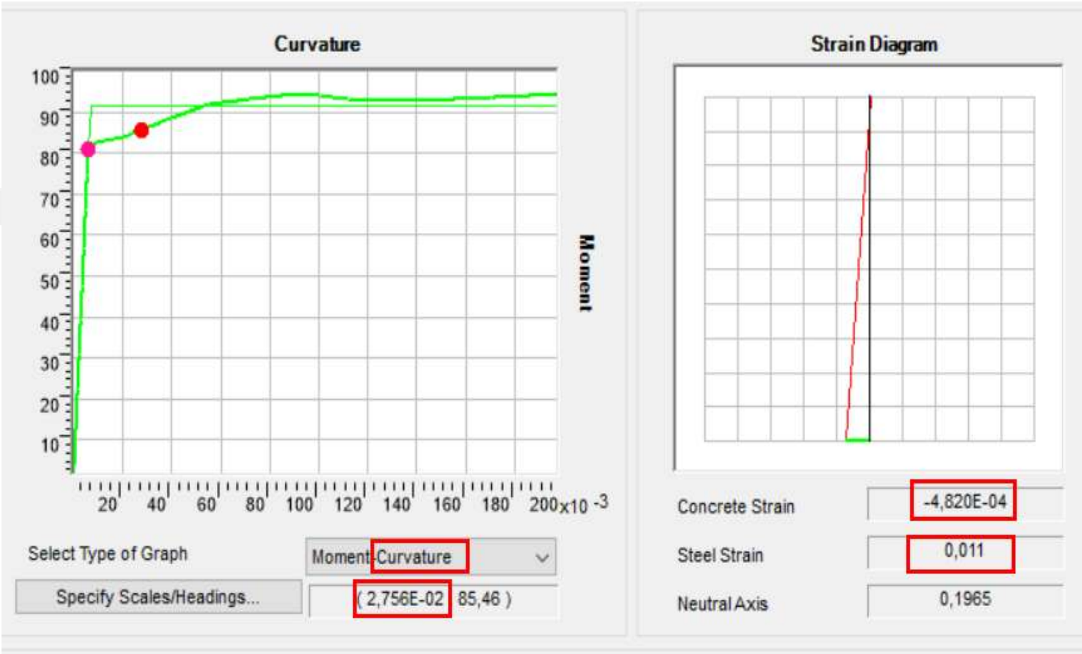

Figure 4.71 The strain of concrete and steel

Table 4.38 The damage limits of strain for a section beam

sec1-3.05		
	εc	εs
SH	0.0025	0.0075
KH	0.005419	0.024
GÖ	0.007225	0.032

Table 4.39 Calculation of damage zone to beams based on strain

AssignHing	R3Plastic	Oy	Curvature-yiled	curvature-plastic	curvature-total	concret-strain	steel-strain	AssignHing	concret-strain	εc-hasar	steel-strain	εs-hasar	HASAR DURUM	Frame	Frame
sec1-3,05	0,00537	0,00151	0,00605	0,02149	0,02754	-0,0005	0,0111	sec1-3,05	0,00048	Sınırlı hasar(SH)	0,0111	Kontrollü Hasar (KH)	Kontrollü Hasar (KH)		1
sec1-3,05	0,00027	0,00151	0,00605	0,00108	0,00713	-0,0004	0,0026	sec1-3,05	0,00044	Sınırlı hasar(SH	0,0026	Sınırlı hasar(SH			1
sec1-3,05	0,00621	0,00151	0,00605	0,02483	0,03088	-0,0005	0,0125	sec1-3,05	0,00049	Sınırlı hasar(SH)	0,0125	Kontrollü Hasar (KH)		1	1
sec1-4,3	0,0067	0,00151	0,00605	0,02679	0,03284	-0,0005	0,0133	sec1-4,3	0,00049	Sınırlı hasar(SH	0,0133	Kontrollü Hasar	Kontrollü Hasar (KH)		2
sec1-4,3	0,00865	0,00151	0,00605	0,03461	0,04066	-0,0005	0,0166	sec1-4,3	0,00051	hasar(SH)	0,0166	Hasar (KH)			2
sec19-4,3	0,00071	0,00165	0,00658	0,00282	0,0094	-0,0007	0,00326	sec19-4,3	0,00072	hasar(SH)	0,00326	hasar(SH)			2
sec19-4,3	0,00099	0,00165	0,00658	0,00395	0,01053	-0,0007	0,00371	sec19-4,3	0,00075	Sınırlı hasar(SH)	0,00371	Sınırlı hasar(SH)		2	2
sec1-3,35	0,00048	0,00151	0,00605	0,00192	0,00797	-0,0004	0,00291	sec1-3,35	0,00045	Sınırlı hasar(SH)	0,00291	Sınırlı hasar(SH)	Kontrollü Hasar (KH)		3
sec1-3,35	0,00624	0,00151	0,00605	0,02496	0,03101	-0,0005	0,0125	sec1-3,35	0,00049	Sınırlı hasar(SH)	0,0125	Kontrollü Hasar (KH)			3
sec1-3,35	0,00064	0,00151	0,00605	0,00254	0,00859	-0,0005	0,00318	sec1-3,35	0,00045	hasar(SH)	0,00318	hasar(SH)			3
sec1-3,35	0,00746	0,00151	0,00605	0,02983	0,03588	-0,0005	0,0145	sec1-3,35	0,0005	Sınırlı hasar(SH)	0,0145	Kontrollü Hasar (KH)		3	3
sec1-4,35	0,00656	0,00151	0,00605	0,02625	0,0323	-0,0005	0,013	sec1-4,35	0,00049	Sınırlı hasar(SH	0,013	Kontrollü Hasar	Kontrollü Hasar (KH)		4
sec1-4,35	0,00603	0,00151	0,00605	0,02412	0,03017	-0,0005	0,0121	sec1-4,35	0,00049	Sınırlı hasar(SH	0,0121	Kontrollü Hasar			4
sec7-4,35	0,00497	0,0015	0,006	0,01989	0,02589	-0,0005	0,0103	sec7-4,35	0,00046	Sınırlı hasar(SH	0,0103	Kontrollü Hasar			4
sec7-4,35	0,00767	0,0015	0,006	0,03066	0,03666	-0,0005	0,0149	sec7-4,35	0,00049	hasar(SH)	0,0149	Hasar (KH)		4	4
										hasar(SH		Hasar			

Table 4.40 The damage of beams base on strain according to time history (Erzincan-1)

strain		Number				%			
	Number of beams	SHB	BHB	İLB	GB	SHB	BHB	İLB	GB
Basement	43	43	0	0	0	100.00	0.00	0.00	0
Ground floor	63	36	27	0	0	57.14	42.86	0.00	0
1. Story	63	34	29	0	0	53.97	46.03	0.00	0
2. Story	63	33	30	0	0	52.38	47.62	0.00	0
3. Story	63	33	30	0	0	52.38	47.62	0.00	0
4. Story	63	29	34	0	0	46.03	53.97	0.00	0
5. Story	63	29	33	1	0	46.03	52,38	1.59	0
6. Story	63	29	33	1	0	46.03	52.38	1.59	0
7. Story	63	30	32	1	0	47.62	50.79	1.59	0
8. Story	63	28	34	1	0	44.44	53.97	1.59	0
9. Story	63	27	35	1	0	42.86	55.56	1.59	0
10. Story	63	29	34	0	0	46.03	53.97	0.00	0
11. Story	63	30	33	0	0	47.62	52.38	0.00	0
12. Story	63	42	21	0	0	66.67	33.33	0.00	0
Total	862	452	405	5	0	52.44	46.98	0.58	0

Table 4.41 The damage of columns base on strain according to time history (Erzincan-1)

strain		Number				%			
	Number of columns	SHB	BHB	İLB	GB	SHB	BHB	İLB	GB
Basement	15	15	0	0	0	100.00	0.00	0.00	0
Ground floor	15	3	12	0	0	20.00	80.00	0.00	0
1. Story	15	14	1	0	0	93.33	6.67	0.00	0
2. Story	15	15	0	0	0	100.00	0.00	0.00	0
3. Story	15	15	0	0	0	100.00	0.00	0.00	0
4. Story	15	15	0	0	0	100.00	0,00	0.00	0
5. Story	15	15	0	0	0	100.00	0,00	0.00	0
6. Story	15	15	0	0	0	100.00	0,00	0.00	0
7. Story	15	15	0	0	0	100.00	0,00	0.00	0
8. Story	15	15	0	0	0	100.00	0,00	0.00	0
9. Story	15	15	0	0	0	100.00	0,00	0.00	0
10. Story	15	15	0	0	0	100.00	0,00	0.00	0
11. Story	15	15	0	0	0	100.00	0,00	0.00	0
12. Story	15	11	4	0	0	73.33	26.67	0.00	0
Total	210	193	17	0	0	91.90	8.10	0.00	0.00

Table 4.42 The damage of shear walls base on strain according to time history (Erzincan-1)

strain		Number				%			
	Numbe r of shear walls	SHB	BHB	İLB	GB	SHB	BHB	İLB	GB
Basemen t	24	24	0	0	0	100.00	0.00	0.00	0
Ground floor	24	21	3	0	0	87.50	12.50	0.00	0
1. Story	24	23	1	0	0	95.83	4.17	0.00	0
2. Story	24	23	1	0	0	95.83	4.17	0.00	0
3. Story	24	24	0	0	0	100.00	0.00	0.00	0
4. Story	24	24	0	0	0	100.00	0.00	0.00	0
5. Story	24	24	0	0	0	100.00	0.00	0.00	0
6. Story	24	24	0	0	0	100.00	0.00	0.00	0
7. Story	24	24	0	0	0	100.00	0.00	0.00	0
8. Story	24	24	0	0	0	100.00	0.00	0.00	0
9. Story	24	24	0	0	0	100.00	0.00	0.00	0
10. Story	24	24	0	0	0	100.00	0.00	0.00	0
11. Story	24	24	0	0	0	100.00	0.00	0.00	0
12. Story	24	24	0	0	0	100.00	0.00	0.00	0
Total	336	331	5	0	0	98.51	1.51	0	0

Thus, the building performance by using Erzincan earthquake record has been classified as Controlled damage. Because the percentage of the beam on the floor has exceeded 20% in the Significant Damage Zone as shown in Table 4.39. On some floors, it may even exceed 50%. Also, no structural elements were recorded in the advanced damage zone as shown in Table 4.40 and Table 4.41. In addition, no brittle elements were recorded.

4.4 The effect of soil type on performance

In this chapter, the effect of soil type was studied by using the pushover method according to TSC2018 rules. The STA4CAD program has been implemented. The example building is a 3-story. The pushover analysis has been carried out four times to consider different soil conditions such as ZB, ZC, ZD, ZE. Finally, the results have been compared.

Table 4.43 Building data

Building Information	
The Number of stories	3 story
floor Hight	3 m
Total Building Hight	9 m
Concrete Class	C20
Rebar Class	S420
Column (Number, Section Dimension)	30, (25x60, 60x35)
Beam (Section Dimension)	(25x60) for all beams
Seismic Zone	DD2
Latitude	37.65425
Longitude	41.234

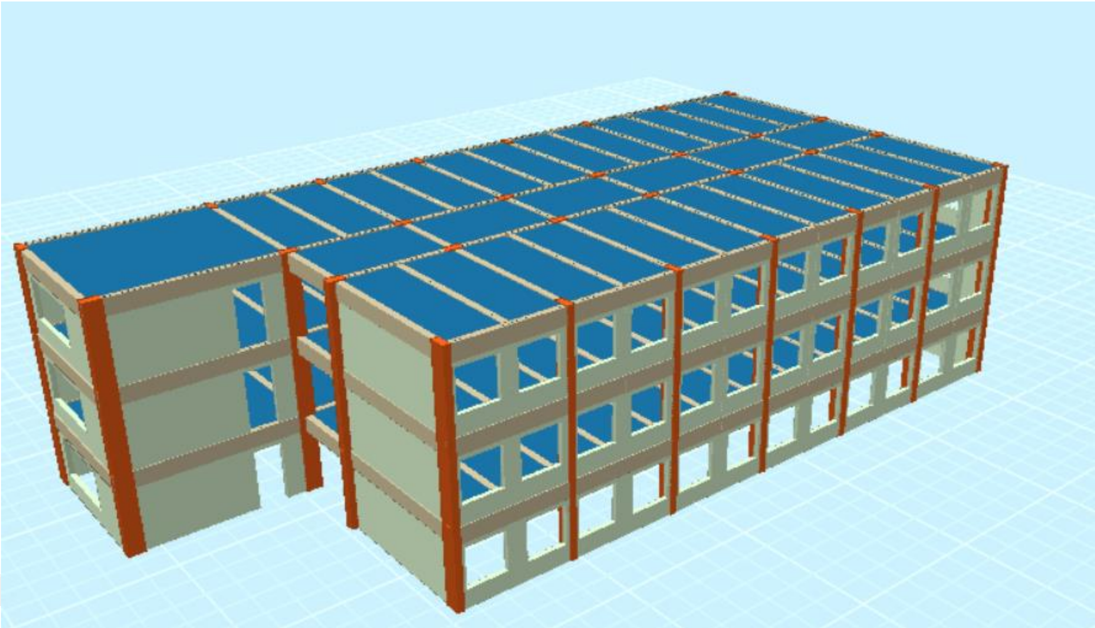

Figure 4.72 3d STA4CAD view of the building

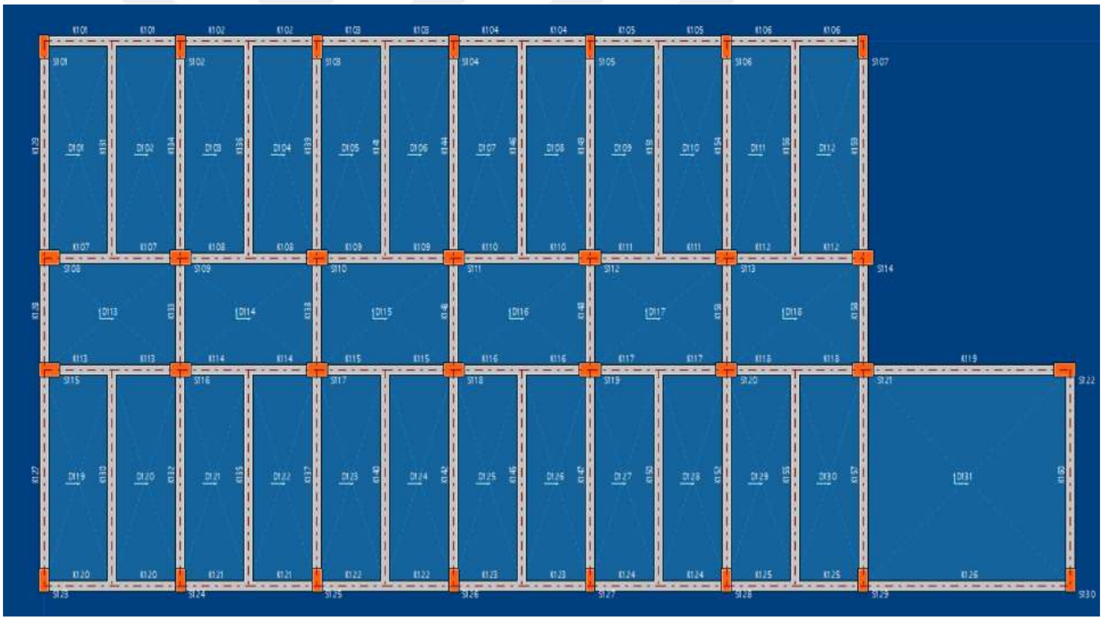

Figure 4.73 2d view floor plan

4.4.1 Definition of soil type in the STA4CAD program

The pushover analysis has been done four times for different soil types (ZB, ZC, ZD, ZE) as given in Figure 4.73 and the results have been given comparatively.

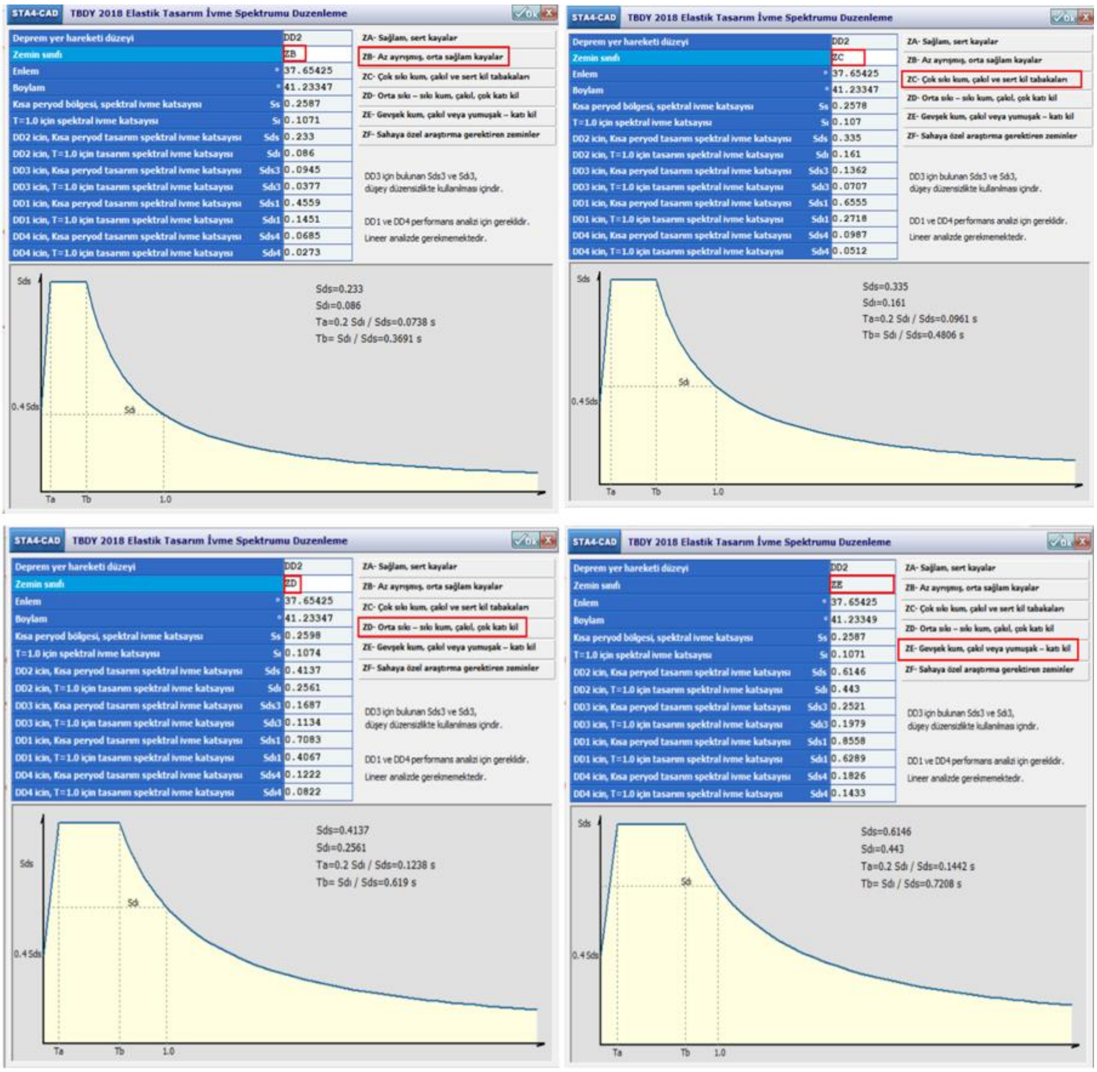

Figure 4.74 Definition of soil classes (ZB, ZC, ZD, ZE) in the Sta4cad program

4.4.2 Analysis results

The performance of building was known for different soil type as shown below. The tables below show the percentage of damage caused to the beams and columns. Based on these ratios, the performance of the building was determined.

Table 4.44 Damage that occurred to beams and columns according to ZB soil class

	Beam damage percentages for ZB class							
	(X) Direction				(Y) Direction			
	SH	BH	IH	GB	SH	BH	IH	GB
3	100	0	0	0	100	0	0	0
2	80.8	19.2	0	0	97.1	0	0	0
1	100	0	0	0	100	0	0	0
Max	100	19.2						

Table 4.44 (Continue)

Column shear force distribution for ZB class								
	(X) Direction				(Y) Direction			
	SH	BH	IH	GB	SH	BH	IH	GB
1	100	0	0	0	100	0	0	0
2	100	0	0	0	100	0	0	0
3	100	0	0	0	100	0	0	0
Max.	100							

Columns Exceeding The Significant Damage Zone In The Lower And Upper Sections, Column shear force distribution (for ZB class)				
	(X) SH+BH	(X) IH+BH	(Y) SH+BH	(Y) IH+BH
3	100	0	100	0
2	100	0	100	0
1	100	0	100	0
Max.	100			

Building performance result for ZB soil class:

Beam significant damage rate= %19.2 < = %20→ Performance building is Limited Damage √.

For ZC soil class:

Table 4.45 Damage that occurred to beams and columns according to ZC soil class

	Beam damage percentages for ZC class							
	(X) Direction				(Y) Direction			
	SH	BH	IH	GB	SH	BH	IH	GB
3	0	100	0	0	35.3	64.7	0	0
2	0	100	0	0	35.3	64.7	0	0
1	3.8	96.2	0	0	38.2	61.8	0	0
Max		100			38.2			
Column shear force distribution for ZC class								
	(X) Direction				(Y) Direction			
	SH	BH	IH	GB	SH	BH	IH	GB
1	100	0	0	0	100	0	0	0
2	100	0	0	0	100	0	0	0
3	100	0	0	0	95.5	4.5	0	0
Max.	100							

Table 4.45 (Continue)

Columns Exceeding The Significant Damage Zone In The Lower And Upper Sections, Column shear force distribution (for ZC class)				
	(X) SH+BH	(X) IH+BH	(Y) SH+BH	(Y) IH+BH
3	100	0	100	0
2	100	0	100	0
1	100	0	100	0
Max.	100			

Building performance result for Zc soil class:

Performance building in Controlled damage level.

Controlled damage performance adequacy check:

Beam Damage rate= (IH= % 0.0 < = % 30 √), (GB= %0 √).

Column Damage rate= (IH= % 0.0 < = % 20 √), (GB= %0 √).

Top floor Vc rate= (IH= % 0.0 < = % 40 √), (GB= %0 √).

Plasticizing column Vc rate= (IH+ GB= % 0.0 < = % 30) √.

For ZD soil class:

Table 4.46 Damage that occurred to beams and columns according to ZD soil class

	Beam damage percentages for ZD class							
	(X) Direction				(Y) Direction			
	SH	BH	IH	GB	SH	BH	IH	GB
3	0	100	0	0	35.3	64.7	0	0
2	0	100	0	0	35.3	64.7	0	0
1	0	100	0	0	35.3	64.7	0	0
Max		100			35.3			
Column shear force distribution for ZD class								
	(X) Direction				(Y) Direction			
	SH	BH	IH	GB	SH	BH	IH	GB
1	100	0	0	0	100	0	0	0
2	100	0	0	0	100	0	0	0
3	94.5	5.5	0	0	82.8	17.2	0	0
Max.	100					17.2		

Table 4.46 (Continue)

Columns Exceeding The Significant Damage Zone In The Lower And Upper Sections, Column shear force distribution (for ZDclass)				
	(X) SH+BH	(X) IH+BH	(Y) SH+BH	(Y) IH+BH
3	100	0	100	0
2	100	0	100	0
1	100	0	100	0
Max.	100			

Building performance result for ZD soil class:

Performance building in Controlled damage level.

Controlled damage performance adequacy check:

Beam Damage rate= (IH= % 0.0 < = % 30 √), (GB= %0 √).

Column Damage rate= (IH= % 0.0 < = % 20 √), (GB= %0 √).

Top floor Vc rate= (IH= % 0.0 < = % 40 √), (GB= %0 √).

Plasticizing column Vc rate= (IH+ GB= % 0.0 < = % 30) √.

For ZE soil class:

Table 4.47 Damage that occurred to beams and columns according to ZE soil class

	Beam damage percentages for ZE class							
	(X) Direction				(Y) Direction			
	SH	BH	IH	GB	SH	BH	IH	GB
3	0	7.7	92.3	0	35.3	17.6	20.6	26.5
2	0	3.8	96.2	0	35.3	17.6	26.5	20.6
1	0	100	0	0	35.3	35.3	17.6	11.8
Max		100	96.2		35.3			26.5
Column shear force distribution for ZE class								
	(X) Direction				(Y) Direction			
	SH	BH	IH	GB	SH	BH	IH	GB
1	100	0	0	0	100	0	0	0
2	100	0	0	0	100	0	0	0
3	0	100	0	0	52.9	36.4	7.9	2.8
Max.		100					7.9	2.8
Columns Exceeding The Significant Damage Zone In The Lower And Upper Sections, Column shear force distribution (for ZE class)								

Table 4.47 (Continue)

	(X) SH+BH	(X) IH+BH	(Y) SH+BH	(Y) IH+BH
3	100	0	100	0
2	100	0	100	0
1	100	0	100	0
Max.	100			

Building performance result for ZE soil class:

In Collapse zone beam damage rate= %26.5 > %20

Performance building in Collapse level, the building needed to retrofitting.

Collapse prevention performance adequacy check:

In Collapse level beam damage rate= %26.5 > %20 not ok.

Column Vc rate= % 0.0 < = % 20 ok.

Top floor Vc rate= % 0.0 < = % 40 ok.

Plasticizing column Vc rate= % 0.0 < = % 30 ok.

→ Insufficient columns need to retrofitting by FRP.

5. RESULTS, CONCLUSIONS, AND FUTURE WORK

The purpose of this thesis is to investigate the non-linear behavior of RC high-rise buildings by using different displacements base nonlinear static and dynamic analysis methods considering both Turkish (TSC-2018) and Eurocode (EC8) rules. In these analyses, different parameters such as the effect of quality of concrete and torsion effect have been considered. General information about the topic has been provided in the first chapter. The second chapter included the evaluation of the related literature. Furthermore, the concept of pushover analysis has been explained in the third chapter. The performance analysis according to TSC-2018 and EC8 code rules was also discussed in this chapter.

The fourth chapter is a case study, where this chapter has been divided into four parts. The pushover analysis has been applied on a simple two-storey frame then the results for the case considering TSC2018, and EC8 rules have been compared. It is noteworthy to mention that it was intended that the outcome of this study is to be a simplified and a clarified reference for engineers.

Consequently, the pushover curves of the TSC2018 and EC8 were found to be similar, and the damage was similar at the performance point. On the other hand, it was noted that the beam damage at around failure was more in the case of EC8 compared to the TSC2018. Contrary to the case of beams, the damage of columns was more for TSC2018. The reason is likely that the effective section of stiffness for beams was 0.35 for TSC2018 while it was 0.5 for EC8. Furthermore, for the columns, the coefficient was 0.7 and 0.5 for TSC2018 and EC8, respectively. In addition, the rotation limits of the plastic hinges are lower in EC8 compared to TSC2018. Yet, these results are not valid for all types of concrete.

The quality of concrete on the building performance according to the TSC2018 and EC8 has been studied in the fourth chapter. To investigate the effect of concrete strength, three types of concrete classes have been considered as C40, C20, and C10. The pushover analysis method was implemented for a 14-storey frame. Consequently, it has been figured out that the frame has been brittle in the case of the C10 concrete class, according to both TSC2018 and EC8. It has been asserted that the performance of the frame was improved when the quality of the concrete was improved, where the damage of beams and columns has been noticeably reduced. Concerning the pushover curve for C10 concrete and C40 concrete, according to both codes, the outcomes were identical. The only difference is the lower displacement capacity in the case of TSC2018 for the C20 concrete class.

The third part of the fourth chapter includes the performance analysis of a 14-storey building having a torsion-dominated behavior. The pushover procedure and time history analysis have been applied by considering TSC2018 and EC8 rules. The plastic deformations of RC members have been compared, further, the structural performance was evaluated on the base of strains according to the TSC2018. In these evaluations, Erzincan earthquake data has been used.

The results proved that the pushover curves according to TSC-2018 and EC8 were almost identical. Correspondingly, the results obtained from the time history solutions showed that the plastic hinge deformations for the case of the Bingol earthquake were the best in comparison to the Erzincan and Duzce earthquakes. No plastic deformations appeared in the columns under the Bingöl earthquake, but in the Duzce and Erzincan earthquake, it was noticed that the number of damaged columns increased on the top floor.

Regarding the damage of the beams and columns, as mentioned previously, the number of damaged beams was higher according to EC8. On the other hand, the number of damaged columns was higher according to TSC-2018. It should be noted that the structural performance has been investigated in terms of controlled damage for the Erzincan earthquake record.

As for the last part of this chapter, the effect of soil type on building performance according to the TSC2018 has been studied by using the STA4CAD program. The pushover analysis has been done for a three-storey building considering (ZB, ZC, ZD, and ZE) soil types. As a result for the example building when the soil type is ZB limited damage level has been achieved. For ZC and ZD controlled damage level has been achieved. For soil type ZE the performance level is collapse level.

Finally, for future works, to know the effect of torsion clearly on the performance according to the non-linear method, it is advisable to compare between two buildings, one with torsion and the other without torsion, by changing the direction of the shear wall and comparing the results.

REFERENCES

ABYYHY (1998). Afet Bölgelerinde Yapılacak Yapılar Hakkında Yönetmelik,

Bayındırlık ve İskan Bakanlığı, Türkiye.

Afet ve Acil Durum Yönetimi Başkanlığı, Türkiye Deprem Tehlikeleri Haritaları https://www.afad.gov.tr/turkiye-deprem-tehlike-haritasi.

ATC-40. (1996). Seismic Evaluation and Retrofit of Concrete Buildings. Applied

Technology Council. California Seismic Safety Commission.

Buğday, D. (2014). Performansa Dayalı Tasarım İlkeleri İle Betonarme Çerçeve Yapılar İçin Pratik Hasar Tahmin Yöntemi. (Master's Thesis). İstanbul Teknik Üniversitesi, Fen Bilimleri Enstitüsü, İstanbul.

Buzuk, J. (2019). Seismic Performance Evaluation Of 24 Story Rc Building By Nonlinear Time History Analysis Utilizing TBDY2018 And EC8. (Master's Thesis). İstanbul Teknik Üniversitesi, Fen Bilimleri Enstitüsü, İstanbul.

Bedirhanoglu, I., Ilki, A. (2004). Theoretical Moment-Curvature Relationships for Reinforced Concrete Members and Comparison with Experimental Data. 6th International Congress on Advances in Civil Engineering, pages: 231-240, 6-8 October, Bogazici University, Istanbul, Turkey. ISBN: 975-518-230-6

Bedirhanoglu, I. 2009. "The behavior of reinforced concrete columns and joints with low strength concrete under earthquake loads: an investigation and improvement." Ph.D. thesis, Civil Engineering Faculty, Istanbul Technical Univ.

Bedirhanoglu, I., Ilki, A., Pujol, S., and Kumbasar, N. (2010). Behavior of Deficient Joints with Plain Bars and Low-Strength Concrete. ACI Structural Journal, Vol. 107, No.3, pp. 300-310., May-June 2010. DOI: 10.14359/51663695

Bedirhanoglu, I. (2011a). Tekin Apartmanında Meydana Gelen Kolon Hasarı Sonucu Yapının Göçme Riskinin İredelenmesi ve Alınması Gereken Acil Önlemler. Dicle Üniversitesi Mühendislik Fak. İnşaat Müh. Bölümü İçin Rapor.

Bedirhanoglu I. (2011b). Preliminary Report on 23 October 2011 Van Earthquake (Mw : 7.2), Chamber of Civil Engineers, Diyarbakir Branch, 1 November 2011. DOI: 10.13140/RG.2.1.5059.7920

Bedirhanoğlu İ., Erdemli S.G. (2013). Beton kalitesinin yapı denetimi kapsamında denetlenmesi. 3. Yapı Denetimi Sempozyumu,5-6 Ekim 2013 Diyarbakır. . pp. 365-376. ISBN: 978-605-01-0576-6. DOI: 10.13140/RG.2.1.1790.0884.

Bedirhanoglu I. (2014). A practical neuro-fuzzy model for estimating modulus of elasticity of concrete." Structural Engineering and Mechanics Vol. 51, No.2, pp.249-265, 2014. DOI: http://dx.doi.org/10.12989/sem.2014.51.2.249.

Bedirhanoglu I. (2015). Building Inventory in Diyarbakir District. Diyarbakır ve Çevresinin Yapı Stoku. Diyarbakır ve Çevresinin Doğal Afet Riski Çalıştayı, 29-

30 Nisan, Diyarbakır. DOI: 10.13140/RG.2.1.4081.5522.

Bedirhanoglu I., Polat B. (2017). Diyarbakır'daki Yapıların Deprem Dayanımı Açısından Değerlendirilmesi (Evaluation of Existing Buildings In Diyarbakir In Terms Of Earthquake Resistance). 4. Uluslararası Deprem Mühendisliği ve sismoloji Konferansı, 11-13 Ekim, Anadolu Üniversitesi-Eskişehir.

Bedirhanoglu I., Ilki, A., and Triantafillou, T. (2022). Seismic Behavior of Repaired and Externally FRP Jacketed Short Columns Built with Extremely Low-Strength Concrete. ASCE Journal of Composites for Construction. Vol. 26, No.1, pp.04021068-1-20, 2022. DOI: 10.1061/(ASCE)CC.1943-5614.0001179.

Erkan, M. Performans Bazlı Tasarım İtme (Pushover) Analizi - Temel Kavramlar Ve Metot.

ESİN, D. (2005). Statik İtme Analizi Yöntemiyle Mevcut Bir Betonarme Yapının İncelenmesi Ve Uygulanması. (Master's Thesis). İstanbul Teknik Üniversitesi, Fen Bilimleri Enstitüsü, İstanbul.

Eurocode 8. (2004). Design of structures for earthquake resistance -Part 1: General rules, seismic actions and rules for buildings. European Committee For Standardization. Brussels.

Eurocode 8. (2004). Design of structures for earthquake resistance -Part 3: Assessment and retrofitting of buildings. European Committee For Standardization. Brussels.

Ilki, A., Darilmaz, K., Demir, C., Bedirhanoglu, I., Kumbasar, N. (2005). NON-Linear Seismic Analysis of A Reinforced Concrete Building With FRP Jacketed Columns. FIB Symposium Keep Concrete Attractive, 23-25 May, Budapest.

Ilki, A., Bedirhanoglu, I., Basegmez, I.H. And Kumbasar, N. (2006). Shear Retrofit Of Low Strength Reinforced Concrete Short Columns With GFRP Composites. Third International Conference On FRP Composites İn Civil Engineering (CICE 2006), December 13-15, Miami, Florida, U.S.A. Pages: 601-604.

İrtem, E. Türker, K. (2004) Türk Deprem Yönetmliğine Göre Tasarlanmış Betonarme Yapıların Performansının Değerlendirilmesi. Altıncı Uluslararası İnşaat Mühendisliğne Gelişmeler Kongresi. Boğaziçi Üniversitesi, İstanbul, Türkiye.

Köse, D . (2008). Artımsal Eşdeğer Deprem Yükü Yöntemiyle Betonarme Bir Yapının Performans Seviyesinin Belirlenmesi. (Master's Thesis). İstanbul Teknik Üniversitesi, Fen Bilimleri Enstitüsü, İstanbul.

Sahin, U. And Bedirhanoglu I. (2014). "A Fuzzy Model Approach To Stress-Strain Relationship Of Concrete in Compression." The Arabian Journal For Science And Engineering, Vol. 39, No. 6, Pp. 4515-4527. DOI: 10.1007/S13369-014-1170-Z

Saritas, F. (2014). Deprem Etkisindeki Elastomer Mesentli Köprü Ayağının Farklı Zemin ve Mesnet Koşullarında Dinamik Davranışı. İmo Teknik Dergi, 2014 6699-6724, Yazı 416.

Saritas, F. (2019). Performance-Based Seismic Assessment Of A Base-İsolated Bridge-Pie. European Journal of Environmental and Civil Engineering. DOI:10.1080/19648189.2019.1647463.

Saritas, F. (2022). Seismic Performance Assessment of an Isolated Multispan Bridge. Arabian Journal for Science and Engineering. https://doi.org/10.1007/s13369-022-06626-7.

SAP2000 Integrated Structural Analysis and Design Softwar, Computer and Structure Inc., Berkeley, California, 2000.

Sta4Cad v14 Structural Analysis for Computer Aided Design.

Şahin, Y. (2019) Mevcut Bir Betonarme Binanın 2019 Türkiye Bina Deprem Yönetmeliği'ne Göre Zaman Tanım Alanında Analizinin Yapılarak Performansının Belirlenmesi Ve Çelik Güçlendirme Önerileri. (Master's Thesis). İstanbul Teknik Üniversitesi, Fen Bilimleri Enstitüsü, İstanbul.

TBDY2018. (2018). Türkiye Bina Deprem Yönetmeliği. T.C. Resmi Gazete 30364.

Oğuz, S. (2005). Evaluation Of Pushover Analysis Procedures for Frame Structures. (Master's Thesis). Middle East Technical University, The Graduate School Of Natural And Applied Sciences, Ankara.

Özer, E. (2009). Yapı Sistemlerinin Doğrusal Olmayan Analizi.

Özuygün, Ş. (2004). Statik itme yöntemiyle bina tahkiki ve güçlendirme hesabı. (Master's thesis). İstanbul Teknik Üniversitesi, Fen Bilimleri Enstitüsü, İstanbul.

Zolmaz, Y. (2019). Mevcut Betonarme bir Binanın Perdelere Güçlendirlmesi ve Yapısal Performansının TBDY-2018 Göre Değerlendirilmesi. (Master's thesis). İstanbul Teknik Üniversitesi, Fen Bilimleri Enstitüsü, İstanbul.

CURRICULUM VITAE

Personal Information

Surname, Name	Arova KONAK
Web Page (Research Gate, Academia, etc.)	

Education

Degree	Institution	Year of Graduation
MS	NATURAL AND APPLIED SCIENCES OF DİCLE UNIVERSITY	2022
BS	EL-FURAT University-CIVIL ENGINEERING/SYRIA	2016
High School	MESHEL SALIBA/ QAMISHLI -SYRIA	2010

Foreign Languages

Arabic- Turkish- Kurdish

DİCLE ÜNİVERSİTESİ
FEN BİLİMLERİ ENSTİTÜSÜ
TEZ BENZERLİK BİLDİRİMİ FORMU

Öğrencinin Adı, Soyadı	Arova KONAK		
Öğrenci No	18806008		
Ana Bilim Dalı	İnşaat Mühendisliği		
Program Türü	Proje ☐	Yüksek Lisans ☒	Doktora ☐
Tez Danışmanı (Ünvanı, Adı, Soyadı)	Doç. Dr. İdris BEDİRHANOĞU		
(Varsa) II. Tez Danışmanı (Ünvanı, Adı, Soyadı)			
Tez Başlığı	**BETONARME BİNALARIN ŞEKİLDEĞEİŞTİRME DAYALI DOĞRUSAL OLMAYAN PERFORMANSE DEĞERLENDİRMESİNİN TBDY2018 VE EC8 KARIŞLAŞTIRMALI OLARAK GEREÇEKLEŞTİRMESİ**		
RAPOR BİLGİLERİ			
Raporlama Aşaması	Tez Savunma Sınavı Sonrası		
Sayfa Sayısı	130		
Raporlama Tarihi	22.03.2022		
Benzerlik Oranı (%)	21%		

Yukarıda bilgileri verilen tez çalışmamın toplam 130 sayfalık kısmına ilişkin, 22/03/2022 tarihinde şahsım/tez danışmanım tarafından *Turnitin* isimli intihal tespit programından aşağıda belirtilen filtrelemeler uygulanarak alınmış olan intihal raporuna göre, tezimin benzerlik oranı 21% olarak tespit edilmiştir.

Uygulanan filtrelemeler:

☐Başlangıç Bölümleri (Kabul ve Onay sayfası, Teşekkür sayfası, Özet/Abstract) hariç

☐Kaynaklar hariç

☐Alıntılar hariç/dâhil

☒Diğer (Her şey dahil)

Tezimin benzerlik oranı, Dicle Üniversitesi Fen Bilimleri Enstitüsü İntihal Raporu Uygulama Esaslarında belirtilen üst sınır benzerlik oranını aşmamaktadır. Benzerlik oranım üst sınır benzerlik oranının altında olsa dahi aksinin tespit edilmesi durumunda her türlü yasal sorumluğu kabul ettiğimi ve hukuki sonuçlarına razı olduğumu bildirir,
gereğini arz ederim.

Öğrencinin Adı, Soyadı: Arova KONAK
Tarih:
İmza:

Danışman Adı, Soyadı: Doç. Dr. İdris BEDİRHANOĞU İmza:

Tarih:

Ana Bilim Dalı Başkanı: Adı, Soyadı: Prof. Dr. Z. Fuat TOPRAK İmza:

Tarih: